ELUCIDATING THE BIOSYNTHESIS OF POLYKETIDES ACCUMULATING IN BARLEY (*HORDEUM VULGARE*) CUTICULAR WAX

by

Alberto Ruiz Orduna

B.Sc., Universitat de Barcelona, 2012

M.Sc., Université de Montréal, 2015

A THESIS SUBMITTED IN PARTIAL FULFILLMENT OF

THE REQUIREMENTS FOR THE DEGREE OF

MASTER OF SCIENCE

in

THE FACULTY OF GRADUATE AND POSTDOCTORAL STUDIES

(Chemistry)

THE UNIVERSITY OF BRITISH COLUMBIA

(Vancouver)

November 2019

The following individuals certify that they have read, and recommend to the Faculty of Graduate and Postdoctoral Studies for acceptance, a thesis/dissertation entitled:

Elucidating the biosynthesis of polyketides accumulating in barley (*Hordeum vulgare*) cuticular wax

submitted by Alberto Ruiz Orduna in partial fulfillment of the requirements for

the degree of Master of Science

in Chemistry

Examining Committee:

Dr. Reinhard Jetter
Supervisor

Dr. Martin Tanner
Supervisory Committee Member

Dr. Harry Brumer
Supervisory Committee Member

Abstract

The epicuticular waxes covering the uppermost organs of the barley plant, including spikes, peduncles and flag leaf sheaths, are dominated by β-diketones and related hydroxy-β-diketones. Cultivars characterized by higher amounts of these compounds display improved resistance to water loss, therefore resulting in higher production yields. It was recently shown that biosynthesis of the different β-diketones and hydroxy-β-diketones relies on (1) a hydrolase known to participate in the formation of β-keto fatty acids, (2) a type-III polyketide synthase involved in β-diketone formation, and (3) a cytochrome P450 believed to perform the final hydroxylation of β-diketones. So far, only the hydrolase has been partially characterized, and the mechanism through which these enzymes form the different β-diketone-related compounds remains to be demonstrated.

Here, a detailed chemical analysis of the β-diketone-related compounds found in the wax of barley *cv.* Morex spikes has revealed the presence of a novel β-diketone whose structure cannot be explained with the currently assumed biosynthesis pathways. In addition, a natural isotope abundance analysis of the predominant barley β-diketone revealed ^{13}C enrichment also conflicting with previous biosynthesis hypotheses and prompting detailed studies of the polyketide synthase involved in β-diketone formation. This barley diketone metabolism polyketide synthase, DMP, was characterized in yeast and *in vitro*, revealing that it catalyzes the formation of β-diketones via head-to-head condensation between β-ketoacids and fatty acyl-CoAs. In the light of further results confirming that the first pathway enzyme, diketone metabolism hydrolase (DMH), delivers mainly C_{16} β-ketoacid as substrate for DMP, a revised pathway for β-diketone biosynthesis in barley may now be proposed.

Overall, the contribution of this research to the knowledge of barley β-diketones biosynthesis represents an important step towards the breeding of new cultivars with enhanced drought resistance and higher yield production. Interestingly, it seems very likely that current findings for β-diketone biosynthesis can be extrapolated from barley to wheat as a very closely related species, ultimately also enabling the breeding of stress-resistant wheat cultivars.

Lay Summary

The above-ground organs of plants are covered by mixtures of highly hydrophobic compounds, known as cuticular waxes, which protect the tissue against environmental stresses such as excessive water loss, of particular importance due to the serious climate challenging crop production. The uppermost organs of barley are covered by wax compounds with characteristic β-diketone structures playing a central role in protecting the plant late in the growing season and, thus, preventing crop failures. The mechanisms through which barley cells form these compounds remain elusive, and the principal goal of the present research was to characterize the central enzyme involved in β-diketone formation. The results show that these compounds are synthesized in a manner different from the previously hypothesized. The presented findings represent a big step forward in our understanding of cuticular wax formation in barley that may enable the breeding of new cultivars with improved drought resistance and enhanced crop yields.

Preface

My supervisor Dr. Reinhard Jetter, fellow graduate student Yulin Sun and I designed all the experiments presented in this research.

I grew the plant material used in Chapter 2, sampled the wax mixtures, analyzed them by GC-MS, and performed all the data analysis and processing. Dr. Sarah Feakins performed the isotopic measurements of purified wax compounds.

Dr. Asaph Aharoni provided the *E. coli* constructs for *Hv*DMH and *Hv*DMP. Yulin Sun performed the subcloning, heterologous expression of *Hv*DMH and *Hv*DMP in yeast and *E. coli*, and *Hv*DMP recombinant protein purification. I synthesized all substrates, and together with Yulin Sun performed the different feeding experiments, yeast and *E. coli* extractions, product analyses by GC-MS and data processing for the experiments presented in Chapters 3 and 4.

I performed all the literature searches, figure preparation and, with Dr. Reinhard Jetter, wrote the contents of this thesis.

Table of Contents

List of Tables

List of Figures

List of Abbreviations

°C	degrees Celsius
$\delta^{13}C$	conventional delta notation
µg	microgram
µl	microliter
µm	micrometer
ACP	acyl carrier protein
ALT	acyl-lipid thioesterase
amu	atomic mass unit
ARS	alkylresorcinol synthases
***At*LACS1**	*Arabidopsis thaliana* long chain acyl-CoA synthetase 1
BBS	bibenzyl synthase
BHFA	β-hydroxy fatty acid
BKA	β-keto acid
BKFA	β-keto fatty acid
BSTFA	bis-N,O trimethylsilyltrifluoroacetamide
C	carbon
CAM	crassulacean acid metabolism
cer	*eceriferum*
CHS	chalcone synthase
cm	centimeters

CoA	coenzyme A
CURS	curcumin synthase
CUS	curcuminoid synthase
cv.	cultivar
CYP	cytochrome P450
DCS	diketide-CoA synthase
DMC	β-diketone metabolism cytochrome P450
DMH	β-diketone metabolism hydrolase
DMP	β-diketone metabolism polyketide synthase
DNA	deoxyribonucleic acid
E. coli	*Escherichia coli*
EAR	enoyl-ACP reductase
ECR	enoyl-CoA reductase
ER	endoplasmic reticulum
eV	electron volts
FA	fatty acid
FAE	fatty acid elongation
FAME	fatty acyl methyl ester
FAS	fatty acid synthase
FAT	fatty acyl-ACP thioesterase
g	relative centrifugal force
g	gram

GC	gas chromatography
GC-FID	gas chromatography coupled to flame ionization detection
GC-IRMS	gas chromatography isotopic ratio mass spectrometry
GC-MS	gas chromatography coupled to mass spectrometry
HAD	hydroxyacyl-ACP dehydratase
HCD	ketoacyl-CoA dehydratase
***Hv*DMC**	*Hordeum vulgare* β-diketone metabolism cytochrome P450
***Hv*DMH**	*Hordeum vulgare* β-diketone metabolism hydrolase
***Hv*DMP**	*Hordeum vulgare* β-diketone metabolism polyketide synthase
IPTG	isopropyl β-D-1-thiogalactopyranoside
IUPAC	International Union of Pure and Applied Chemistry
KAR	ketoacyl- ACP reductase
KAS	β-ketoacyl-ACP synthase
KCR	ketoacyl-CoA reductase
KCS	ketoacyl-CoA synthase
l	liter
LACS1	long chain acyl-CoA synthetase 1
LB	Luria-Bertani
LCFA	long chain fatty acids
MAH1	mid-chain-hydroxylase 1
M	molar
M^+	molecular ion

m/z	mass to charge ratio
mg	milligram
min	minute
MK	methylketone
MKS	methylketone synthase
ml	milliliter
mM	millimolar
mm	millimeter
MS	mass spectrometry
nm	nanometer
OD	optical density
PCR	polymerase chain reaction
PKS	polyketide synthase
Rf	retention factor
Rt	retention time
RuBisCO	ribulose bisphosphate carboxylase/oxygenase
TE	thioesterase
TLC	thin layer chromatography
TMS	trimethylsilyl
UV	ultra violet
VLCFA	very long chain fatty acid
VPDB	Vienna Pee Dee Belemnite

WS wax synthetase

Acknowledgements

I would like to take this opportunity express my most sincere gratitude to my supervisor Dr. Reinhard Jetter for, firstly, giving me the opportunity to work on this exciting project, and secondly, for his tremendous support and guidance throughout these years. Without his patience, motivation and knowledge this dissertation, and the contained scientific contribution, would not be possible.

Thanks to all the Jetter lab members, Daisy Zhang, Jedrzej Gozdzik for all their support and a special thanks to Yulin Sun for her crucial participation on the success of this project. I will always keep with me all those great and special moments we spent together all these years.

Last but not the least, offer my sincere gratitude to first, my family, who from the distance always believed on me and kept supporting and encouraging me every single day. Secondly, to my Vancouver family, for all the great experiences, adventures, laughs, and infinite support which helped me go through the most difficult moments.

Chapter 1: **Introduction**

1.1 Plant cuticle composition, structure and function

The epidermis of land plants is covered by a multilayered hydrophobic structure called the cuticle. The inner domain of the cuticle, known as cuticular layer, sits right on top of the polysaccharide cell wall surrounding epidermal cells. The cuticular layer consists of cell wall polysaccharides embedded into a cutin polyester matrix. It is considered as a transition zone between the cell wall and the overlaid lipid-enriched cuticle proper, where waxes are deposited. Divided in two layers, the inner compartment of the cuticle proper consists of intracuticular wax embedded into the cutin matrix, whereas the outermost layer is devoid of cutin and consists of so-called epicuticular wax[1] (Figure 1.1).

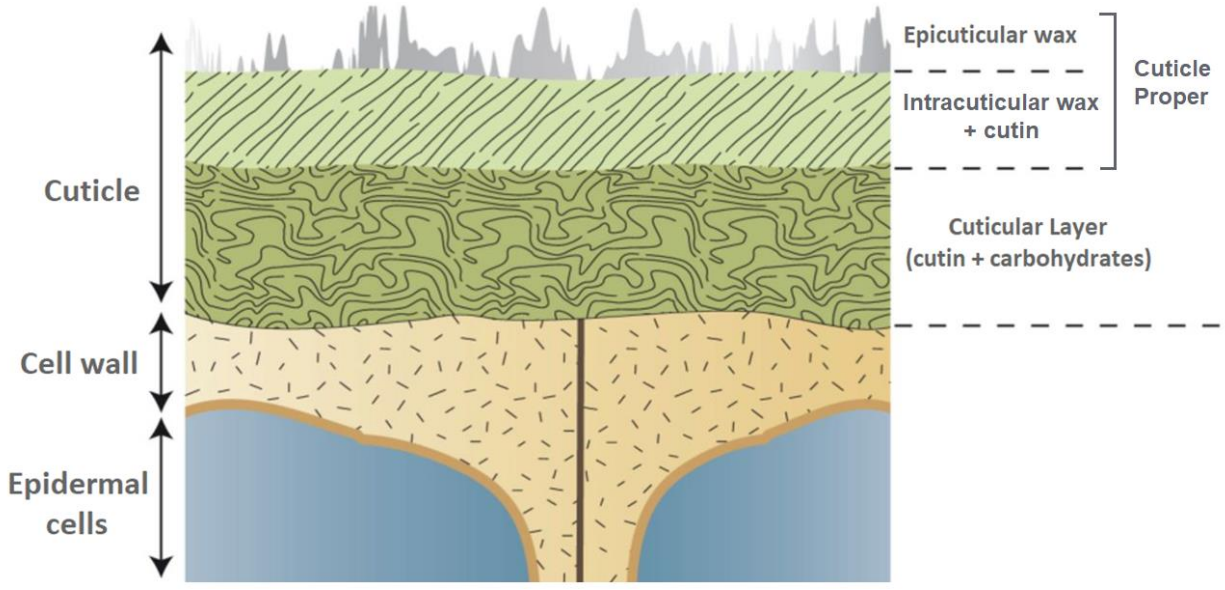

Figure 1.1: **Schematic cross-section of the plant epidermis.** Adapted from Kourounioti et al. 2013[2].

The overall cuticular waxes, consisting of intra- and epicuticular waxes, are complex mixtures of highly hydrophobic compounds. The waxes of most plant species comprise mono-functionalized very-long-chain aliphatics, including carboxylic acids, primary alcohols, alkyl esters, aldehydes, secondary alcohols and ketones, as well as alkanes. In some plant species the waxes contain further special compounds, and these may even be the predominant compound classes of the mixture. For example, plants belonging to the Poaceae family, including wheat and barley, accumulate high amounts of aliphatic β-diketones and hydroxy-β-diketones in the waxes covering certain organs. Chain lengths of wax compounds typically range from C_{20} to C_{36}, with homologs containing even numbers of carbons dominating in most compound classes except alkanes, secondary alcohols, ketones or β-diketones. Alicyclic compounds, such as terpenoids, and aromatics, such alkylresorcinols or phenolic esters, are also present in wax mixtures of some plant species. Hence, composition and compound class distribution of wax mixtures can highly vary not only between different plant species but also between organs within a species[3].

Epicuticular waxes aggregate to form microscopic crystals with a wide variety of shapes (Figure 1.2). Wax crystal morphology is mainly determined by the nature of the predominant wax compound, but can also be affected by presence of minor amounts of other compound classes. In some cases, epicuticular wax mixtures are complex mixtures not dominated by a specific compound class, and in these cases the correlation between crystal morphology and composition is sometimes unclear. In general, mixtures dominated by non-functionalized linear alkanes result in amorphous wax films, whereas wax mixtures dominated by compounds with terminal functionalities such as primary alcohols, aldehydes or fatty acids commonly lead to the formation of wax platelets. Finally, mixtures dominated by in-chain functionalized compounds such as

secondary alcohols or β-diketones lead to relatively complex crystal shapes, including tubules, helices or transversely ridged rodlets[4].

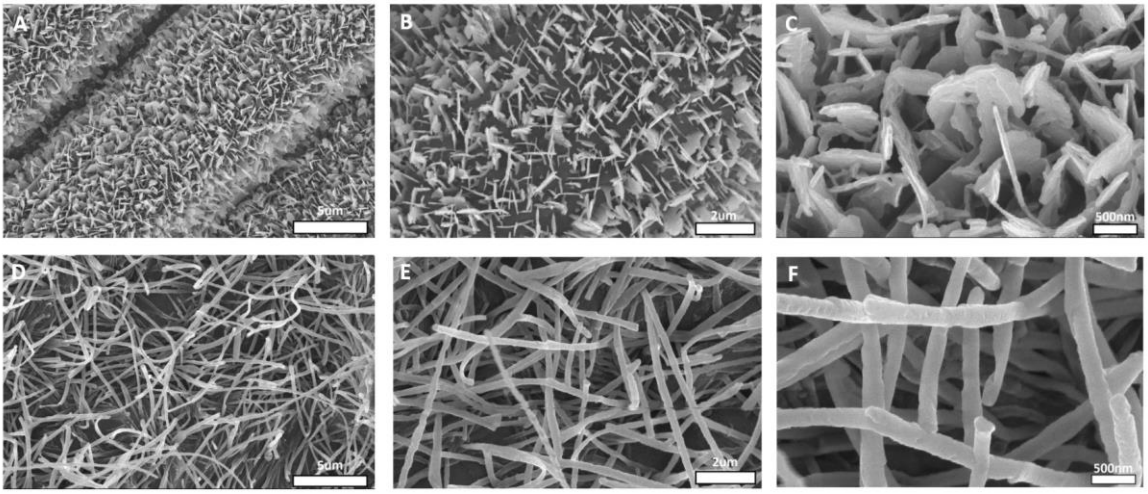

Figure 1.2: **SEM images of the surface of barley *cv.* Morex showing the morphology of the epicuticular wax crystals. A. B. C.** SEM images of flag leaf blades, presenting platelet-shaped crystals dominated by C_{26} primary alcohol and **D. E. F**. Flag leaf sheaths, presenting tubule-shaped crystals dominated by hentriacontane-14,16-dione. Magnifications x5.000 (**A** and **D**), x10.000 (**B** and **E**) and x30.000 (**C** and **F**) are presented.

The composition of cuticular waxes, combined with their crystalline disposition, confers crucial physical properties and biological functions to plants. The highly hydrophobic character of the overall cuticular waxes enables them, for example, to limit excessive water loss, protect from pathogen infection and proliferation, and avoid organ fusion, whereas the particular morphology of epicuticular crystals may specially help plants on protecting against ultra violet (UV) radiation by light refraction or to enhance hydrophobicity of their surfaces, conferring self-cleaning properties, or protection against herbivorous insects thanks to a reduced surface contact[5].

1.2 Formation of ubiquitous wax compounds in the model plant Arabidopsis

Classically, wax biosynthesis has been studied using the model plant species *Arabidopsis thaliana*, chosen for its small size, fast growth, small diploid genome, and many other advantageous traits. The metabolic pathways leading to major constituents of Arabidopsis cuticular waxes have already been established, and most of the genes encoding wax biosynthesis enzymes in this species have been identified. Accordingly, the biosynthesis of wax components is known to occur in epidermal cells (Figure 1.3).

In Arabidopsis, long-chain fatty acids (LCFA) (C_{16} and C_{18}) are biosynthesized through the so-called *de novo* fatty acid synthesis in plastids. A multi-enzyme complex known as fatty acid synthase (FAS) catalyzes LCFA biosynthesis by four sequential reactions. Initially, a β-ketoacyl-acyl carrier protein synthase (KAS) catalyzes the condensation of a acyl carrier protein (ACP) bound malonyl with coenzyme A (CoA) bounded acetyls or acyl-ACPs, resulting in the addition of two-carbon units to yield β-ketoacyl-ACPs. These are then reduced by ketoacyl-ACP reductase (KAR), resulting in 3-hydroxyacyl-ACPs, further dehydrated by a hydroxyacyl-ACP dehydratase (HAD) to yield Δ-trans-enoyl-ACPs, followed by double-bond reduction catalyzed by an enoyl-ACP reductase (EAR) to generate acyl-ACPs elongated by two carbon units. These resulting acyl-ACPs will then reenter the cycle, and in several repeats, will be elongated up to C_{16} or C_{18}. Elongation terminates by acyl-ACP interception by fatty acyl-ACP thioesterase (FAT)-B, which hydrolyzes the ACP group, and the resulting LCFA can then be transported to the endoplasmic reticulum (ER) for further elongation[6].

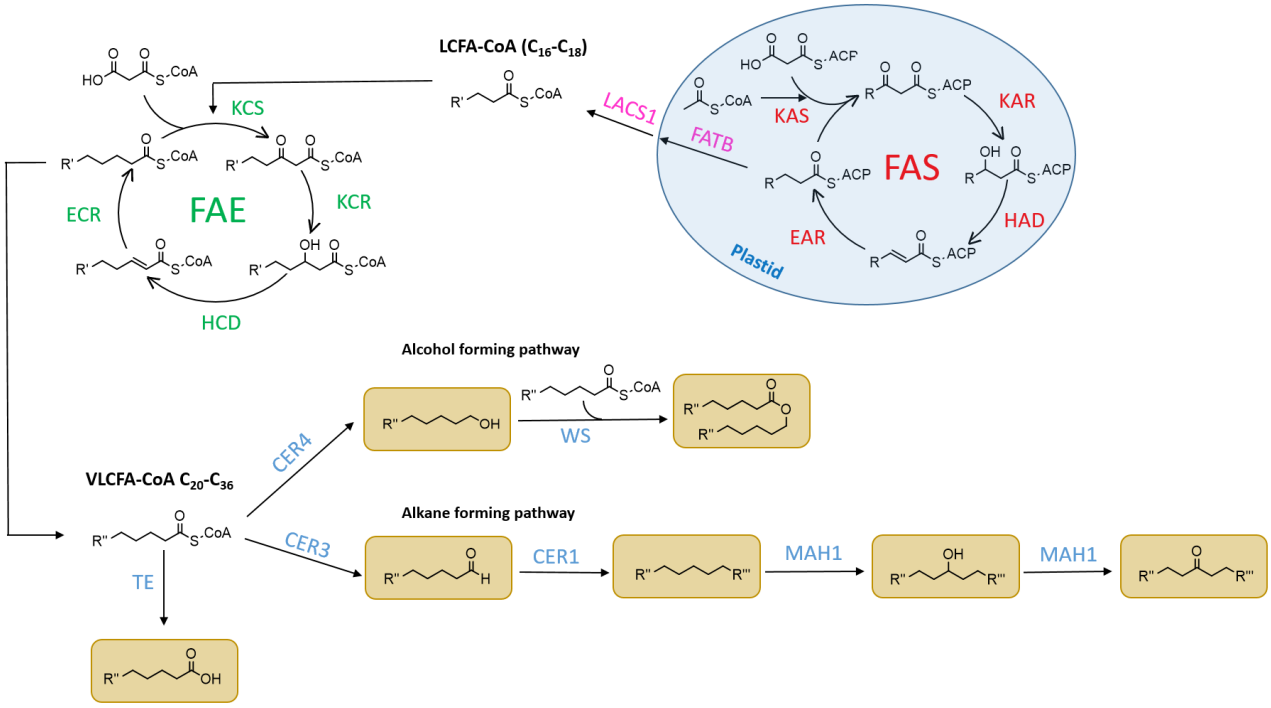

Figure 1.3: **Biosynthesis of ubiquitous wax compounds in Arabidopsis.** In epidermal cell, wax compounds are biosynthesized from plastidial LCFAs. In the ER LCFAs are elongated into VLCFAs before suffering head group and/or in chain modifications resulting in the different wax compound classes.

At the ER, LCFA are converted into acyl-CoAs by long chain acyl-CoA synthetase 1 (LACS1) and elongated into very-long-chain fatty acids (VLCFA) (C_{20} to C_{36}) by multi-enzyme complexes fatty acid elongation (FAE) analogous to the FAS. Elongation at the FAE complex is also mediated by the condensation between acyl-CoAs and a single unit of malonyl-CoA, β-keto group reduction, hydroxyacyl dehydration and enoyl reduction, catalyzed by a ketoacyl-CoA synthase (KCS), ketoacyl-CoA reductase (KCR), ketoacyl-CoA dehydratase (HCD) and enoyl-CoA reductase (ECR), respectively[7]. Again, each round of the cycle results in the extension of the chain by two carbons.

Elongated very long chain acyl-CoAs can either be converted into free VLCFAs though the action of a thioesterase (TE), or they can also undergo further modification of the head group towards

various wax components. Head group modification can occur through two different pathways: the acyl reduction (also known as alcohol-forming pathway) or through the decarbonylation pathway (also known as alkane-forming pathway). On the former pathway, reduction of very long chain acyl-CoAs into primary alcohols is catalyzed by ECERIFERUM (CER)-4, an enzyme characterized as a selective fatty acyl-CoA reductase[8]. The final step of the acyl reduction pathway is the synthesis of alkyl esters by a wax synthetase (WS), an acyltransferase catalyzing the esterification of acyl-CoAs with fatty alcohols[9].

On the other hand, very long chain acyl-CoAs can also undergo reduction to aldehydes and decarbonylation, resulting in the formation of alkanes. Both steps of this pathway are known to be carried out by a complex of two enzymes, CER3 and CER1. Even though the exact function of each enzyme is not fully understood, the initial reduction is thought to be catalyzed by CER3 and the C-C bond cleavage by CER1[10]. In addition, secondary alcohols and ketones are also formed on the alkane-forming pathway. The mid-chain-hydroxylase 1 (MAH1), a cytochrome P450 (CYP) monooxygenase, catalyzes the hydroxylation of alkanes into secondary alcohols in Arabidopsis, and likely also a further oxidation to the corresponding ketones[11].

1.3 Formation of Poaceae-specific wax compounds

The wax biosynthesis pathways in Poaceae species, including wheat (*Triticum aestivum*), barley (*Hordeum vulgare*), rye (*Secale cereale*) and oat (*Avena sativa*), are not as well characterized as in Arabidopsis. Biosynthesis of ubiquitous wax compounds, such as very long chain aliphatic carboxylic acids, alcohols, esters, aldehydes or alkanes, are assumed to happen in most species through routes analogous to those in Arabidopsis. For example, biosynthesis of primary alcohols in the Poaceae species wheat, was recently reported to be mediated by several enzymes

homologous to the Arabidopsis CER4[12]. However, the biosynthetic mechanisms forming the various Poaceae-specific wax components such as β-diketones, hydroxy-β-diketones and alkan-2-ol esters are still far from being understood.

Early genetic studies on the diploid Poaceae species barley identified a gene locus named *CER-CQU*, with three differentiated activities responsible for the formation of β-diketones (nonacosane-12,14-dione, nonacosane-14,16-dione, hentriacontane-14,16-dione and tritriacontane-16,18-dione), hydroxy-β-diketone (25-hydroxy-hentriacontane-14,16-dione) and alkan-2-ol esters (C_{33} to C_{37} alkan-2-ol esters) (for more details on the composition of β-diketone-related compounds see Chapter 2). Barley *cer-q* mutant lines lacked all β-diketone-related wax compounds, whereas *cer-c* mutants had just alkan-2-ol esters but no β-diketones or hydroxy-β-diketones. *Cer-u* mutants, instead, lacked only hydroxy-β-diketone. These observations suggested that β-diketones, hydroxy-β-diketones and alkan-2-ol esters were sharing a common precursor[13].

Intense research ensued to decipher the mechanisms for biosynthesis of β-diketone-related compounds. This research was performed primarily by incubating barley spike slices, tissue presenting large amounts of β-diketones on its surface, with different ^{14}C-radiolabeled substrates. The resulting β-diketones were extracted, fragmented via iodoform reaction into two fatty acid (FA) moieties, and then further degraded into shorter FAs by chemical α-oxidation. Analysis of the reaction products by radio-gas chromatography was then performed to determine the position of the incorporated radiolabeled carbons.

Tissue incubation with [2-^{14}C-acetate] resulted in characteristic ^{14}C incorporation into the carbon skeleton of the predominant hentriacontane-14,16-dione. Three regions with differentiated patterns of label incorporation were found. The C_{16} FA moiety obtained by iodoform fragmentation of the β-diketone presented a label pattern consistent with the incorporation of C_2

units into an intermediate with up to 16 carbons in length by a unique mechanism. Two other uniformly labeled regions were found between C-17 to C-19 of hentriacontane-14,16-dione and from C-20 to C-31. These results suggested that the entire carbon skeleton of the predominant β-diketone is biosynthesized by three independent mechanisms and, hence, ruled out a possible biosynthesis of hentriacontane-14,16-dione via condensation between C_{16} FA, C_{14} FA and a malonate unit, as this would presumably involve formation of C_{16} FA and C_{14} FA moieties by overlapping rather than independent mechanisms[14].

Further experiments testing tissue incubation with radiolabeled FAs revealed that these were optimal substrates for β-diketone biosynthesis. C_{12} FA, C_{14} FA and C_{16} FA were efficiently incorporated into the β-diketones, with C_{14} being the preferred substrate chain length, whereas C_{18} was found not to be incorporated[15]. It was then assumed that β-diketones were synthesized from FA substrates via elongation through successive malonyl incorporation similar to other wax compounds. However, at this point the moiety of the β-diketone originating from the FA, and hence the direction of further elongation, could not be unequivocally determined. Further tests of the FA precursors for β-diketone formation as well as the direction of elongation were performed by incubation with labeled C_{15} FA, resulting in the formation of an unnatural even-numbered β-diketone, triacontane-14,16-dione. Both its moieties, arising from the FA and further elongation, could be distinguished, suggesting that triacontane-14,16-dione elongation occurred from C-30 to C-1, opposite to nomenclature counting. This interpretation implied that C_{15} FA undergoes five rounds of elongation with retention of the β-diketone group. Interestingly, this mechanism was also consistent with the β-diketones obtained from feeding other FAs, where C_{16}, C_{15} and C_{14} FAs gave C_{31}, C_{30} and C_{29} β-diketones. It was inferred that the predominant barley β-diketone,

hentriacontane-14,16-dione, was biosynthesized from a C_{16} FA precursor via elongation from C-31 to the C-1 end of the molecule[16].

Similar experiments were also employed to study the biosynthetic relationship between the β-diketones and the alkan-2-ol esters. Labeled pentadecan-2-ol and pentadecan-2-one as well as β-keto fatty acyl-CoA were all successfully incorporated into the alkan-2-ol esters, in contrast to β-hydroxy fatty acid. These results confirmed the original hypothesis that β-diketones and alkan-2-ol esters have a common precursor, and that a reductase is involved in the branch pathway leading to the alkan-2-ol esters[17].

All observations taken together in 1984 led to a pathway hypothesis, where CER-Q would possess β-ketoacyl elongase activity mediating the condensation of a fatty acyl-CoA with a malonyl-CoA unit to form a β-ketoacyl-CoA intermediate. CER-C would then act as type-III polyketide synthase (PKS) catalyzing the condensation of the β-keto acyl-CoA intermediate with two malonyl-CoA extender units, retaining the two original carbonyls and forming a tetraketide intermediate. The resulting tetraketide would undergo elongation analogous to other wax compounds, via five rounds of elongation in one or more FAE complexes, followed by head group decarboxylation analogous to the formation of wax alkanes. The β-diketone product of this process would finally be hydroxylated by CER-U to form the hydroxy-β-diketone. On the other hand, CoA hydrolysis could give a β-ketoacid intermediate, which after decarboxylation and reduction would yield alkan-2-ols that serve as substrates for formation of alkan-2-ol esters (Figure 1.4)[18]. However, at this point the identity of the enzymes as well as whether the *CER-CQU* gene locus encoded a single protein possessing three domains with these three activities or if actually three genes encoded three different enzymes was still unclear[19,20].

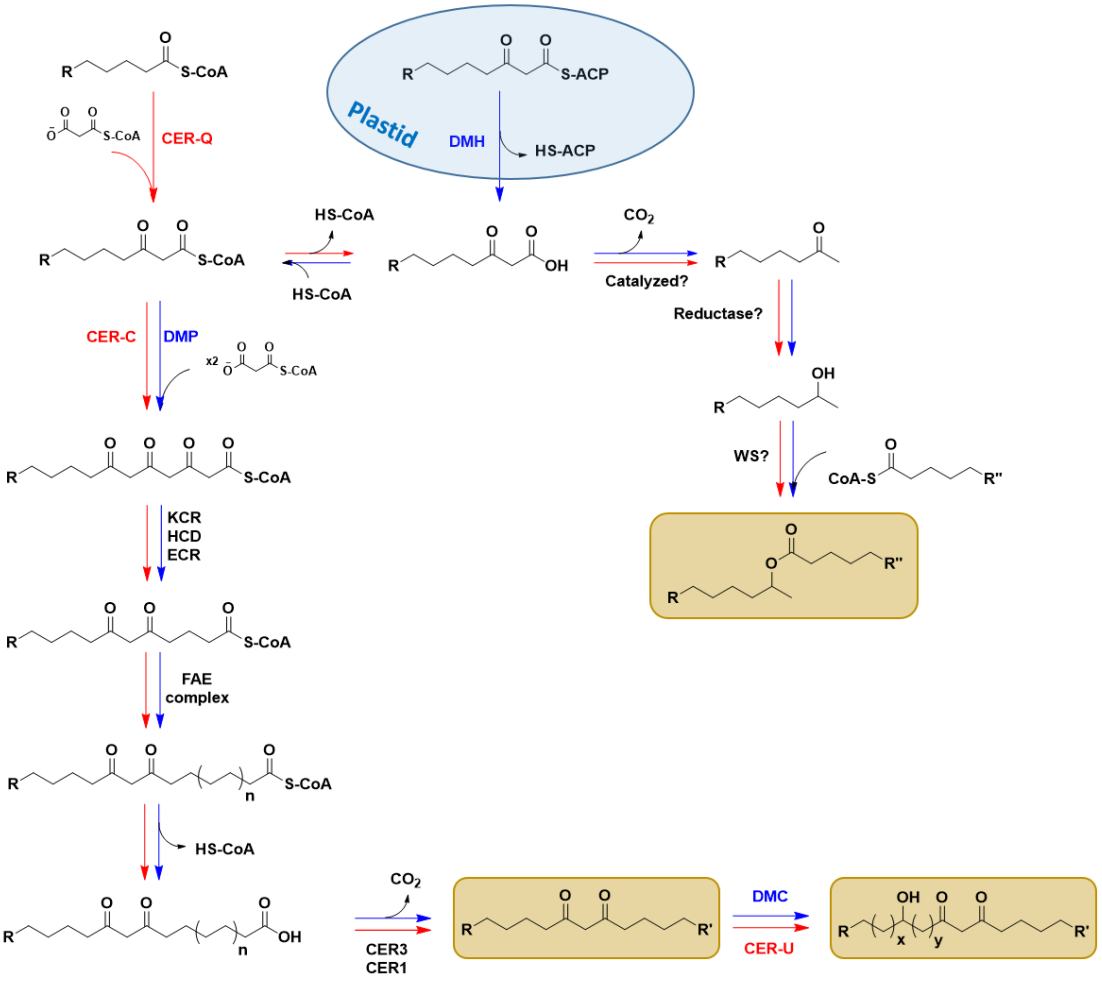

Figure 1.4**: Hypothesized pathway for biosynthesis of β-diketone-related barley and wheat wax compounds.** The pathway assumed since 1984 involving a β-ketoacyl-CoA intermediate is indicated in red. The alternative pathway newly hypothesized in 2016-2017, after the discovery that CER-Q is a hydrolase (now designated as *Hv*DMH), is indicated in blue.

The original β-diketone pathway hypothesis could finally be tested once the barley genome was sequenced and, in 2016, the barley *CER-CQU* gene locus was identified. It proved to be a gene cluster[20] encoding, among others, three enzymes newly annotated as *Hordeum vulgare* β-diketone metabolism hydrolase (*Hv*DMH), *Hordeum vulgare* β-diketone metabolism polyketide synthase (*Hv*DMP) and a *Hordeum vulgare* β-diketone metabolism cytochrome P450 (*Hv*DMC) based on their predicted protein sequences[21]. Deoxyribonucleic acid (DNA) sequencing of the *cer-c*, *cer-q*

and *cer-u* mutants confirmed that the three newly annotated reading frames were identical with the original *CER-Q*, *CER-C* and *CER-U* locus, respectively, implying that the CER-Q protein should not have β-keto acyl elongase activity as surmised in the old pathway model, but instead should be a hydrolase. Since the first enzyme on the pathway might thus generate free acid intermediates, this raised doubt whether the originally proposed β-ketoacyl-CoA intermediate would indeed be a precursor for β-diketones.

In further research, the barley DMH enzyme has since been partially characterized using *in vivo* assays in *Escherichia coli* (*E. coli*)[21]. These experiments demonstrated the hydrolase activity of *Hv*DMH, and in particular that it can intercept β-keto acyl-ACP intermediates of fatty acid elongation and hydrolyze them into free β-keto fatty acid (BKFA) species. *Hv*DMH has substrate/product specificity towards the formation of C_{16} BKFA, however, that this first step of the pathway may also occur on C_{18} BKFA precursors as the original hypothesis involves cannot be ruled out at this point (for details see chapter 3). Interestingly, the observed preference of *Hv*DMH for C_{16} BKFA correlates well with the homolog distribution of the esterified alkan-2-ol esters but not with the BKFA chain length assumed to serve as precursor for β-diketone biosynthesis. As pointed out in a recent review summarizing our current understanding of biosynthetic pathways leading to β-diketone-related compounds in barley, *Hv*DMH still needs to be better characterized and its specificity for different β-ketoacyl-CoA chain lengths further evaluated[22].

The function of the second enzyme on the β-diketone formation pathway, *Hv*DMP, remains unresolved at this point. This enzyme may act similar to other plant type-III PKSs, by performing successive condensations of two malonyl-CoA units with the now established central intermediate of the pathway, a β-keto fatty acid, to form a tetraketide intermediate. This intermediate could then

be further elongated into the β-diketones, in a manner analogous to most of the wax compound classes (Figure 1.4). So far, the tetraketide-forming activity of *Hv*DMP has not been demonstrated, and its occurrence relies solely on the distinct pattern of labeled acetate and C_{16} FA incorporation into the β-diketones. Interestingly, analysis of the predicted *Hv*DMP sequence, based on the newly published barley genome information, revealed significant similarity to curcuminoid synthase (CUS)[21]. This plant type-III PKS does not catalyze condensation of a starter acyl-CoA with malonyl extenders, but instead forms curcuminoids via head-to-head condensation between an aromatic acyl-CoA and an aromatic β-ketoacid (further details are presented in chapter 4). The sequence similarity between *Hv*DMP and CUS suggests that *Hv*DMP may also have activities other than the malonyl condensation commonly assumed for type-III PKSs.

*Hv*DMC is assumed to be the last enzyme in the pathway acting by precisely hydroxylating β-diketones on C-25 to form hydroxy-β-diketones. This conclusion is primarily based on the phenotype that *cer-u* barley mutant plants present. However, its involvement has not been directly demonstrated, most likely due to the highly hydrophobic nature of its substrate. Even though other pathways involving an early hydroxylation of the FA precursor for the β-diketones cannot be completely ruled out, this stands as a less likely alternative.

1.4 Aims of the presented research

After more than 40 years of intense research, the recent identification of the enzymes encoded in the *CER-CQU* gene cluster and the first attempts on characterizing these enzymes now enabled further experiments, testing the currently assumed pathway as well as alternative pathways such head-to-head condensation between a BKFA and a fatty acyl-CoA. The latter alternative had been discarded early based on the displayed labeled acetate incorporation pattern into the β-diketones.

However, the observed incorporation of C_{16} FA into the predominant β-diketone, the new observation that C_{16} BKFA is the main product of *Hv*DMH, and the reported *Hv*DMP similarities with CUS indicates that this alternative needs to be re-visited.

The investigations presented here on the mechanisms underlying barley β-diketone biosynthesis first focus on a detailed chemical analysis of the different β-diketone-related compounds found in barley (Chapter 2), in order to acquire comprehensive information on homolog and isomer distributions that may be indicative of enzyme activities. Then, *Hv*DMH was extensively characterized using heterologous expression in *E. coli* (Chapter 3). Since this is the first enzyme acting in the pathway, identification of all its products is crucial, especially as previous results had indicated that the enzyme product may not fit the earlier pathway hypotheses. Based on the *Hv*DMH products, further studies into the activity of *Hv*DMP could then be undertaken *in vivo* and *in vitro.* Heterologous expression in yeast as well as *in vitro* assays combined with feeding of the BKFA products of *Hv*DMH was used to query the *Hv*DMP activity (Chapter 4). Finally, all the combined results will be discussed to draw novel conclusions on β-diketone biosynthesis (Chapter 5).

Chapter 2: **A survey on barley *cv.* Morex cuticular wax, β-diketone homologs and isomers, and ^{13}C content among compound classes**

2.1 Introduction

Current knowledge on barley wax composition is mainly based on studies undertaken about four decades ago on the cultivars Bonus and Foma, as well as on different mutant lines derived from them. The surfaces of flag leaf sheaths, exposed peduncle and spikes are covered with tubule-shaped epicuticular wax crystals characteristic of β-diketones, causing grey-bluish appearance of these organs[23]. Instead, *cer-c* and *cer-q* mutant plants present a phenotype where the surface of the above-mentioned organs was bright green, indicating a lack of β-diketones[13]. Therefore, these mutants, along with the related *cer-u* mutant, were of special interest for investigations into the biochemistry of the β-diketone-related compounds characteristic of barley and other Poaceae, and the wax mixtures of their flag blades and sheaths, spikes and awns were analyzed in some detail.

2.1.1 Distribution of wax compounds among the mixtures covering barley organs

Analysis of the different components that constitute barley cuticular waxes were originally performed by first separating β-diketones and hydroxy-β-diketones from the crude wax by the formation of copper complexes that can be easily separated, for example by column or thin layer chromatography (TLC). The remaining lipids were then subjected to TLC purification. Identification of the compound class contained in each TLC band was performed based on retention factor (Rf) and confirmed by infrared spectroscopy[23,13,24] or, in some cases such as alkan-2-ol esters[25] and secondary alcohols[24], by gas chromatography coupled to mass spectrometry (GC-

MS). Quantification of each homolog within each compound class was achieved by gas chromatography coupled to flame ionization detection (GC-FID) analysis.

The wax mixtures on different barley organs were found to contain β-diketones, hydroxy-β-diketones, alkanes, primary alcohols, esters (of alkan-1-ols and alkan-2-ols), fatty acids, aldehydes and, in some cultivars, secondary alcohols. Between organs, the proportion of each compound class varied highly, and in some organs compounds such as β-diketone-related compounds lacked completely. In addition, the relative abundance of the different homologs within each compound class also differed strongly. Leaf waxes were principally dominated by C_{26} primary alcohol, accounting for approximately 72% of the total wax, and these lacked β-diketone-related compunds[14]. β-Diketones and hydroxy-β-diketones instead dominated the wax mixtures of flag leaf sheaths, constituting approximately 63% of the total wax. Awn wax was dominated by alkanes, with the C_{31} homolog predominant, except for the barley *cv.* Foma which also had secondary alcohols with chain lengths similar to the alkanes[24].

C*er-u* mutant spikes, lacking hydroxy-β-diketones and accumulating β-diketones, have received special interest owing to the relatively even distribution of compound classes in their wax, making them most suitable for observing alterations in the different classes of compounds and hence facilitating studies into possible biosynthetic relationships between β-diketone-related compounds and other wax components and possible shared mechanisms of elongation. *Cer-u* spikes have been shown to contain β-diketones, accumulating to around 50% of the total wax. Alkanes, as the second-most abundant compound class, constituted 16% of the total wax, with chain lengths ranging from C_{27} to C_{33} and the C_{31} homolog predominant[18]. Esters made up 11% of the total wax, including alkan-1-ol esters and alkan-2-ol esters. Chain lengths ranged from C_{33} to C_{37} for the alkan-2-ols, with C_{35} as the predominant homolog, and from C_{38} to C_{50} for the alkan-1-ols, with

C_{44} the predominant. Other compound classes were found in much lower abundance, including aldehydes (4%), primary alcohols (3%), and free acids (5%). The remaining 11% included compounds that could not be identified[26].

2.1.2 Homologs and isomers of β-diketone-related compounds

Identification of the different homologs and isomers of β-diketones were originally performed by saponification of the β-diketones. GC-FID analysis of the resulting FAs and methylketones was used to determine β-diketone chain lengths as well as carbonyl group positions, revealing that the barley β-diketones consisted primarily of a single homolog and a single isomer, hentriacontane-14,16-dione[23]. Later, this was confirmed by GC-MS analysis of the isolated diketone fraction after reduction to the respective β-diols and trimethylsilyl (TMS) ether-derivatization. GC-MS analysis of these species facilitated structure elucidation their mass spectra presented abundant fragment ions corresponding to the four possible α-cleavages occurring at both sides of the hydroxyl groups. Interestingly, this method permitted to determine that in fact four different homologs and/or isomers were present in barley *cv.* Bonus spikes, including hentriacontane-14,16-dione (95.8%), nonacosane-14,16-dione and nonacosane-12,14-dione (together 0.4%), and tritriacontane-16,18-dione (3.8%)[16].

β-Diketone structure assignments were corroborated in further studies involving GC-MS analysis of either the intact molecule or its TMS derivative. Mass spectra of the intact β-diketones displayed a base peak *m/z* 100 thought to be generated by double McLafferty rearrangement on both sides of the two carbonyl groups, which was therefore recognized as a hallmark of the β-diketone structure. Even though the α-fragments used for structure identification had much lower abundance than the McLafferty product, GC-MS analysis of the underivatized β-diketone was shown to be suitable

for structure elucidation[27]. On the other hand, TMS derivatization of β-diketones resulted in β-ketoenol TMS ethers whose mass spectrometry (MS) fragmentation was shown to greatly reduce McLafferty rearrangements and enhance α-cleavage, to some extent facilitating MS spectrum interpretation[28]. However, it was observed that TMS derivatization of β-diketones was sometimes incomplete, resulting in mixtures of derivatized and underivatized β-diketones[29] and somewhat impeding this approach.

The possible presence of different isomers and homologs of the hydroxy-β-diketones has been also evaluated by GC-MS analysis of TMS derivatives, in this case containing two TMS groups. Contrary to the β-diketones, its hydroxy derivatives have been reported to be present as a single homolog and isomer, 25-hydroxy hertriacontane-14,16-dione[28].

Barley *cv.* Bonus spikes have also been the focus of investigations into the composition of the alkan-2-ol esters thought to be biosynthetically related to β-diketones. The structures of these esters, as well as the presence of different homologs and isomers, were determined by GC-MS analysis of the alkan-2-ol fraction after ester saponification and by comparison of their mass spectra with those of authentic standards. The different homologs identified within this compound class encompass the odd-numbered chain lengths C_{33}, C_{35} and C_{37}, with C_{35} dominating (52.5%) along with C_{33} (31.4%). Alkan-2-ol esters presented the same esterified acid moiety as the alkan-1-ol esters, with chain lengths ranging from C_{16} to C_{22} and C_{20} being the predominant homolog (60%). However, both ester classes greatly differed in esterified alcohol chain lengths, comprising C_{20} to C_{28} alkan-1-ols with C_{22} (38.0%) and C_{24} (40.1%) dominating, and C_{13}, C_{15} and C_{17} alkan-2-ols with C_{15} accounting for 60.5%, C_{13} 38.9%, and C_{17} 0.6% respectively[18,25,26].

The development of more efficient gas chromatography (GC) columns and more sensitive MS instrumentation in the last four decades may allow the detection and identification of novel minor compounds that may have been previously overlooked. Such compounds are of great interest, as they might be intermediates or side products from specific wax biosynthesis pathways.

Differences between barley cultivars have been observed on the composition of the waxes covering certain organs, for example barley *cv.* Foma was found to contain secondary alcohols in their awns, whereas barley *cv.* Bonus did not present this compound class[24]. The recent sequencing of barley genome, on its cultivar Morex[30], pointed out the need of acquiring comprehensive data on the composition of the waxes covering the organs of this cultivar, as no literature is currently available, in order to facilitate the characterization of newly identified enzymes involved in wax biosynthesis. To fill important gaps in our knowledge of barley wax composition and lay the groundwork for investigations into the biosynthesis of β-diketone-related compounds, the first goal of the present work was to provide detailed information on the chemistry of waxes covering barley spikes and flag leaf sheath on its cultivar Morex. TLC was used to purify the crude wax and the different TLC fractions were exhaustively analyzed by GC-MS in order to determine the presence of novel homologs and isomers of the different β-diketone-related compounds which can reveal some insights on the mechanisms through which β-diketones are biosynthesized. In this context, as shown in previous studies[16], β-diketones with even carbon numbers are of special interest, because in them the moiety corresponding to the precursor can be distinguished from the moiety formed by elongation. Commonly, wax compound classes comprise homologous series with even- and odd-chain lengths, one of them strongly dominating depending on biosynthesis pathways. However, natural even-chain length β-diketones have not yet been identified. A special effort will

therefore be put into their identification, in order to provide further evidence testing the currently assumed pathway.

2.1.3 ^{13}C content of wax compounds

Plant metabolites have been shown to present characteristic ^{13}C isotope content encoding information on their plant type of origin as well as on their mechanisms of biosynthesis. C3, C4 and crassulacean acid metabolism (CAM) plants incorporate different amounts of ^{13}C into their metabolites while, within a plant species, differences on ^{13}C content are also found between compound classes biosynthesized through different pathways as well as between homologs within the same compound class. Determination of ^{13}C stable isotope content on wax components stands as a useful approach to complement studies on the elucidation of their biosynthesis.

Carbon and hydrogen are the most abundant elements in plants. Carbon is found in nature as ^{12}C, accompanied by its stable isotope ^{13}C with an abundance of a 1.108%[31]. The ^{13}C content of plant metabolites has been studied, in most cases, by gas chromatography isotopic ratio mass spectrometry (GC-IRMS). ^{13}C relative content determined by GC-IRMS is given as the variation of the ratio between the heavy and the light isotope, i.e. $^{13}C/^{12}C$. Values are conventionally expressed as conventional delta notation ($\delta^{13}C$), which are defined as; $\delta^{13}C=(R_{sample}-R_{standard})*1000/R_{sample}$, where R_{sample} stands for the absolute isotope ratio of the sample and $R_{standard}$ for the absolute isotope ratio of the highly ^{13}C-enriched Vienna Pee Dee Belemnite (VPDB) standard[32]. As just small differences on ^{13}C content are found between compounds, $\delta^{13}C$ values are given as per thousand.

The main source of carbon for plants is CO_2. Terrestrial C3, C4 and CAM plants differ in their mechanisms used for carbon fixation. While C3 plants undergo carbon fixation through the direct

delivery of CO_2 into the Calvin-Benson cycle by the ribulose bisphosphate carboxylase/oxygenase (RuBisCO) enzyme, C4 plants perform carbon fixation through the Hatch-Slack cycle. This pathway involves intracellular CO_2 fixation as HCO_3^- by phosphoenolpyruvate to generate malic acid, which will be then used as a source of carbon for RuBisCO. CAM plants, instead, can perform carbon fixation in different manners, analogous to either C3 or C4 plants[33]. Interestingly, the C3 pathway has been shown to discriminate against ^{13}C, giving rise to low $^{13}C/^{12}C$ ratios, such that C3 total leaf tissue has $\delta^{13}C$ values of -24 to -38 $^0/_{00}$. The C4 pathway, instead, discriminates less against ^{13}C, resulting in higher $^{13}C/^{12}C$ ratios, between -8 and - $16^0/_{00}$, whereas CAM plants present more variable ^{13}C abundances, with $\delta^{13}C$ values typically between -10 to $-34^0/_{00}$[34]. These characteristic ratios of ^{13}C incorporation have been attributed to the different diffusive fluxes of CO_2 containing different isotopes during the process of carbon assimilation[35], in some cases enabling the determination of fixation precursors and, thus, origin, based on ^{13}C content.

Within the same plant species, differences in isotope enrichment of metabolites biosynthesized through distinct pathways are also observed. For example, isotopic composition of FAs and the lipids containing them, derived from the acetogenic pathway, differ from isoprenoid lipids, such as sterols, whose biosynthesis proceeds through the mevalonic acid pathway and condensation of isopentyl pyrophosphate and dimethylallyl pyrophosphate units. VLCFA derivatives have been shown to be enriched in ^{13}C by 2.0-6.4$^0/_{00}$ compared to sterols. This variation on ^{13}C content has been principally attributed to different degrees of isotope discrimination exhorted by the different enzymes involved in each biosynthetic pathway[36].

Interestingly, different C-isotopic ratios have been observed for compounds within the same class, such as for different alkane homologs found in plant cuticular waxes. On C3 plants, alkanes present depletion on $\delta^{13}C$ values as chain length increases, typically ranging between $-35^0/_{00}$ for the short

homologs (C_{27}) to -38.9‰ for the longer homologs (C_{31}), but with high variation between plant species. In addition, alkanes and their derivate compounds, primary alcohols and fatty acids, present quasi-equal ^{13}C content for same chain lengths, indicative of their related biosynthesis[37]. Homologs differ exclusively in the number of cycles of elongation that the LCFA delivered by the plastids experience in the ER. Therefore, the differences on $^{13}C/^{12}C$ content between homologs must result from a characteristic C-isotope incorporation in each of these two cell compartments. Overall, lower ^{13}C values may be expected for those carbons incorporated in the ER as compared to the plastids, in agreement with the expected lower diffusional flux of heavy metabolites[34].

Based on these observations, determination of the ^{13}C content of barley β-diketones by GC-IRMS might be a useful approach to evaluate the relative content of plastidial versus ER carbon and, hence, to give insights on their biosynthesis. Here, in particular the $\delta^{13}C$ values of alkanes, alkan-2-ol and alkan-1-ol esters as well as β-diketones isolated from barley *cv.* Morex spike wax will be determined. Alkanes, based on their known biosynthesis, are the compounds with more ER carbon content as these are elongated from of plastidial C_{16} or C_{18} LCFAs to their corresponding chain lengths (C_{25} to C_{33}) in the ER. On the other hand, alkan-2-ol esters represent the wax compounds with lowest ER-carbon content, because they are formed combining a completely plastidial alkan-2-ol moiety with an acyl moiety largely originating from the plastid as well. Alkan-1-ol esters, instead, are formed by esterification of ER-elongated VLCFAs and very long chain alcohols, resulting in an intermediate ER C content. Therefore, analysis of the ^{13}C content in these compound classes can be used to assess their ER carbon content, and to compare against the ER carbon content of β-diketones. Ultimately, this may enable an evaluation whether β-diketone biosynthesis proceeds either via elongation or head-to-head condensation of BKFA with an acyl-

CoAprecursors, resulting either in a high ER ^{13}C content similar to alkanes or in a low ER carbon content similar to alkan-2-ol esters, respectively.

2.2 Materials and methods

2.2.1 Plant material

Hordeum vulgare cv. Morex seeds (NGB23015) were kindly provided by NordGen, Alnarp, Sweden. Seeds were germinated at room temperature in petri dishes equipped with humidified filter papers for one week. Seedlings grown to around 5 cm were then transferred into plastic pots of 40 cm of diameter containing moistened Sunshine Mix #4 (Sun Gro Horticulture Canada) soil and grown in a growth chamber at The University of British Columbia under 16 hours of light at 21°C and for 8 hours at 19°C in the dark, at 70% relative humidity. After 85 days, plants reached maturity with a fully developed spike, flag leaf and six vegetative leaves. Plants were harvested and dissected at this point, collecting flag leaf sheaths and spikes from which awns were selectively removed. Three independent samples were generated, each by pooling approximately 30 spikes or 30 flag leaf sheaths.

2.2.2 Plant wax extraction

Wax extraction was carried out immediately after the organs were harvested by immersion in $CHCl_3$ twice for 30 seconds, then both $CHCl_3$ fractions were combined and solvent was concentrated under a gentle stream of N_2 gas while heating to 50°C. Concentrated samples were then either transferred into GC autosampler vials with a 250 µl insert for further derivatization, or into 50 ml vials for further TLC purification.

2.2.3 TLC purification of extracted wax mixtures

Crude waxes extracted from barley *cv*. Morex spikes and flag leaf sheaths were purified by TLC. A plate of 0.25 mm thickness (Analtech) was loaded with crude waxes and developed with $CHCl_3$:hexane (1:1). TLC plates were then sprayed with a solution of primuline (1% in acetone) and bands were visualized under UV light (365 nm). Selected bands were scratched from the plate, and wax was extracted from the silica with $CHCl_3$. Extracts were passed through filter paper to remove any silica, and purified extracts were concentrated under a gentle N_2 flow and transferred into GC vials containing a 250 µl insert for GC-MS or GC-IRMS carbon isotopic analysis.

2.2.4 Derivatization reactions

TLC-purified hydroxy-β-diketones were converted into the respective triols by $LiAlH_4$ reduction. For this, wax samples were dissolved in 1 ml of diethyl ether, inside a 2 ml vial, before 10 mg of $LiAlH_4$ (Sigma-Aldrich) were added. The mixture was left to react at room temperature for one hour, then the reaction was quenched with 500 µl of H_2SO_4 (10%) and extracted with diethyl ether (3 x 1 ml). The organic fractions were combined, dried under a gentle N_2 flow and TMS-derivatized as described below.

Wax samples were derivatized prior to GC-MS analysis by conversion into the corresponding TMS derivatives. Dried wax contained in autosampler vial inserts were dissolved in 10 µl of pyridine (Sigma Aldrich) and 10 µl of bis-N,O trimethylsilyltrifluoroacetamide (BSTFA) (Sigma- Aldrich), and the mixtures were incubated at 70°C for 45 min. Excess derivatization reagents were then evaporated under a stream of N_2 gas, and the dry residue was dissolved in 200 µl of $CHCl_3$.

2.2.5 GC-MS analysis of wax samples

Wax samples were analyzed on an Agilent 6890N GC equipped with an on-column injector and a HP-1 capillary column (30 m x 0.32 mm, 1 µm film thickness) and coupled with an Agilent 5793N Mass Selective Detector. Sample was injected into the GC with a He flow through the column of 1.4 ml/min and the oven set to 50ºC. After 2 min the temperature was ramped to 200ºC with a gradient of 40°C/min, the temperature was held for 2 min, raised to 320ºC at 3ºC/min, and then held for 30 min. GC-eluted analytes were detected on the MS detector equipped with an electron impact ionization source working at 70 eV, and ions were detected at 1 scan/second in the range of m/z 50-800.

2.2.6 Compound-specific carbon isotopic analysis (in collaboration with Dr. Sarah Feakins)

Compound-specific carbon isotopic values were obtained using a Thermo Scientific Trace GC equipped with a Rxi-5ms column (30 m x 0.25 mm, 0.25 µm film thickness) and a programmable temperature vaporizing injector operated in solvent split mode was used. The GC was connected via a GC Isolink with a combustion furnace at 1000°C via a Conflo IV interface to a DeltaVPlus isotope ratio mass spectrometer. To check for stability and linearity, the CO_2 reference gas was analyzed daily with a standard deviation of < 0.06‰. Six reference peaks of CO_2 bracket analyte peaks during the course of a GC-IRMS run; two were used for standardization, the rest were used to monitor stability. Samples were interspersed with standard compound mixtures of known isotopic composition. Data were normalized to the VPDB carbon isotopic scale by comparing with

an external standard (A6mix) obtained from A. Schimmelmann, Indiana University, Bloomington, containing 15 alkane compounds (C_{16} to C_{30}), with $\delta^{13}C$ values spanning −33.34 to −26.15‰.

2.2.7 Synthesis of authentic standards

2.2.7.1 Hexadecanal

1 g of hexadecanol (Sigma-Aldrich) was dissolved in 30 ml of CH_2Cl_2 to which 1.5 g of Dess Martin Periodinane (1.5 eq) (Sigma-Aldrich) were added. The mixture was stirred at room temperature until the reaction was found to be completed by monitoring it by TLC ($CHCl_3$ mobile phase). Then, excess reagent was quenched by adding 5 ml of saturated $Na_2S_2O_3$, products were extracted with CH_2Cl_2 (3x 10 ml). Organic fractions were combined and washed with saturated NaH_2CO_3 (10 ml) and H_2O (10 ml), then dried with Na_2SO_4 and concentrated in vacuum. The resulting solid was purified by column chromatography (100% $CHCl_3$). MS analysis of the purified solid revealed that it consisted of hexadecanal, obtained with a 86% yield. The solid was then directly used in the next reaction.

2.2.7.2 16-hydroxy hentriacontane-14-one

0.7 g of pentadecan-2-one were dissolved in 11.5 ml of a 0.1 M lithium diisopropylamide solution in tetrahydrofuran (Sigma-Aldrich), and the mixture was stirred in an ice bath for ten minutes. Then, 0.8 g of hexadecanal (Section 2.2.7.1) dissolved in 2 ml freshly distilled tetrahydrofuran were added, and the reaction mixture was stirred for one hour. Finally, the reaction was quenched by the addition of 5 ml of 20% H_2SO_4, the products were extracted with CH_2Cl_2 (3x 20 ml), the organic fractions were combined and washed with saturated NaH_2CO_3 (10 ml) and H_2O (10 ml),

then dried with Na_2SO_4, and the solvent was evaporated under vacuum. The resulting solid was purified by column chromatography (1:1 hexane:$CHCl_3$). MS analysis of the purified solid revealed that it consisted of 16-hydroxy-hentriacontan-14-one, obtained with a 52% yield. The solid was directly used in the next reaction.

2.2.7.3 Hentriacontane-14,16-dione

In an acetone/dry ice CO_2 bath, 0.5 ml of 1 M oxalyl chloride (5 eq) (Sigma-Aldrich) were added into 2 ml of CH_2Cl_2 and allowed to cool down. Then, 150 µl of dimethyl suloxide (2 eq) were slowly added (3 x 50 µl). When the elution of gas ceased, 0.2 g of 16-hydroxy hentriacontane-14-one (Section 2.2.7.2) dissolved in 3 ml of CH_2Cl_2 were added drop-wise. The reaction mixture was allowed to return to room temperature by removing it from the acetone/dry ice CO_2 bath, then 0.3 ml of Et_3N (5 eq) were added. The resulting solid was re-dissolved by the addition of 5 ml of H_2O, and the reaction products were extracted with CH_2Cl_2 (3x 20 ml). The organic fractions were combined, washed with diluted HCl (10 ml) and H_2O (10 ml), and then dried with Na_2SO_4. Finally, the solvent was evaporated under vacuum, and the resulting solid was purified by column chromatography (3:1 hexane:$CHCl_3$). MS analysis of the purified solid revealed that it consisted of hentriacontane-14,16-dione. Reaction resulted into discrete yields below 8%.

2.3 Results

2.3.1 Identification of β-diketone homologs and isomers in waxes from barley *cv.* Morex flag leaf sheaths and spikes

Exhaustive analysis of the different β-diketone homologs and isomers was performed in two organs known to contain this compound class, spikes (minus awns) and flag leaf sheaths. TLC purification of the crude wax resulted in a band at Rf=0.56 containing β-diketones. Initial identification of this compound class was performed based on comparison of the MS fragmentation pattern and GC retention time (Rt) of the predominant β-diketone with those of a synthetic standard of hentriacontane-14,16-dione (Rt=25.8 min). β-diketones were analyzed by GC-MS with no previous derivatization. GC conditions allowed the separation of the different homologs but not the isomers.

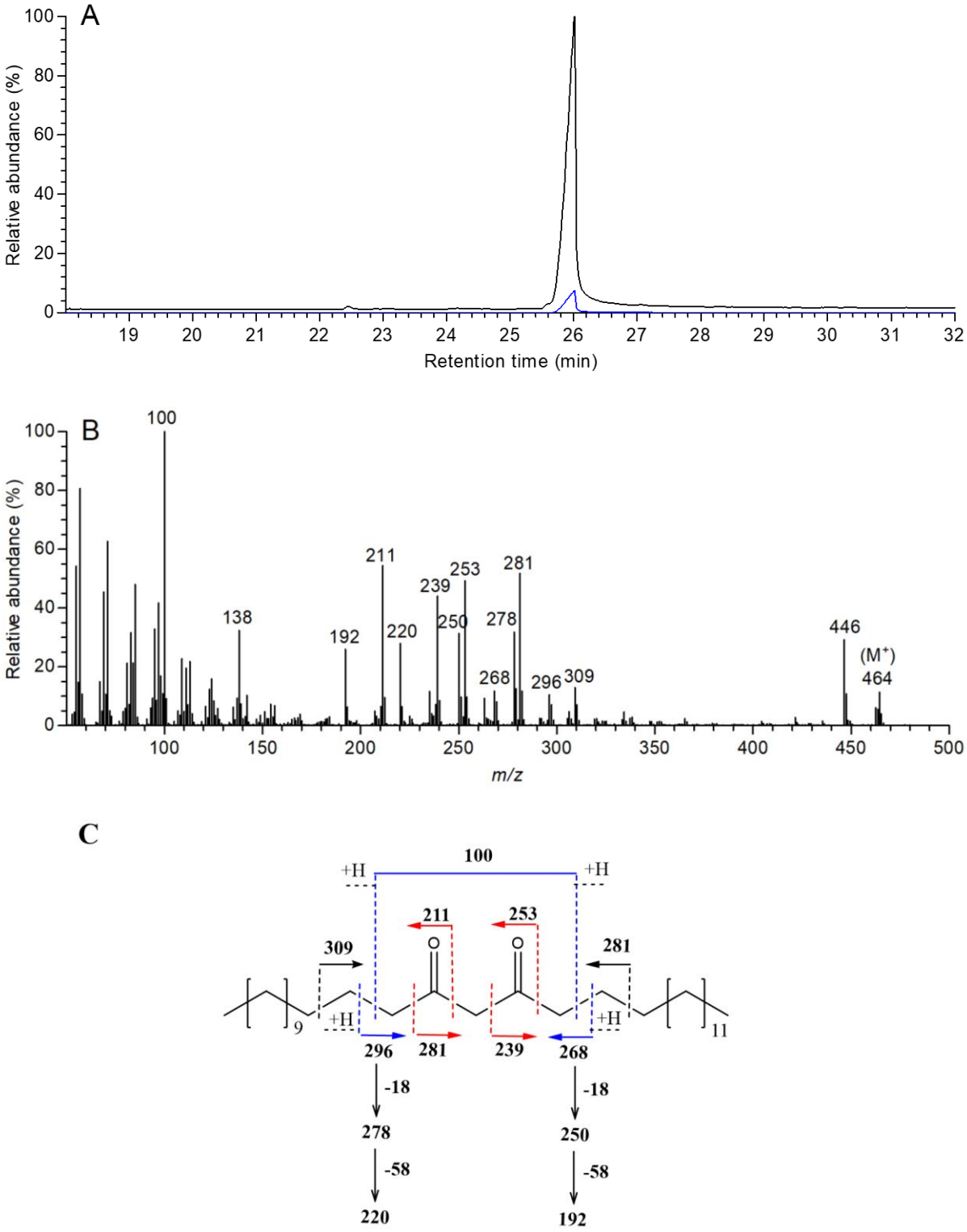

Figure 2.1: **GC-MS analysis of the hentriacontane-14,16-dione authentic standard. A.** Overlapped total ion (black) and *m/z* 100 extracted ion (blue) chromatograms and **B.** mass spectrum. **C.** Schematic showing of the proposed assignment for the major fragments of hentriacontane-14,16-dione.

All other compounds accompanying hentriacontane-14,16-dione in the TLC fraction were identified as β-diketones based on their similar mass spectral characteristics. In particular, they all shared a base peak *m/z* 100 characteristic of this compound class, corresponding to two consecutive McLafferty rearrangement at both carbonyl groups. Fragment ions resulting from the four possible α-cleavages next to the two carbonyl groups were found to be the second most abundant type of fragments. In addition, the two possible fragments resulting from single McLafferty rearrangement were also observed. These were found to undergo further fragmentation, resulting in loss of one molecule each of water (Δ*m/z* -18) and acetone (Δ*m/z* -58). The molecular ion (M^+) was present at very low abundance, accompanied by an ion M^+-18 with higher intensity. In addition, a fragment *m/z* 138 was detected for all β-diketones, indicating that this is a further fragment diagnostic of the β-diketo group. Even though identity of *m/z* 138 could not be assigned rationally, this is most likely the result of the decomposition of the fragments formed by single McLafferty rearrangement[27] (Figure 2.1).

Overall, the signature ion *m/z* 100 was found optimal for monitoring the abundance of different β-diketone homologs, while combinations of M^+ and M^+-18 allowed chain length determination, and α-fragments could be used for isomer identification as well as for quantification.

The TLC fraction containing the β-diketones isolated from spike wax was almost entirely composed of hentriacontane-14,16-dione. A homolog eluting at 23.1 min was identified as a homolog two carbons shorter containing two isomers, nonacosane-12,14-dione and nonacosane-14,16-dione. In addition, a homolog two carbons longer with Rt=28.2 min was identified as the symmetric tritriacontane-16,18-dione, occurring as a single isomer. Interestingly, small amounts of two even-carbon-numbered diketones were also found in the fraction, with C_{30} (Rt=24.5 min) and C_{32} chains (Rt=27.0 min). Their mass spectra revealed that the C_{30} homolog contained a single

isomer, identified as triacontane-14,16-dione, whereas the C_{32} homolog comprised two different isomers, dotriacontane-14,16-dione and dotriacontane-15,17-dione (Figure 2.2).

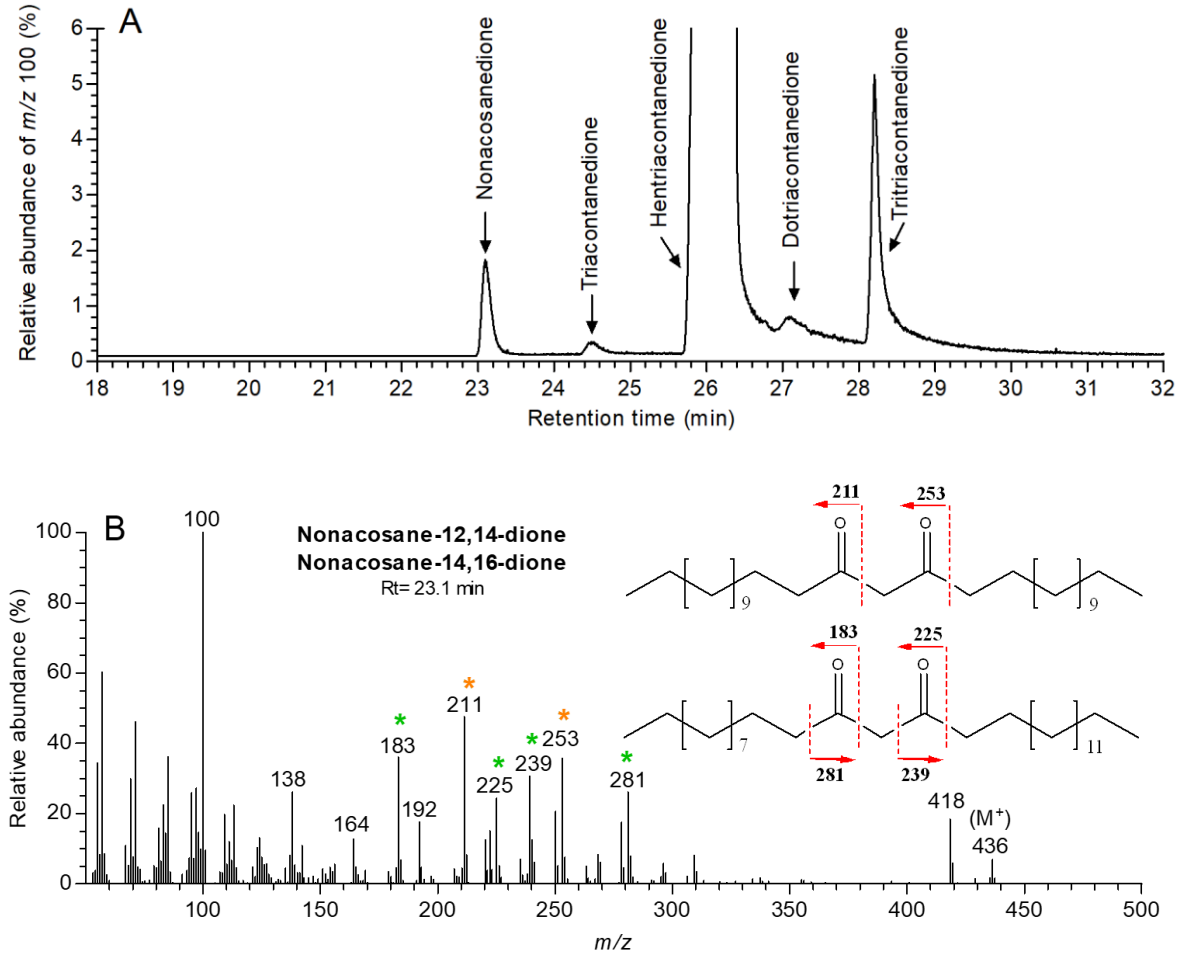

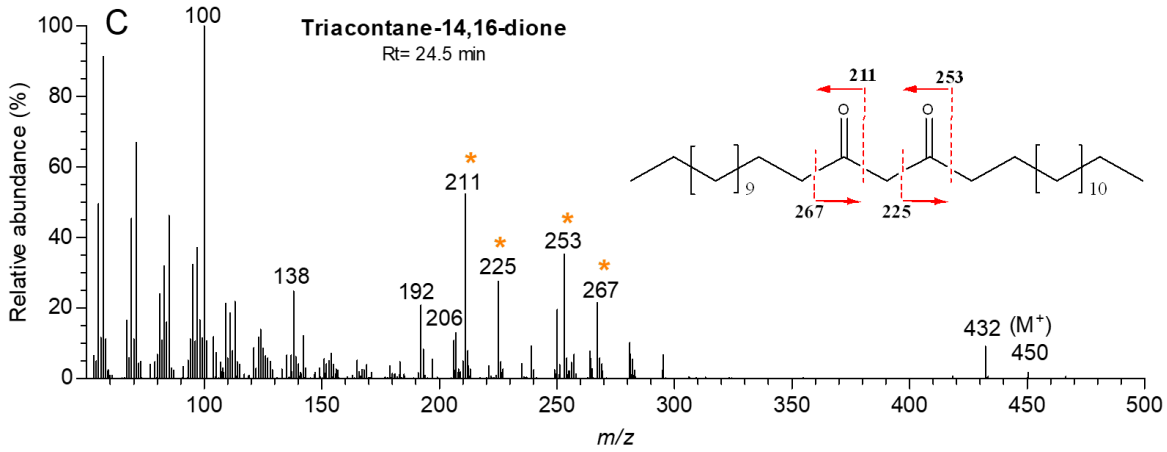
C
Triacontane-14,16-dione
Rt= 24.5 min
Relative abundance (%)
m/z
100
211
253
225
267
138
192
206
432 (M+)
450
9
10

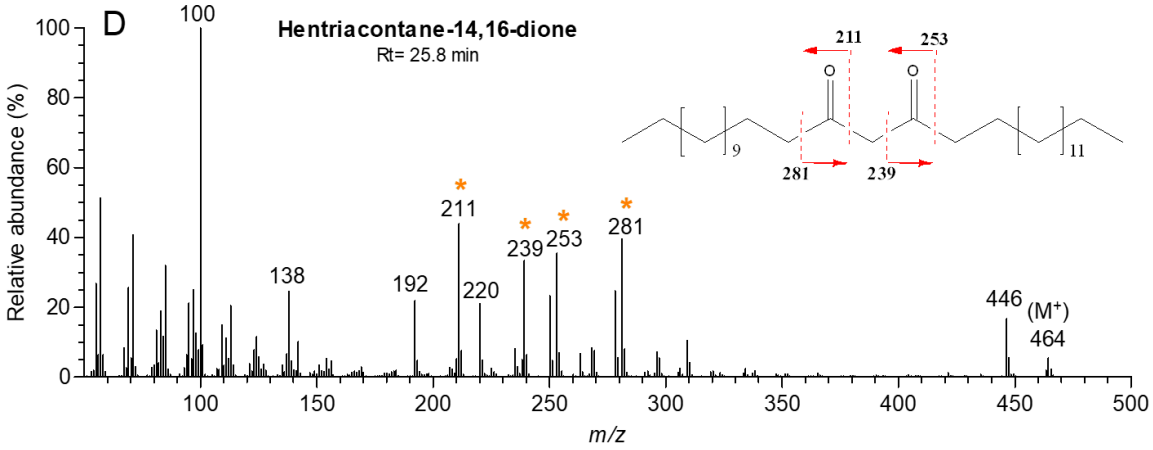
D
Hentriacontane-14,16-dione
Rt= 25.8 min
Relative abundance (%)
m/z
100
211
253
239
281
138
192
220
446 (M+)
464
9
11

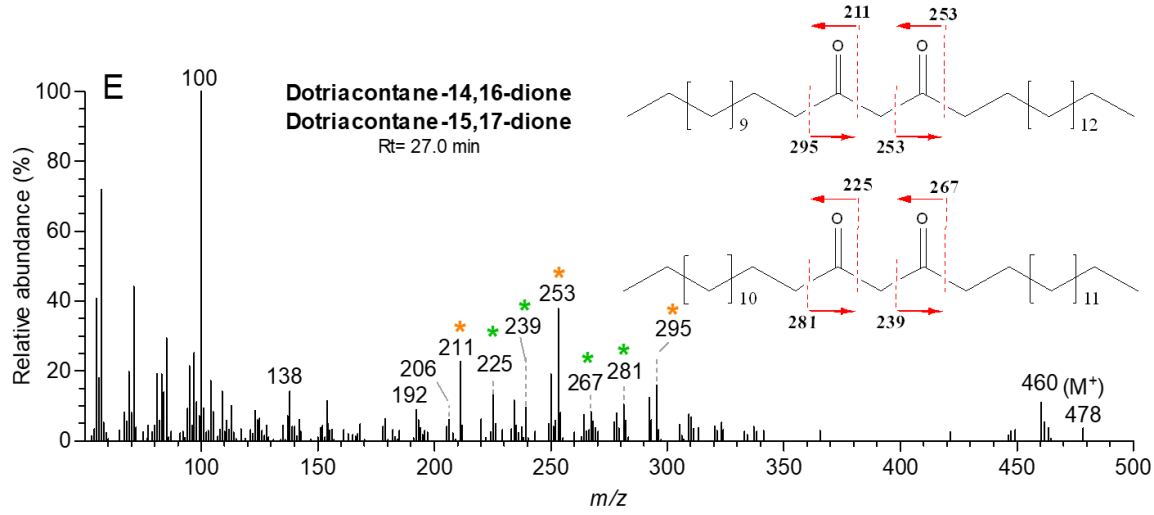
E
Dotriacontane-14,16-dione
Dotriacontane-15,17-dione
Rt= 27.0 min
Relative abundance (%)
m/z
100
211
253
225
267
239
295
281
138
206
192
460 (M+)
478
9
12
10
11

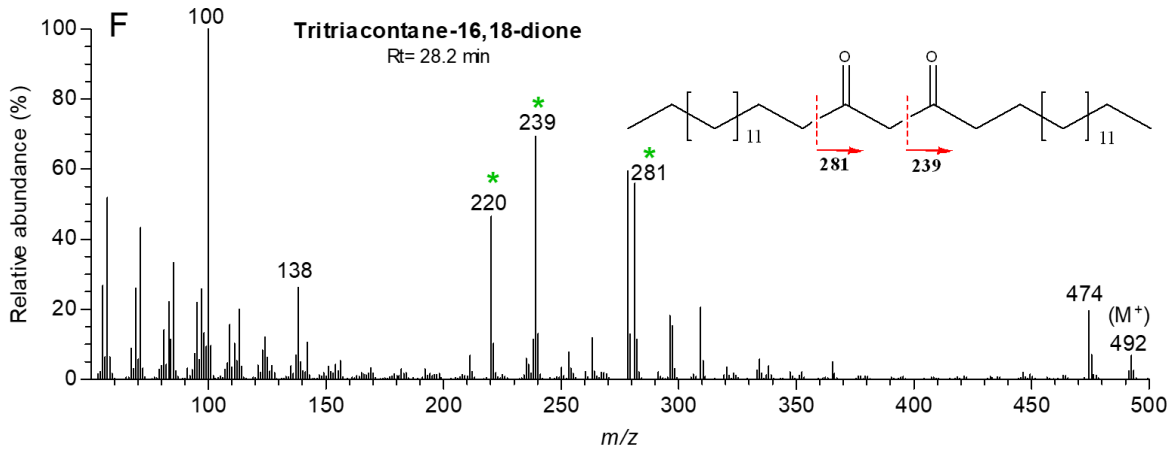

Figure 2.2: **GC-MS analysis of the TLC fraction containing β-diketones from barley *cv.* Morex spike wax. A.** *m/z* 100 extract ion chromatogram. Mass spectra of **B.** Nonacosanedione, composed of the two isomers nonacosane-12,14-dione and nonacosane-14,16-dione. **C.** Triacontanedione represented a single isomer, triacontane-14,16-dione. **D.** Hentriacontanedione as hentriacontane-14,16-dione **E.** Dotriacontanedione contained dotriacontane-14,16-dione and dotriacontane-15,17-dione. **F.** Tritriacontanedione occurred as tritriacontane-16,18-dione. Fragments corresponding to α-cleavage have been starred. Fragments corresponding to 14,16 isomers are indicated in green, the rest of the isomers in orange.

IUPAC convention mandates that β-diketones are named such that functional group positions are given counting carbons from the shorter alkyl end of the molecule. However, the suggested biosynthesis of β-diketones from, mainly, C_{16} FA (or C_{18} BKFA) involves elongation in the inverse direction of International Union of Pure and Applied Chemistry (IUPAC) nomenclature (Figure 2.3). Hence, an abbreviated nomenclature including IUPAC nomenclature and, in brackets, diketone group position counting from the opposite end of the molecule will be used in this thesis (Table 2.1).

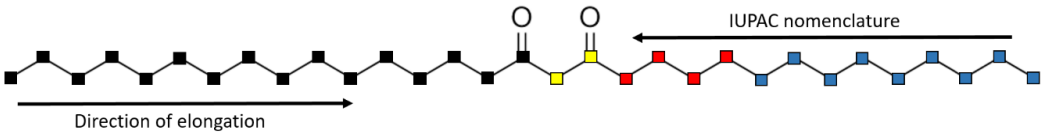

Figure 2.3: **Structure of hentriacontane-14,16-dione.** Carbon atoms originating from the C_{16} fatty acid precursor are indicated in black, carbons in yellow correspond to the single addition of a malonyl-CoA unit involving *Hv*DMH. In red are indicated the two malonyl-CoAs introduced by *Hv*DMP. Blue are carbons introduced during the further elongation by a FAE complex, with the exception of the carbon lost during decarboxylation of the elongated β-diketo fatty acid. The adapted nomenclature considers the position of both keto groups starting from the end of the molecule incorporating the BKFA precursor.

Table 2.1: **IUPAC nomenclature and the adapted nomenclature of the different homologs and isomers detected in barley *cv*. Morex wax.**

Homolog	IUPAC nomenclature	Adapted nomenclature
C_{29}	Nonacosane-12,14-dione	C_{29} 12,14-diketone (C_{29} 16,18-diketone)
	Nonacosane-14,16-dione	C_{29} 14,16-diketone
C_{30}	Triacontane-14,16-dione	C_{30} 14,16-diketone (C_{30} 15,17-diketone)
C_{31}	Hentriacontane-14,16-dione	C_{31} 14,16-diketone (C_{31} 16,18-diketone)
C_{32}	Dotriacontane-14,16-dione	C_{32} 14,16-diketone (C_{32} 17,19-diketone)
	Dotriacontane-15,17-dione	C_{32} 15,17-diketone (C_{32} 16,18-diketone)
C_{33}	Tritriacontane-16,18-dione	C_{33} 16,18-diketone

Quantification of the different isomers within each β-diketone homolog was performed based on the abundance of their shortest characteristic α-fragments, as these did not interfere with other fragments. Accordingly, fragment *m/z* 183 was used to quantify C_{29} 12,14-diketone (C_{29} 16,18-diketone), fragment *m/z* 211 for C_{29} 14,16-diketone, C_{30} 14,16-diketone (C_{30} 15,17-diketone), C_{31} 14,16-diketone (C_{31} 16,18-diketone) and C_{32} 14,16-diketone (C_{32} 17,19-diketone), fragment *m/z* 225 for C_{32} 15,17-diketone (C_{32} 16,18-diketone) and *m/z* 239 for C_{33}16,18-diketone. The homolog C_{29} was found to consist of 42% C_{29} 12,14-diketone (C_{29} 16,18-diketone) and 58% C_{29} 14,16-diketone, and the C_{32} homolog comprised 72% C_{32} 14,16-diketone (C_{32} 17,19-diketone) and 28%

C_{32} 15,17-diketone (C_{32} 16,18-diketone), whereas the other homologs existed as single isomers (Table 2.2).

Table 2.2: **Comparison between spike and flag leaf sheath abundance of each homolog and their isomers.**

	% within homolog		% within compound class	
Compound	**Flag leaf sheath**	**Spike**	**Flag leaf sheath**	**Spike**
C_{29} 12,14-diketone (C_{29} 16,18-diketone)	56.1	41.7	0.3	0.3
C_{29} 14,16-diketone	43.9	58.3	0.2	0.4
C_{30} 14,16-diketone (C_{30} 15,17-diketone)	100.0	100.0	0.2	0.1
C_{31} 14,16-diketone (C_{31} 16,18-diketone)	100.0	100.0	99.0	96.4
C_{32} 14,16-diketone (C_{32} 17,19-diketone)	76.1	71.6	0.1	0.2
C_{32} 15,17-diketone (C_{32} 16,18-diketone)	23.9	28.4	0.1	0.1
C_{33} 16,18-diketone	100.0	100.0	0.4	2.6

The β-diketones of flag leaf sheath wax were analyzed using the same methods, resulting in identification of the same five homologs comprising the same seven isomers. Differences were exclusively found for the relative abundance of homologs, with the predominant β-diketone, C_{31} 14,16-diketone (C_{31} 16,18-diketone) accumulating more in the flag leaf sheaths than the spikes and C_{29} 14,16-diketone and C_{33} 16,18-diketone slightly less on the flag leaf sheath (Figure 2.4).

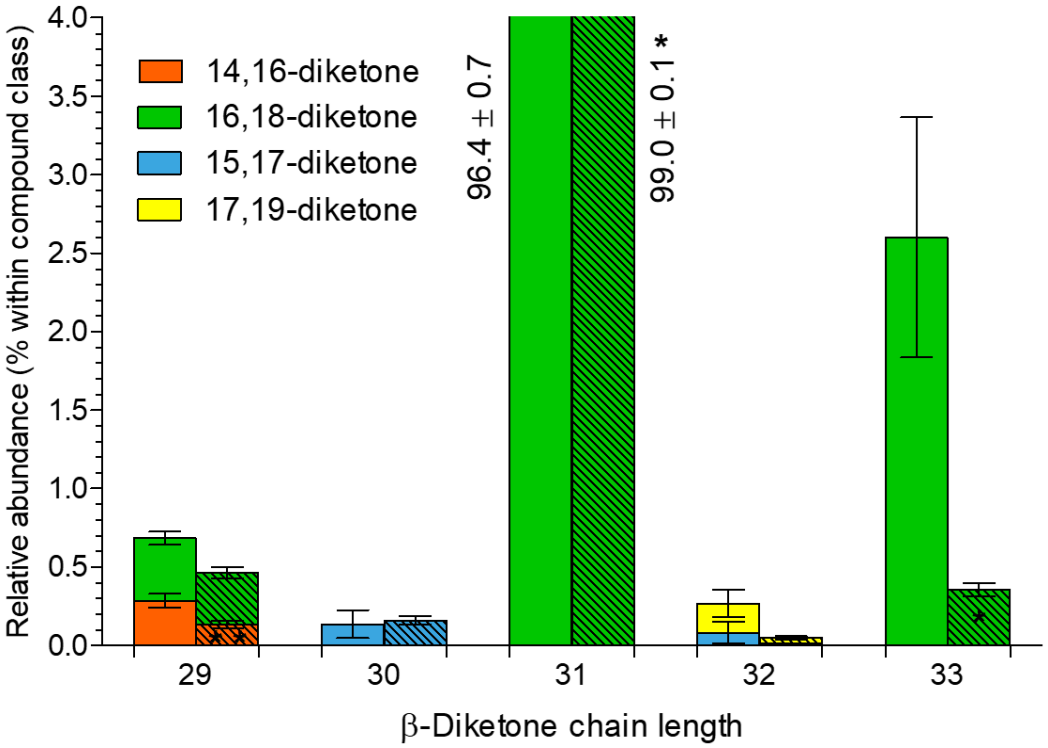

Figure 2.4: **Homolog and isomer distribution among the β-diketones isolated from barley *cv.* Morex spikes (plain bars) and flag leaf sheaths (dashed bars) cuticular wax.** Isomer nomenclature refers to the assumed direction of biosynthesis and, hence, indicates the length of the BKFA precursor. n=3 biological replicates. Error bars represent standard deviation.*p<0.05, **p<0.01.

The presence of different homologs and isomers for the hydroxy-β-diketones in the barley *cv.* Morex spike cuticular wax was also investigated. Analysis of the BSTFA-derivatized TLC fraction (Rf= 0.1) containing the hydroxy-β-diketones revealed mainly C_{31} homolog, accompanied by small amounts of C_{33} and C_{29}. Under the derivatization conditions used here, just derivatization of the hydroxyl group occurred. GC-MS spectra of the hydroxy-β-diketone TMS ethers showed two prominent peaks due to α-cleavage at both sides of the hydroxyl group, along with fragment ions from α-cleavage at the carbonyl groups in much lower abundance. This fragmentation pattern enabled determination of the homolog chain length as well as the distance of the hydroxyl group from the CH_3-terminal of the molecule and its possible isomerism. In addition, identification of

the position of the β-diketone group could also be achieved, however the low abundance of the ions from α-cleavage at the carbonyl groups made it difficult to determine the presence of possible minor components. Therefore, the position of the hydroxyl and carbonyl groups was corroborated by GC-MS analysis of the corresponding triol, generated by $LiAlH_4$ reduction of the hydroxy-β-diketones and analyzed in the form of the triol-TMS derivative (Figure 2.5).

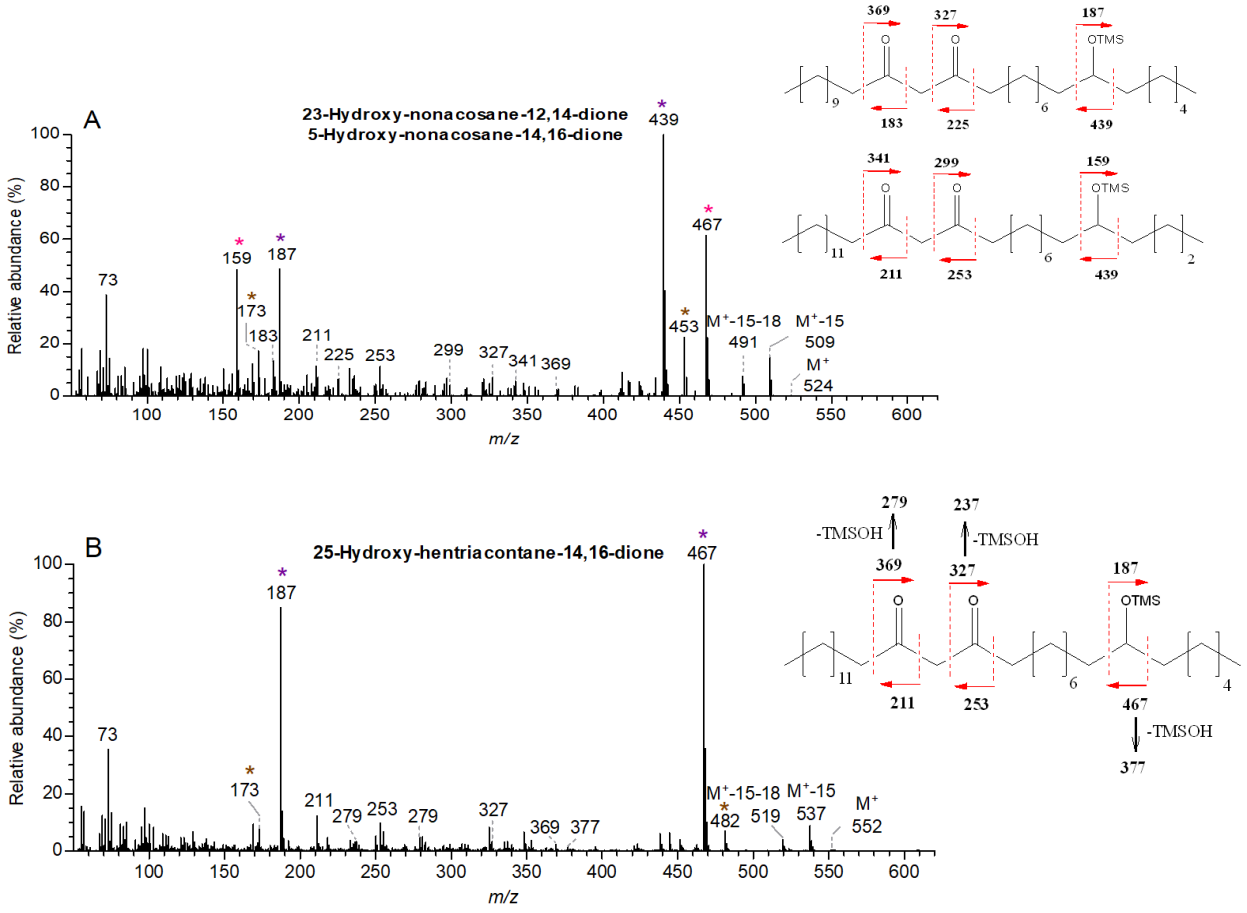

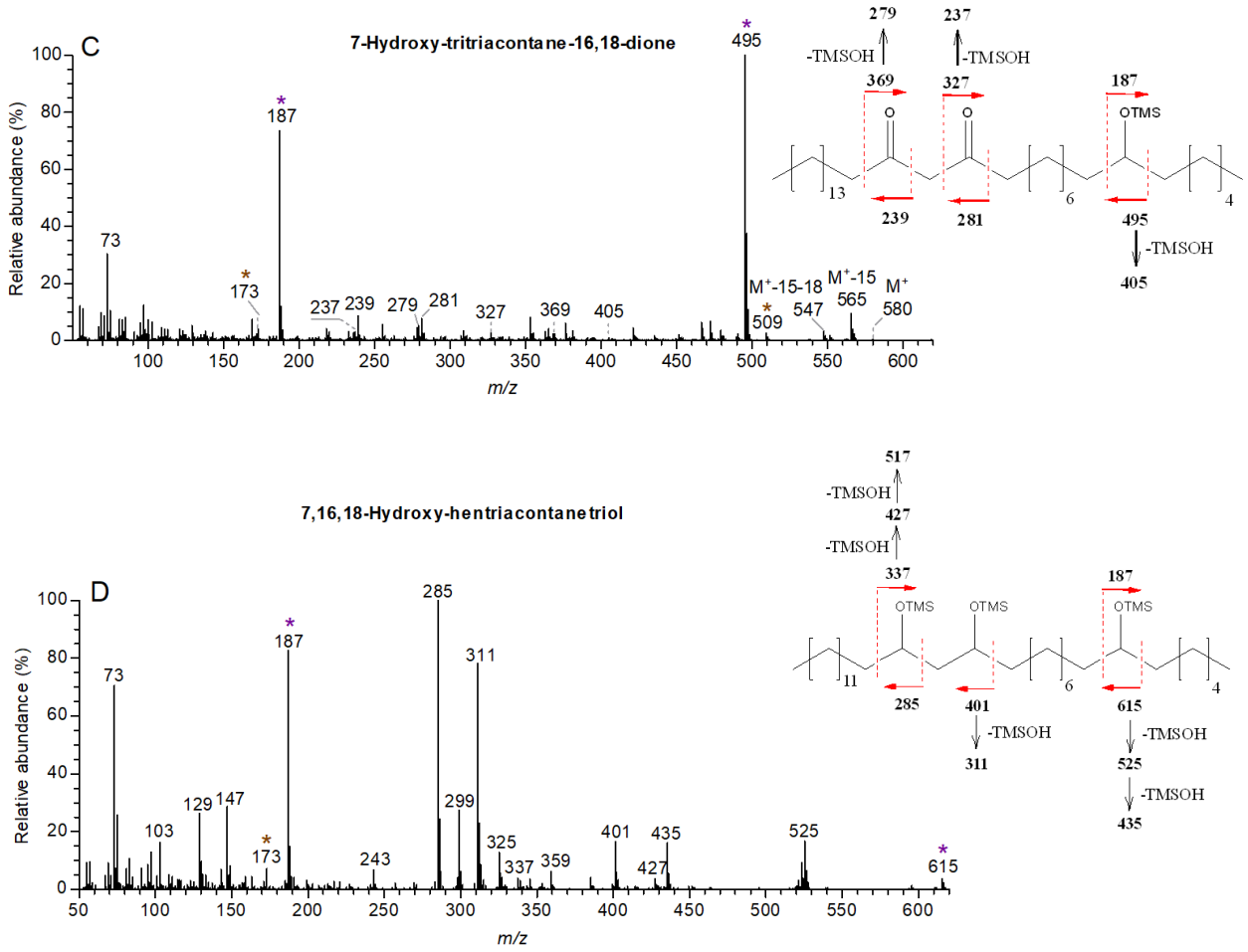

Figure 2.5: **Mass spectra of TMS-derivatized hydroxy-β-diketone homologs A.** C_{29}, **B.** C_{31} and **D.** C_{33}. **E.** Mass spectrum of the triol-TMS derivative of the C_{31} homolog. Inserts show the molecular structures and the proposed fragmentation patterns of the predominant isomers. Fragments resulting from α-cleavage at the hydroxyl group have been starred. Purple, brown and pink asterisks indicate fragments originating from isomers presenting the hydroxyl group on C-7, C-6 and C-5, respectively. M^+-15 fragments corresponds to the loss of a methyl group. M^+-15-18 fragments corresponds to the consecutive loss of a methyl group and a molecule of water, respectively.

The predominant hydroxy-β-diketone was found to be 25-hydroxy-hentriacontane-14,16-dione, with small amounts of 24-hydroxy-hentriacontane-14,16-dione detected based on the mass spectrum of its TMS derivative. These structure assignments were further corroborated by the analysis of the triol-TMS derivative, indicating that both methods permitted the determination of the structure for this homolog. However, the low amounts of the C_{29} and C_{33} homologs did not

allow their detection after conversion into triols. Hence, identification of the possible isomers for the rest of the homologs was exclusively based on interpretation of the mass spectra of the hydroxy-β-diketone TMS derivatives. The C_{29} homolog, was constituted of two isomers respective to the β-diketone group found in similar abundance. The combination of the two isomers shown equal hydroxylation on C-23 (or C-7) and C-21 (or C-5), and to lesser extent on C-22 (or C-6). Despite the low abundance of their characteristic α-fragments, 5-hydroxy-nonacosane-14,16-dione and 23-hydroxy-nonacosane-12,14-dione could be detected, however, it could not be ruled out if in lower extent other isomers respective to the β-diketone group and hydroxylated on carbons with analogous distances, were present. The longer homolog, thanks to the equal length of acyls on either side of the carbonyls, could be unambiguously identified as 7-hydroxy-tritiacontane-16,18-dione, accompanied by small amounts of 6-hydroxy-tritiacontane-16,18-dione (Table 2.3).

Table 2.3: **Hydroxy-β-diketone composition in spike wax of barley *cv.* Morex**

Homolog chain length	% within compound class	Hydroxyl position* within the homolog (%)		
		7	6	5
C_{29}	0.8	42.5	15.1	42.4
C_{31}	96.2	91.8	8.2	-
C_{33}	2.9	95.0	5.0	-

* Position of the hydroxyl group is given by its distance from the closest end of the molecule.

The alkan-2-ol esters were detected in the same TLC fraction as the alkan-1-ol esters, with Rf= 0.73. They were identified based on MS fragmentation as reported before[4], with prominent ions derived from the McLafferty rearrangement occurring on the alcohol side of the carbonyl, and further fragmentation resulting from either a single hydrogen migration or loss of water. In

addition, an alkene fragment resulting from acid elimination was found to be characteristic for the alcohol moiety. The molecular ion, however, could not be observed (Figure 2.6).

Under the GC conditions used, alkan-2-ol and alkan-1-ol ester homologs were all baseline-separated, however without isomer separation. Three alkan-2-ol esters were identified, with total carbon numbers of C_{33}, C_{35} and C_{37} at retention times of 22.6, 26.0 and 29.4 min, respectively. A single even-numbered homolog, C_{36}, was found eluting at 27.7 min. The C_{35} homolog was found to be predominant, accounting for 58.5% of the alkan-2-ol esters, along with 8.3, 30.3 and 2.9% of the C_{33}, C_{37} and C_{36} homologs, respectively. Together, the alkan-2-ol esters contributed 14.0% to the total ester fraction.

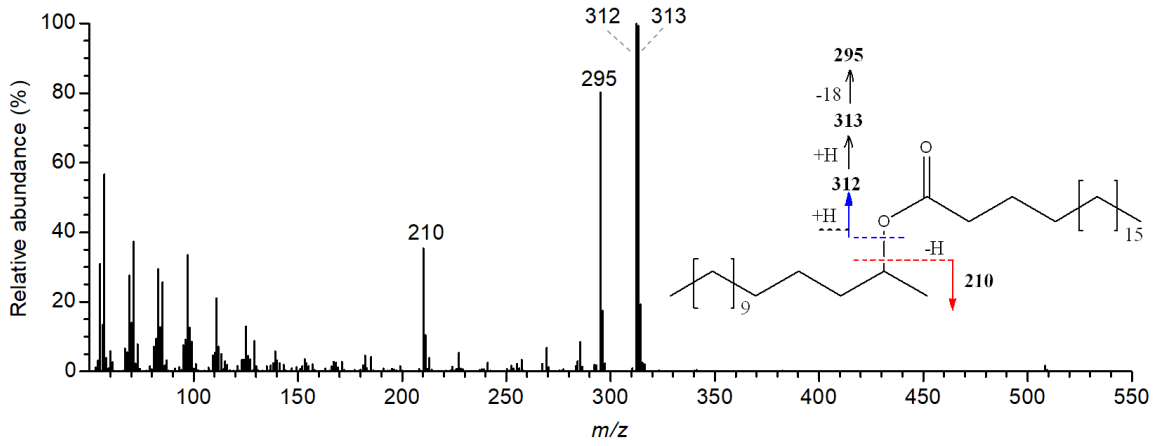

Figure 2.6: **Mass spectrum of the C_{33} alkan-2-ol ester homolog found in barley *cv.* Morex spike wax.**

The distributions of esterified fatty acids and alkan-2-ols within respective ester homologs were determined based on the abundance of the fragments characteristic of the fatty acid moiety (resulting from McLafferty rearrangement and further fragmentation effecting a mass shift $\Delta m/z$ -17) found not to interfere with other fragment ions. Thus, the C_{33} ester was found composed of C_{13} and C_{15} alkan-2-ol esterified with C_{18} and C_{20} acid, respectively. The C_{35} and C_{36} esters consisted

of single isomers, with C_{15} alkan-2-ol esterified with C_{20} or C_{21} acid, respectively, whereas C_{37} ester comprised two isomers, consisting on C_{15} and C_{17} alkan-2-ols esterified with C_{22} and C_{20} acids, respectively.

Multiplication of the isomer percentages within each homolog with the homolog abundances gave the abundance of esterified acids and alcohols across all alkan-2-ol ester homologs. Overall, C_{15} alkan-2-ol was found to be most abundant, whereas a range of acids between C_{18} and C_{22} were present, with C_{20} dominating (Figure 2.7, Table A.1)

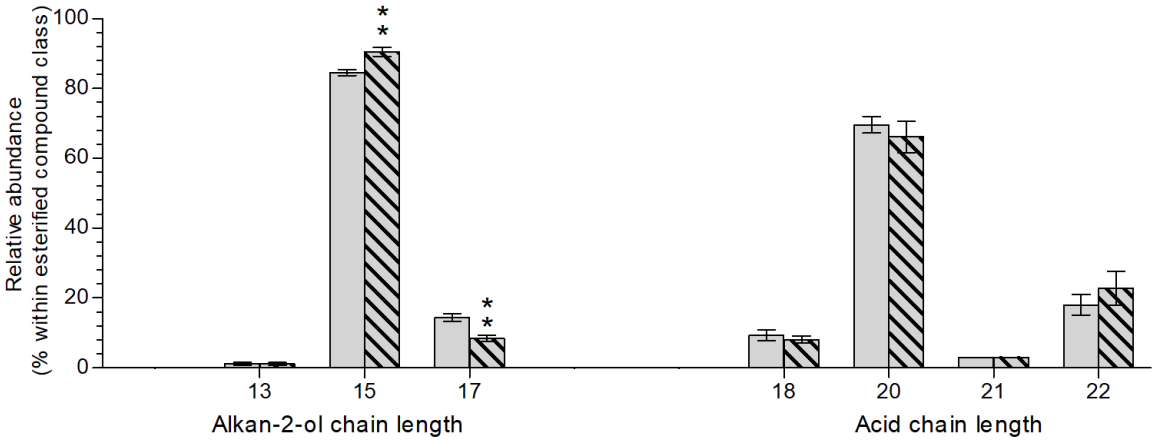

Figure 2.7: **Relative amounts of alcohol and acid moieties in the alkan-2-ol esters of barley *cv.* Morex flag leaf sheath (plain bars) and spike (dashed bars) waxes.** n=3 biological replicates, error bars represent standard deviation. **p<0.01

2.3.2 Isotopic composition of barley *cv.* Morex wax compounds

The relatively homogenous distribution of the different compound classes previously reported in barley spike wax, as compared to other β-diketone-containing waxes on other organs, led to the choice of this organ for performing ^{13}C isotopic ratio analysis among the different homologs and compound classes. Alkanes, esters (of alkan-1-ols and alkan-2-ols) and β-diketones were the primary targets for GC-IRMS analysis, since GC analysis of other compounds including alcohols

or hydroxy-β-diketones would require TMS derivatization with special isotope-depleted reagents in order to achieve a good chromatographic separation.

TLC purification of barley *cv.* Morex spike crude wax yielded a fraction containing the alkanes (Rf= 0.94), which together with the fraction containing the esters was used for comparison with the fraction containing β-diketones. Initially, these fractions were analyzed by GC-MS in order to determine homolog and isomer distributions. Alkanes were identified using authentic standards and homologs assigned based on retention times and molecular ions in the mass spectra. The alkane fraction comprised homologs ranging from C_{23} to C_{33} , with C_{31} predominant, along with trace amounts of even-numbered compounds from C_{26} to C_{30} (Figure 2.8).

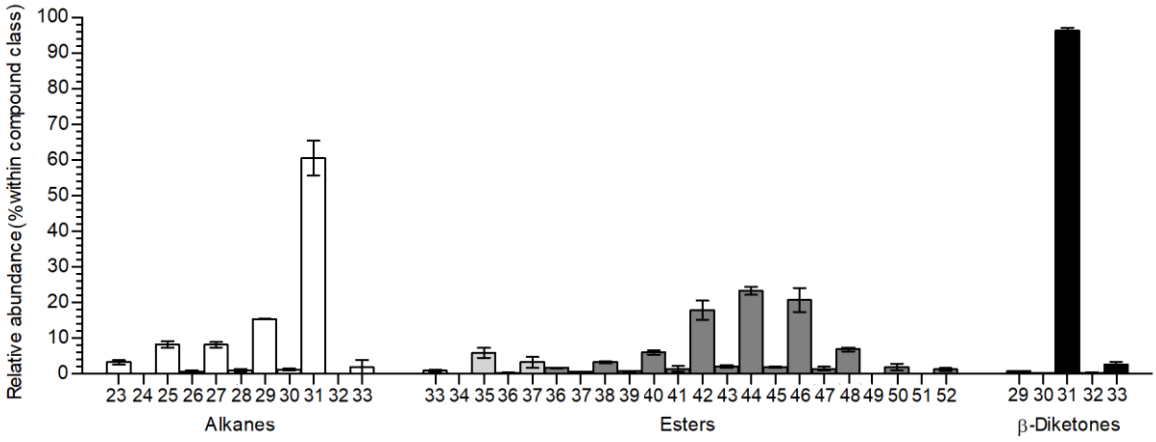

Figure 2.8: **Relative composition of the three fractions isolated by TLC purification of barley *cv.* Morex spike crude wax.** n=3. Error bars represent standard deviation. Alkan-2-ol esters are indicated in light grey. n=3 biological replicates, error bars represent standard deviation.

The ester fraction contained alkan-2-ol esters as described above. The accompanying alkan-1-ol esters were analyzed by GC-MS, such that the CG conditions allowed separation of the different homologs but not isomers. However, the ester mass spectra presented fragments corresponding to the McLafferty rearrangement plus hydrogen transfers similar to those observed for the alkan-2-

ols, indicative of the acyl moieties present and thus enabling direct quantification of the acyl chain length profiles within each ester homolog. Alcohol-characteristic fragments could not be detected, in accordance with previous reports on wax esters of primary alcohols[38]. Nevertheless, the chain length of the alcohol moiety in each ester homolog could be determined based on the known overall chain length of the ester, confirmed by abundant molecular ions, and the acid moieties present.

The ester fraction contained alkan-1-ol esters ranging from C_{38} to C_{52}, with the C_{44} homolog dominating. Odd-numbered alkan-1-ol esters were also found in small amounts, ranging from C_{39} to C_{47}. Each homolog contained several different isomers, where the C_{44} ester was principally composed of C_{20} acid esterified with C_{24} alcohol and, for example, the C_{42} and C_{48} homologs also dominated by the same acid moiety esterified with other alcohols (Figure 2.9). Overall, 44.7% of the esters contained C_{20} acid esterified, along with 21.5% C_{22}, 10% C_{18} and 13% C_{16}. The esterified alcohols displayed a roughly Gaussian distribution of chain lengths ranging from C_{14} to C_{36}, peaking at the C_{24} alcohol (Figure A.1 and A.2).

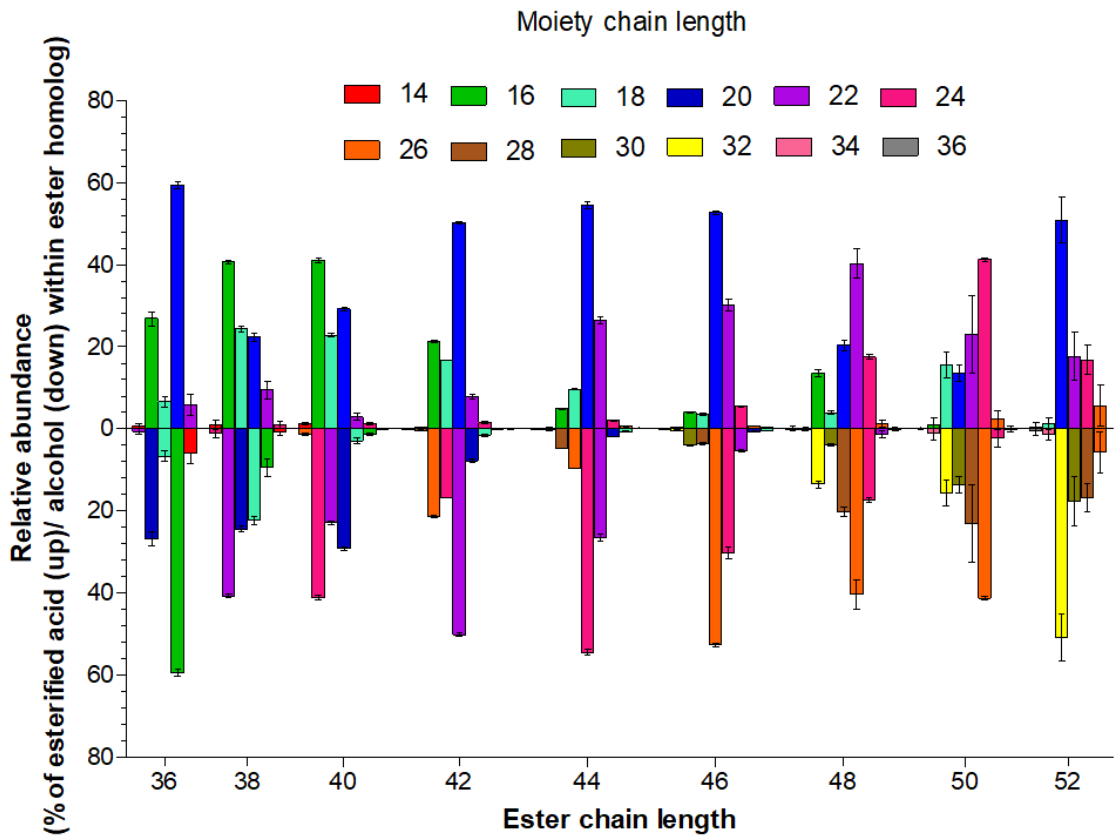

Figure 2.9: **Distribution of acids and alcohols esterified within the predominant even-numbered alkan-1-ol ester homologs found in barley *cv.* Morex spike wax.** Each group of bars represent the percentage of acids (up) and alcohols (down) esterified within a particular homolog. Bars represent the averages and standard errors of three independent biological replicates.

Within the three fractions submitted for GC-IRMS analysis, just the most dominant compounds were found to have the necessary concentration for ^{13}C quantification. Within the alkane fraction, the C_{25}, C_{27}, C_{29} and C_{31} homologs could be analyzed for ^{13}C content. The shortest alkane homolog, C_{25}, showed the highest isotope ratio with a $\delta^{13}C$ of -38.62. Longer homologs presented a nearly linear decrease on $\delta^{13}C$ values, with $\delta^{13}C$ of -38,8 and -39.7 for C_{27} and C_{31}, respectively. However, the C_{29} homolog had a $\delta^{13}C$ of -41.34 (Figure 2.10).

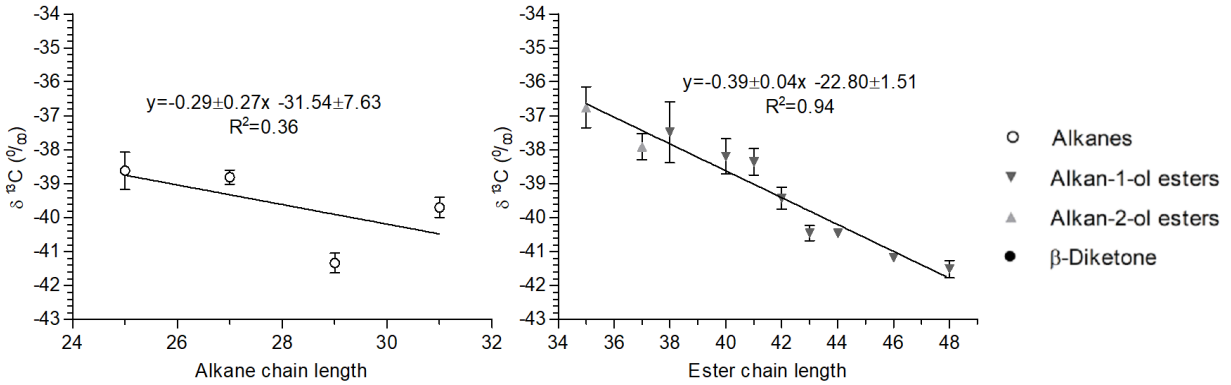

Figure 2.10: **δ^{13}C values of different alkane and ester homologs in barley *cv.* Morex spike wax.** Error bars represent standard deviation of a minimum of three independent replicates.

Within the ester fraction, the ^{13}C ratio for the C_{35} and C_{37} alkan-2-ol esters and the C_{38}, C_{40}, C_{41}, C_{42}, C_{43}, C_{44}, C_{46} and C_{48} alkan-1-ol esters could be determined. The δ^{13}C values for the different esters showed steady decrease with increasing homolog chain length. The longest ester homolog, C_{46}, presented the smallest δ^{13}C of -41.52, whereas the shortest compound, the C_{35} alkan-2-ol ester, had the highest δ^{13}C value of -36.76. Overall, the δ^{13}C values were inversely proportional to chain length, with a regression coefficient of 0.94. It was also observed that δ^{13}C values for compounds at low concentrations varied more than those of the major compounds, as indicated by respective standard deviations, showing the limitations of this technique.

For the fraction containing the β-diketones, the ^{13}C content of the C_{31} 14,16-diketone (C_{31} 16,18-diketone) could be measured. This showed a δ^{13}C value of -34.99, much higher than the ^{13}C values determined for both the alkanes and the esters.

2.4 Discussion

2.4.1 Insights into the diverse β-diketone homologs and isomers found in barley *cv.* Morex cuticular waxes

The GC-MS analyses of barley *cv.* Morex waxes performed here have permitted the identification of novel β-diketone-related compounds, including novel homologs and isomers of β-diketones, hydroxy-β-diketones and alkan-2-ol esters.

Firstly, analysis of the fraction containing the β-diketones isolated from barley *cv.* Morex spikes and flag leaf sheaths showed the same three homologs and four isomers reported in the literature for the spikes of barley *cv.* Bonus cultivars[16], also in similar relative amounts. However, the two even-numbered homologs detected, C_{30} and C_{32}, had not been identified in barley wax before. The low abundance of these homologs might not have permitted their identification by methods involving either β-diketone saponification, reduction to diols or incomplete TMS derivatization. These even-numbered compounds were of special interest, since they have one odd- and one even-numbered acyl moiety, permitting to differentiate between both sides of the molecule.

From the natural even-numbered β-diketones identified here, the chain length of their BKFA precursor can be easily determined based on the odd- and even-numbered acyl moieties. Since elongation can only occur by addition of two-carbon units, it will only yield even-numbered acyl moieties. The odd-numbered acyl moiety of the even-numbered β-diketones must, therefore, originate from an odd-chain length BKFA starter (biosynthesized from propanoyl-CoA). Hence, C_{30} 14,16-diketone (C_{30} 15,17-diketone) and C_{32} 14,16-diketone (C_{32} 17,19-diketone) must be biosynthesized from C_{17} BKFA and C_{19} BKFA, respectively. Assuming that biosynthesis proceeds via elongation of BKFA precursors, the chain lengths of these even-numbered β-diketones then

implies that they are both formed via five rounds of FAE elongation after *Hv*DMP action, similar to what has been proposed for the predominant C_{31} homolog. Therefore, the new β-diketone analyses thus far are in accordance with previous experiments, where feeding of radiolabeled C_{15} FA (precursor for C_{17} BKFA) to spike tissue slices led to the formation of an unnatural even-numbered homolog, C_{30} 14,16-diketone (C_{30} 15,17-diketone)[16], consistent with the expected five rounds of FAE elongation and demonstrating that elongation of the tetraketide resulting from C_{17} BKFA also occurs analogous to the predominant β-diketone[22].

However, the present barley spike wax analyses revealed a second C_{32} β-diketone, C_{32} 16,18-diketone (C_{32} 15,17-diketone). Assuming elongation mechanisms, this isomer must be formed via C_{17} BKFA, but involving six rounds of FAE elongation. Intriguingly, both C_{32} 14,16-diketone (C_{32} 17,19-diketone) and C_{32} 16,18-diketone were found in roughly equal amounts, and thus the reactions leading to them via five and six FAE elongations must also occur with similar frequency. In this, the biosynthesis of the novel β-diketone isomers appears to be conflicting with the assumed elongation pathways leading to the odd-numbered homologs, where the large majority is formed through five FAE elongation rounds (Figure 2.11). The homolog and isomer analysis presented here, thus, casts some doubt on the simple elongation hypothesis assumed so far.

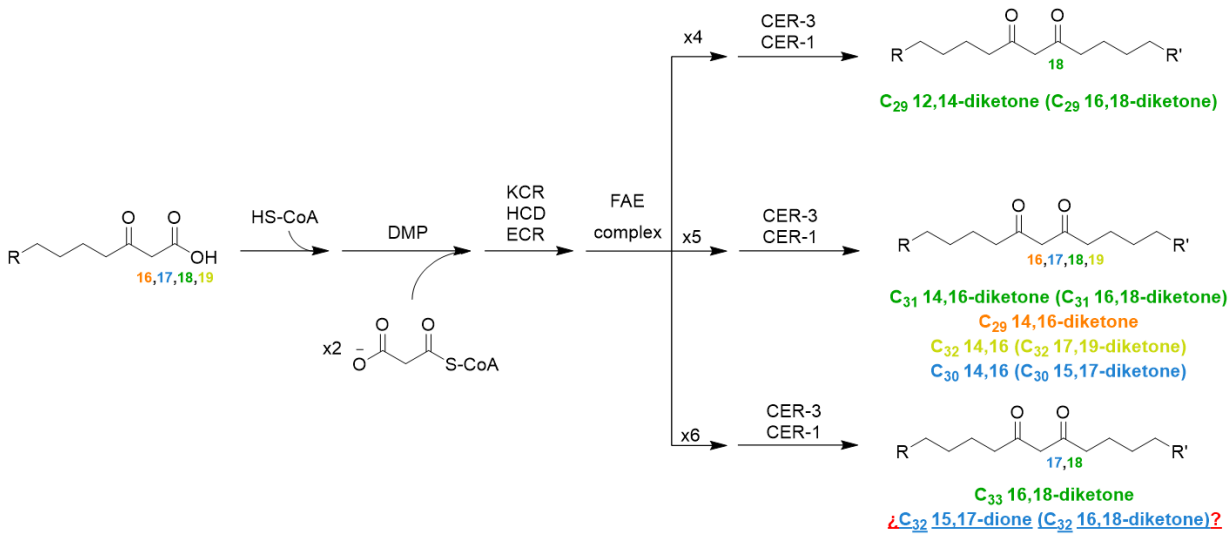

Figure 2.11: **Simplified assumed biosynthetic pathway leading to the formation of different β-diketone homologs and isomers found in barley *cv.* Morex.** Based on the assumed biosynthesis of the predominant odd-chain lengths, biosynthesis of even-numbered β-diketones must involve odd-numbered BKFA starters.

Secondly, the different alkan-2-ol esters identified in barley *cv.* Morex spike and flag leaf sheath waxes also enabled further interpretation of wax biosynthesis pathways leading to β-diketone-related compounds. Overall, the alkan-2-ol ester compositions reported here match those previously reported for barley *cv.* Bonus[25], with the exception of one novel even-numbered homolog, C_{36}. It was also confirmed for barley *cv.* Morex that the alkan-1-ol esters and alkan-2-ol esters comprised similar acyl moieties, and that the alkan-2-ol esters were largely dominated by C_{15} alcohol. Interestingly, the relative amounts of the esterified alkan-2-ol homologs thus do not correlate with the relative abundances of the BKFA homologs assumed to be involved in the biosynthesis of the β-diketones, even though both compound classes are thought to be biosynthetically related. Conversely, the alkan-2-ol ester analyses presented here suggest that C_{16} BKFA might be the most abundant endogenous BKFA, accompanied by much lesser amounts of respective C_{18} and C_{14} homologs. Obviously, the current chemical data cannot be taken as firm

evidence for intermediate pool compositions, since the enzymes involved in the biosynthesis of the different alkan-2-ol esters and β-diketones may also exhibit substrate chain length specificities that further affect product profiles. Nonetheless, the present alkan-2-ol profiles cast further doubt on the simple elongation hypotheses for β-diketone biosynthesis.

In this context, it should be noted that barley *Hv*DMH had recently been found to preferentially form C_{16} BKFA when expressed in *E.coli*, thus matching the predominant chain length of the alkan-2-ol found esterified in barley wax[21]. The *Hv*DMH activity in planta is expected to be analogous to that in *E. coli*, according to previous reports on plant hydrolase characterization in *E. coli* (see chapter 3). Finally, it is also worth noting that the depletion of esterified C_{13} and C_{17} alkan-2-ols observed on the flag leaf sheaths as compared to the spikes is paralleled by lower amounts of C_{29} 12,14-diketone (C_{29} 16,18-diketone) and C_{33} 16,18-diketone in the spike wax, suggesting a relation between these homologs. Taken together, these observations again challenge the current hypothesis of β-diketone biosynthesis assuming elongation of a tetraketide intermediate.

In summary, the alkan-2-ol ester profiles imply that the predominant BKFA starter chain length should be C_{16} BKFA rather than C_{18} BKFA, as previously assumed, and the structure and relative abundance of C_{32} 15,17-diketone (C_{32} 16,18-diketone) argue further against the currently assumed pathway based on elongation. Together, this evidence may be taken to suggest a *Hv*DMP activity analogous to its closely related CUS, catalyzing the biosynthesis of C_{31} 14,16-diketone (C_{31} 16,18-diketone) by head-to-head condensation of C_{16} BKFA with C_{16} acyl-CoA, a pathway alternative that had been discarded early-on based on acetate incorporation patterns.

2.4.2 IRMS analysis of barley *cv.* Morex spike wax reveals an unexpected ^{13}C content of C_{31} 14,16-diketone (C_{31} 16,18-diketone).

Based on the assumption that the first 16 carbons of all wax intermediates are exclusively incorporated in the plastids during *de novo* fatty acid biosynthesis, the percentage of ER carbons for the different compounds can be calculated (Table 2.4). Respective percentages of ER carbon can be used as a reference parameter to plot $\delta^{13}C$ values of various wax compounds, to test in how far plastidial and/or ER incorporation of carbon discriminates for isotope composition.

Table 2.4: **Assumed proportion of plastidial ER carbons for the different compounds analyzed by IR-MS**

	Alkan-2-ol esters		Alkan-1-ol esters							
	C_{35}	C_{37}	C_{38}	C_{40}	C_{41}	C_{42}	C_{43}	C_{44}	C_{46}	C_{48}
Plastidial:ER C	31:4	31:6	32:6	32:8	32:9	32:10	32:11	32:12	32:14	32:16
% ER C	11.4	16.2	15.8	20.0	22.0	23.8	25.6	27.3	30.4	33.3

	Alkanes				β-Diketone		
	C_{25}	C_{27}	C_{29}	C_{31}	C_{31}		
Plastidial:ER C	16:9	16:11	16:13	16:15	31:0[1]	16:15[2]	18:13[3]
% ER C	36.0	40.7	44.8	48.4	0.0	48.4	41.9

* C_{31} 14,16-diketone (C_{31} 16,18-diketone) ER carbon content was calculated as three possible alternatives, 1. assuming β-diketone biosynthesis through head-to-head condensation and 2. and 3. assuming β-diketone biosynthesis via elongation from plastidial C_{16} or C_{18} BKFA, respectively.

As expected, negative $\delta^{13}C$ values were obtained for all the compounds as a result of the use of ^{13}C-enriched standards. As reported in previous literature, $\delta^{13}C$ values were found to decrease with increasing chain length within a compound class[38]. This tendency was also observed when $\delta^{13}C$ values were represented as a function of the theoretical percentage of ER carbon. In fact, the $\delta^{13}C$ values of the ten barley wax esters were found to be proportional to the ER-derived carbon

amounts. Hence, a higher incorporation of ^{13}C during plastidial biosynthesis was observed as compared to ER elongation.

As alkanes were observed to follow the same tendency of ^{13}C enrichment respective to the percentage of plastidial carbon, and despite their more disperse $\delta^{13}C$ values, alkane and ester values were combined, and a linear regression analysis for all the compounds was performed and the 95% confidence interval of the regression curve determined (Figure 2.12). Even though the linearity of the resulting overall dataset was relatively weak (regression coefficient of 0.39), the combined plot showed clearly decreasing ^{13}C content as a function of increasing ER carbon content.

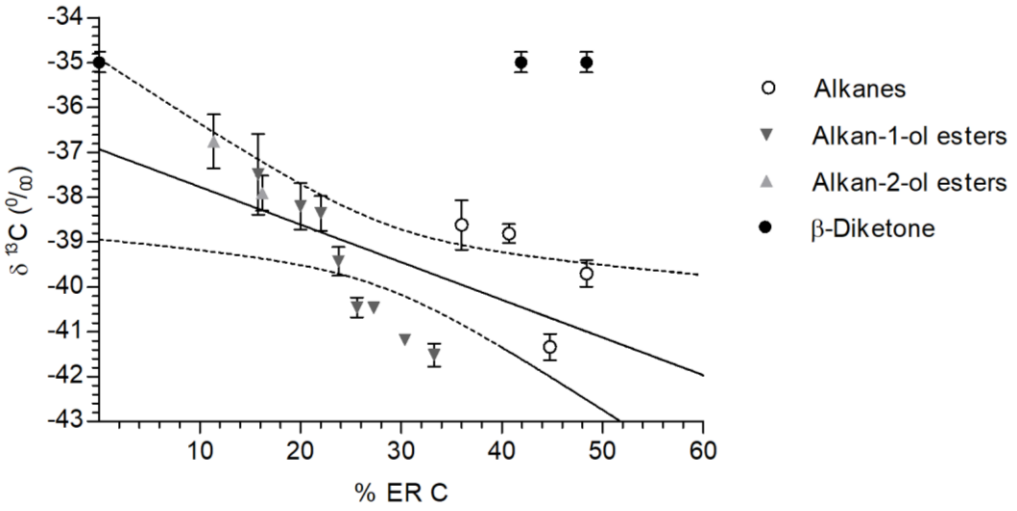

Figure 2.12: **$\delta^{13}C$ values for alkanes, alkan-1-ol and alkan-2-ol esters and C_{31} 14,16-diketone (C_{31} 16,18-diketone) isolated from barley *cv.* Morex spike wax, plotted versus its assumed percentage of plastidial carbon.** The $\delta^{13}C$ value obtained for the β-diketone was plotted for three different scenarios, two of them assuming that plastidial precursors with 16 or 18 carbons are elongated in the ER, leading to additional incorporation of 15 or 13 carbons in the ER and, thus containing 41.8% or 38.7% of ER carbon. In the third scenario, plastidial precursors with 16 or 18 carbons may be combined with a second moiety also containing 16 or 14 carbons from plastidial pathways, leading to 0% ER carbon content. Error bars represent standard deviation of a minimum of three independent replicates. The dashed lines indicate the 95% confidence interval of the linear regression.

Surprisingly, the $\delta^{13}C$ value of C_{31} 14,16-diketone (C_{31} 16,18-diketone) was found to be outside the 95% confidence interval of the linear regression if assuming ER elongation of precursors containing 16 nor 18 plastidial carbons. In sharp contrast, the obtained $\delta^{13}C$ value did agree with the correlation between $\delta^{13}C$ and ER carbon contents defined by the alkanes and esters, if β-diketone biosynthesis is assumed to proceed via head-to-head condensation of two units that are both formed in the plastid. Interestingly, this result is in line with the previous findings for *Hv*DMH product specificity, alkan-2-ol profiles, β-diketone isomer distributions, and organ-specific ratios of alkan-2-ols and β-diketones, all together questioning the elongation pathway hypothesis to β-diketones. Once again the isotope profiling results strongly agree with the discarded hypothesis involving head-to-head condensation of C_{16} acyl-CoA and C_{16} BKFA, since this should give β-diketones with 0% content of ER carbon. All the results presented here suggest that head-to-head condensation should be reconsidered and that further research should also evaluate this alternative.

Chapter 3: **Functional characterization of barley DMH**

3.1 Introduction

3.1.1 Thioesterases

Thioesterase (TE) enzymes are a special type of hydrolases that catalyze the hydrolysis of thioester bonds between a carbonyl group and a sulfur atom to form free acids. TEs are thus capable of cleaving acyl-activating groups such ACP and CoA, making this type of enzyme crucial for the regulation of lipid metabolism and trafficking.

Found distributed in different subcellular compartments such as the cytosol, ER, mitochondria, plastids, and peroxisome in eukaryotic organisms[39,40,41], their most remarkable function is the interception of acyl-ACPs during fatty acid *de novo* biosynthesis to give rise to free, and metabolically inactive, fatty acids. The latter can be exported from the plastids to the cytosol and ER, where they are esterified with HSCoA and used for further metabolic purposes such as incorporation into membrane lipids, storage as triacylglycerols or, in plant epidermal cells, elongation and modification to give rise to the diverse VLCFA derivatives constituting plant cuticular waxes. Conversely, TEs are also crucial for the catabolism of VLCFAs occurring in the peroxisomes and mitochondria.

TEs are a very diverse group of enzymes sharing the same biochemical function but largely differing in their structures, catalytic residues and reaction mechanisms. They are classified into families, where members share strong primary structure similarities, almost identical tertiary structure and same catalytic residues and mechanisms. Within a family, TEs are also grouped into clans primarily based on folding similarities. The large majority of hydrolases identified so far

present either α/β-hydrolase fold or hotdog fold structures, consisting of eight β-sheets surrounded by alpha helices or five to seven antiparallel β-sheets surrounding a central α-helix, respectively[42]. TEs have been mostly characterized by heterologous expression in bacteria, especially in *E. coli*, as this organism presents large amounts of the acyl-ACP substrates required by the enzymes. It has been observed that the activity displayed by TEs in *E. coli* can slightly differ from those *in planta*, as a result of differences in the available acyl-ACP pool. Specifically, *E. coli* contains unsaturated acyl-ACPs which are found in much lesser extent *in planta*. On top of that, different ACP isoforms are present in eukaryotic and prokaryotic organisms[43], including between bacterial and plant ACPs[44], and might influence the observed TE activities. Finally, it is also possible that altered protein folding in *E. coli* as compared to the TE structures in native organism may account for further differences in TE activity.

3.1.2 Plant thioesterases

An extended repertoire of TEs has been identified in plants, some of them being also characterized in detail. The majority of plant TEs characterized so far are involved exclusively in the generation of FAs, such as the different FATs differing in substrate specificity. Some plant TEs have been shown to be able to, in addition, also produce BKFAs such as the different acyl-lipid thioesterase (ALT) enzymes, whereas in other cases, such as for the tomato methylketone synthase (MKS) enzymes or the partially characterized barley DMH, these might present a principal activity towards the production of BKFAs.

FAT-A and FAT-B were first isolated from *Umbellularia californica*, where they were found to be highly important for controlling fatty acid levels in seeds[45]. Further studies revealed that homologs of these enzymes are found across the plant kingdom and are distributed among different

organs. Interestingly, FAT-A and FAT-B have been proposed to be the main enzymes responsible for controlling fatty acid pools in plants[46,47]. These enzymes were found to have a double hotdog fold and be localized in the plastids where they act by hydrolyzing diverse acyl-ACP substrates. Characterization of FAT-A and FAT-B in *E. coli* revealed that these enzymes possessed different substrate specificity and that differences also existed between different plant species despite the minimal differences in primary sequence. While *Umbellularia californica* FAT-B possess high specificity towards saturated C_{12} acyl-ACP[48], *Arabidopsis thaliana* FAT-B displayed preference for C_{16} acyl-ACP[49]. *Arabidopsis thaliana* FAT-A, instead, had strong specificity for unsaturated acyl-ACPs, especially for $C_{18:1}$ acyl-ACP.

The crucial biological role of FAT-A and FAT-B prompted their further investigation *in vitro* and *in planta*. *In vitro* characterization using partially purified enzymes isolated from *E. coli*, combined with external feeding of a series of acyl-ACPs, revealed small differences in substrate specificities between *E. coli* and *in vitro* assays, mainly in the enzyme preferences for unsaturated substrates which are highly abundant in *E. coli*, but also small differences in chain length preferences attributed to different ACP isoforms[50]. In addition, *in planta* characterization of FAT-B in Arabidopsis using antisense technology pointed out the importance of this enzyme in controlling C_{16} FA levels in different plant tissues, especially in seeds and flowers, where the protein is highly expressed[51]. Together, FAT-B and FAT-A are crucial for regulating the availability of different plant lipids including triacylglycerols, cuticular waxes, cutin and suberin.

ALTs are another important family of TEs also present in most plant taxa also belonging to the hotdog fold clan[52]. Four ALTs have been identified in *Arabidopsis thaliana*, all localized in the plastids and each expressed in specific organs. Homologs of Arabidopsis ATL1-4 identified from

different plant taxa were shown to differ in substrate specificity either for different chain lengths or degrees of unsaturation, or between acyl- or β-ketoacyl-ACP substrates[53]. So far, the role of ALTs *in planta* is still unknown, but the high differences in substrate specificity suggest that each ALT can have very different roles, including the control of available free fatty acids or the production of volatile methylketones from BKFA hypothesized to protect plants from numerous pests[54].

E. coli expression of Arabidopsis ALTs revealed that, in addition to generating free fatty acids, ALTs are also capable of producing BKFAs. Specifically, ATL-1 and ATL-4 were found to catalyze the formation of saturated FA with preferences for C_{12} and C_6-C_8 FAs, respectively. On the other hand, ATL-2 and ATL-3 possess main activity towards the formation of BKFAs, with short, saturated BKFAs (C_7-C_9) as predominant products of ATL-2 and longer, unsaturated C_{13} BKFA for ALT-3. It is worth noting that their activity towards the formation of BKFAs was determined based on the detection of their degradation products, including methylketone (MK) and alkan-2-ol products. BKFAs are relatively unstable compounds which undergo spontaneous decarboxylation especially under non-physiological temperatures and pH, resulting in MKs[55]. In addition, it was found that in *E. coli* MKs also undergo reduction into their corresponding alkan-2-ols as a result of the presence of unidentified endogenous reductases.

On the other hand, two TEs identified in the wild tomato species *Solanum habrochaites*, and named as methylketone synthases MKS-1 and MKS-2, were the first TEs described with primary activity towards the biosynthesis of either BKFAs or their respective decarboxylation products, MKs[54]. Unlike other TEs, MKSs are capable of intercepting and hydrolyzing β-ketoacyl-ACPs to yield free BKFAs, which either through spontaneous or catalyzed decarboxylation lead to the production

of the MKs. Both TEs were found to be expressed in the trichome cells of this tomato species, where these metabolites accumulate, and like most of the TEs were found to be localized in the plastids. The activities of MKS-1 and MKS-2 were found to differ along with their quaternary structure. While MKS-1 belongs to the α/β-hydrolase fold clan, MKS-2 presents a hotdog fold. Characterization of MKS-1 and MKS-2 in *E. coli* and *in vitro* revealed that MKS-2 possesses primarily TE activity, catalyzing the hydrolysis of different β-ketoacyl-ACP substrates and perhaps, as spontaneous and catalyzed decarboxylation can be difficult to be distinguished, the subsequent decarboxylation of the resulting BKFAs. Specifically, MKS-2 characterization in *E. coli* demonstrated the ability of this enzyme to produce mainly saturated and unsaturated C_{13} MK, both in similar proportions, smaller amounts of saturated $C_{11:0}$ and unsaturated $C_{15:1}$, and traces of the $C_{9:0}$ homolog[56,57]. MKS-1, instead, was shown to display decarboxylase activity catalyzing the decarboxylation of MKS-2 products, as well as to present a reduced TE activity complementary to MKS-2. However, neither enzyme presented activity towards the formation of FAs[54].This observed activity suggested that *in planta* both enzymes might be linked, with MKS-2 acting upstream of MKS-1. Interestingly, *Solanum habrochaites* trichomes have been reported to contain mainly C_{13} and C_{11} MKs, and in smaller extent C_{15} MK[58], indicating that MKSs display a similar substrate preference *in planta* as compared to *E. coli*. MKS-2 homologs have been identified in other model plant species such as in Arabidopsis and in the Poaceae species rice, but their function still needs to be investigated[56].

The recent characterization of barley *Hv*DMH suggested that this enzyme may possess an activity analogous to MKS-2, producing exclusively BKFAs. In particular, characterization of *Hv*DMH in *E. coli* revealed that its function was restricted to the production of a single BKFA chain length,

C_{16} BKFA, in contrast to the wider chain length range of products displayed by the majority of TEs. Interestingly, the presence of esterified alkan-2-ols with diverse chain lengths in barley wax also indicated that at least C_{14} - C_{18} BKFAs should be products of *Hv*DMH. In addition, *Hv*DMH was also found to form different β-hydroxy fatty acid (BHFA) homologs, even though this was not its main activity. However, other functions such as its involvement in producing free FAs have not been tested.

Based on computational modeling, *Hv*DMH was predicted to present a particular fold consisting of two domains, one with high similarity to bacterial heroin esterase with an α/β-hydrolase fold, and the other one (with lower confidence modeling) with a structure distant from any other annotated hydrolase. In addition, the *Hv*DMH primary sequence was found to present low similarity to the previously described TEs[20]. The presence of the two domains in *Hv*DMH might also indicate that this enzyme possesses dual activity. Its subcellular localization still remains to be experimentally determined, however its activity in heterologous expression in *E. coli* and transit peptide prediction suggest that *Hv*DMH is localized in the plastids[21].

Hence, a more extended characterization of this enzyme still remains to be done, including the determination of other possible BKFA chain lengths produced and evaluation of *Hv*DMH activity towards the formation of FAs and BHFAs formation. These will be the aims of the present chapter.

3.2 Materials and methods

3.2.1 Synthesis of authentic standards

3.2.1.1 Heneicosan-2-ol

500 mg of heneicosan-2-one (C_{21} MK) (Roth) were dissolved in 10 ml of CH_2Cl_2, to which 91 mg (1.5 eq.) of $LiAlH_4$ 95% powder (Aldrich) were added. The reaction was allowed to proceed at room temperature until completed (monitoring by TLC with $CHCl_3$ mobile phase). Unreacted $LiAlH_4$ was quenched by adding 2 ml of 1 N HCl, and reaction products were recovered by extraction with $CHCl_3$ (3x 10 ml). Organic fractions were combined and washed with saturated NaH_2CO_3 (10 ml) and H_2O (10 ml), dried with Na_2SO_4 and concentrated under vacuum. The resulting solid was then purified by column chromatography (100% $CHCl_3$). 420 mg of heneicosan-2-ol (C_{21} alkan-2-ol) (84% yield) were obtained as determined from structure and purity determination by GCMS analysis of the obtained solid.

3.2.2 Constructs, *E. coli* transformation and colony selection (performed in collaboration with Y. Sun)

Two constructs, pET28-HvDMH and pET28-HvDMP, containing barley DMH (HORVU2Hr1G002620.1, MLOC_13397) and DMP (HORVU2Hr1G002640.1, MLOC_59804) in pET28-TEVH plasmids, respectively, were kindly provided by Dr. Asaph Aharoni (Weizmann Institute of Science, Rehovot)[29]. *E. coli* competent cells BL21 (DE3) (Invitrogen) were transformed with pET28-HvDMH or pET28-HvDMP plasmids according to the manufacturer's protocol. The resulting transformed *E. coli* were verified by colony polymerase chain reaction

(PCR) and Sanger sequencing. Three independent colonies of each transformation were grown in 2 ml of Luria-Bertani (LB) medium supplemented with 50 µg/ml kanamycin at 37°C overnight. The resulting *E. coli* cultures were mixed with glycerol and stored at -80°C for further use.

3.2.3 *E.coli* in vivo assay (performed in collaboration with Y. Sun)

The three selected colonies of *E. coli* BL21 (DE3) carrying pET28-HvDMH were grown in 1 ml LB medium with kanamycin at 37°C overnight. *E. coli* BL21 (DE3) carrying the empty vector pET28-TEVH was used as control. Each sample was diluted 1:100 in 100 ml LB media supplemented with kanamycin and grown at 37°C. Recombinant His-HvDMH protein expression was then induced by adding isopropyl β-D-1-thiogalactopyranoside (IPTG) to a concentration of 0.5 mM, followed by incubation at 22°C overnight. *E. coli* cells were harvested by centrifugation, washed with double-distilled water, collected again by centrifugation and allowed to air dry.

3.2.3.1 Transesterification of *E. coli* cells (in collaboration with Y. Sun)

E. coli cell pellets were resuspended in 1 ml methanol containing 0.5 M H_2SO_4 and 2% dimethoxypropane. To each sample, 400 µl of heneicosan-2-one (C_{21} MK) 0.104 mg/ml (Roht), 80 µl of 0.19 mg/ml heneicosan-2-ol (C_{21} alkan-2-ol) (Section 3.2.1.1) and 80 µl of 0.23 mg/ml 2-hydroxy-eicosanoic acid (available repertoire of authentic standards) in $CHCl_3$ were added as internal standards. The transmethylation reaction was performed by incubation of the suspension at 80°C for 3 h, after which 1 ml of sodium chloride solution (2.5%) was incorporated. Lipids were then extracted with hexane (3x 5 ml), organic fractions were combined in a glass tube, concentrated under a gentle nitrogen stream, transferred to GC vials equipped with an insert, and placed under a nitrogen stream until dryness.

3.2.3.2 Analysis of *E. coli* transmethylation products

E.coli transmethylation products were derivatized prior to GC-MS analysis by conversion into the corresponding trimethylsilyl derivatives as described in Section 2.2.4. GC-MS analysis of derivatized samples was performed as described on Section 2.2.5, with a modified GC method with oven temperature set to 50ºC and after 2 min ramped to 100ºC on a gradient of 40°C/min, held at this temperature for 2 min, raised to 320ºC at 3ºC/min, and then held for 5 min.

3.2.3.3 Determination of GC-MS response factor between 2-hydroxy-eicosanoyl methyl ester and 3-hydroxy-hexadecanoyl methyl ester

In quintuples, 100 µl or 0.23 mg/ml 2-hydroxy-eicosanoic acid and 100 µl 0.23 mg/ml 3-hydroxy-hexadecanoic acid (available repertoire of authentic standards) were transferred into a caped tube and converted into their respective methyl esters by transmethylation as described in Section 3.2.3.1. Samples were derivatized as described in Section 2.2.4 and analyzed by GC-MS as described in Section 3.2.3.2. Response factor was then determined to be 2.2 based on the peak area ratio between both compounds.

3.3 Results

The TE function of *Hv*DMH was examined by heterologous expression of this enzyme in *E. coli* and GC-MS analysis of the solvent-extracted lipids after transmethylation reaction. Lipids from *E. coli* cells expressing *Hv*DMH were found to contain 6.7 mg/OD·l of MKs and 2.9 mg/OD·l of alkan-2-ols as determined by using heneicosan-2-one (C_{21} MK) and heneicosan-2-ol for identification and quantification. The cells also contained 10.1 mg/OD·l of free BHFAs quantified using 2-hydroxy eicosanoic acid, both detected as their respective methyl esters. Finally, C_{21} MK reference standard was also used to determine the relative abundance of each FA homolog contained on the extracted lipids, being also detected as their respective methyl esters and identified based on their mass spectral characteristics. All compounds were quantified from total ion chromatograms (Figure 3.1).

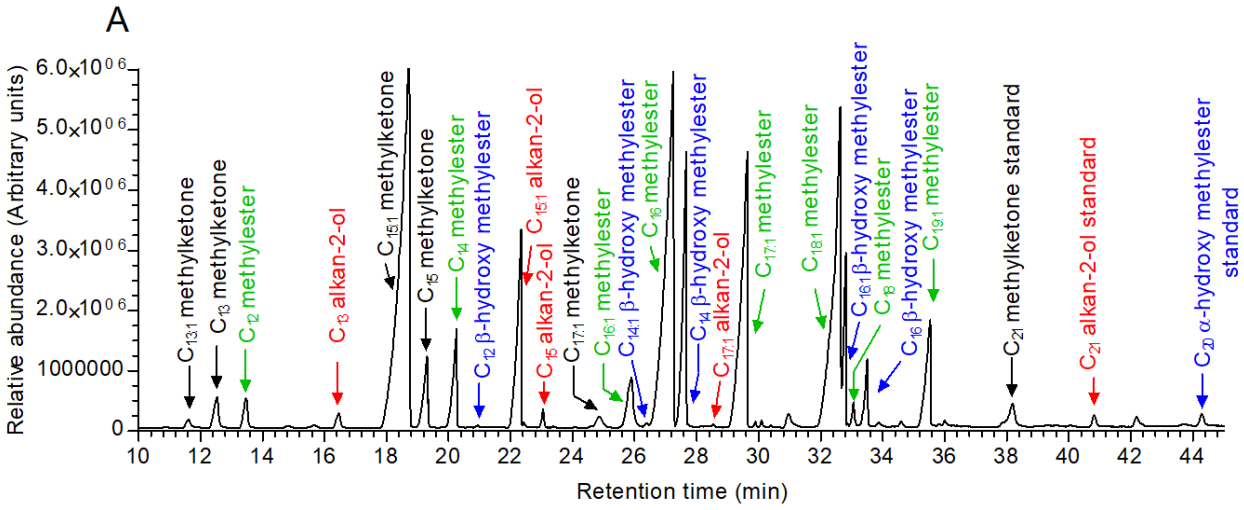

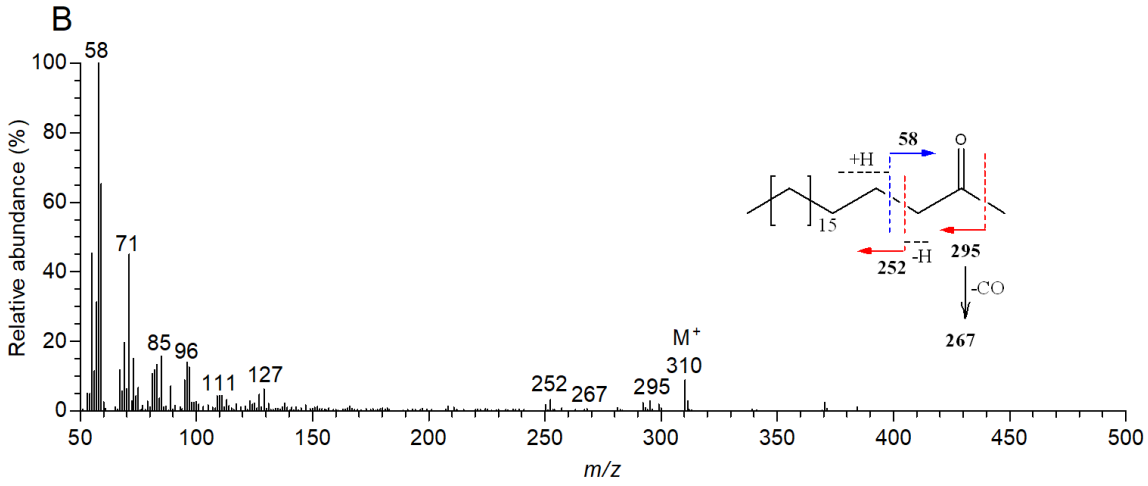
B
Relative abundance (%)
m/z
58
71
85
96
111
127
252
267
295
M+
310
+H
-H
-CO
252
267
295

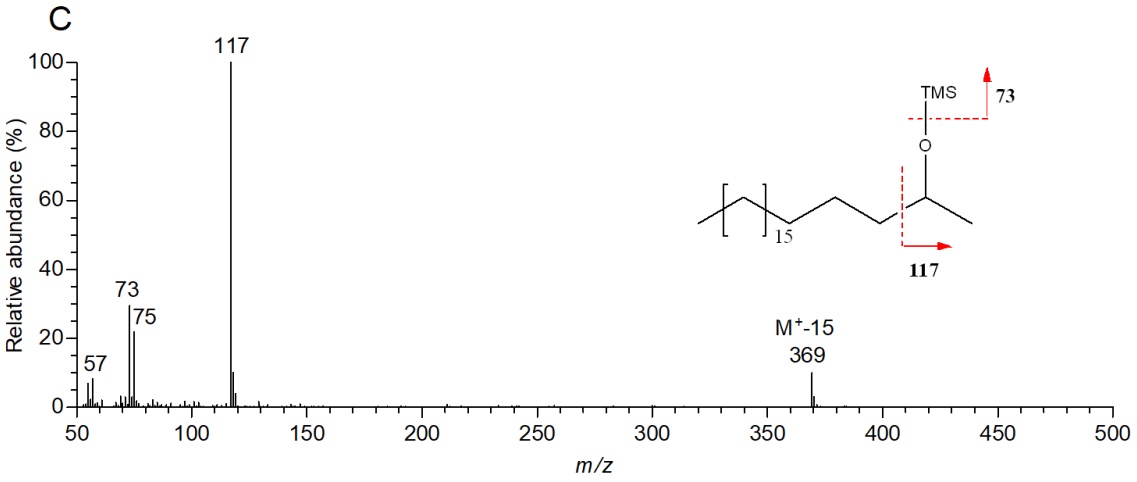
C
Relative abundance (%)
m/z
117
73
75
57
M+-15
369
TMS
73
117

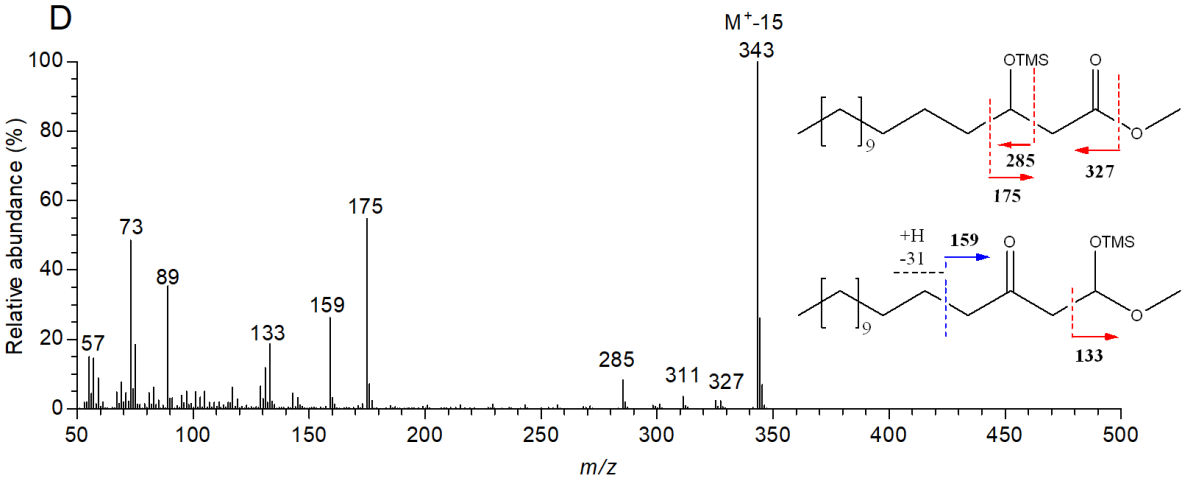
D
Relative abundance (%)
m/z
M+-15
343
73
89
175
159
133
57
285
311
327
OTMS
285
327
175
+H
-31
159
133

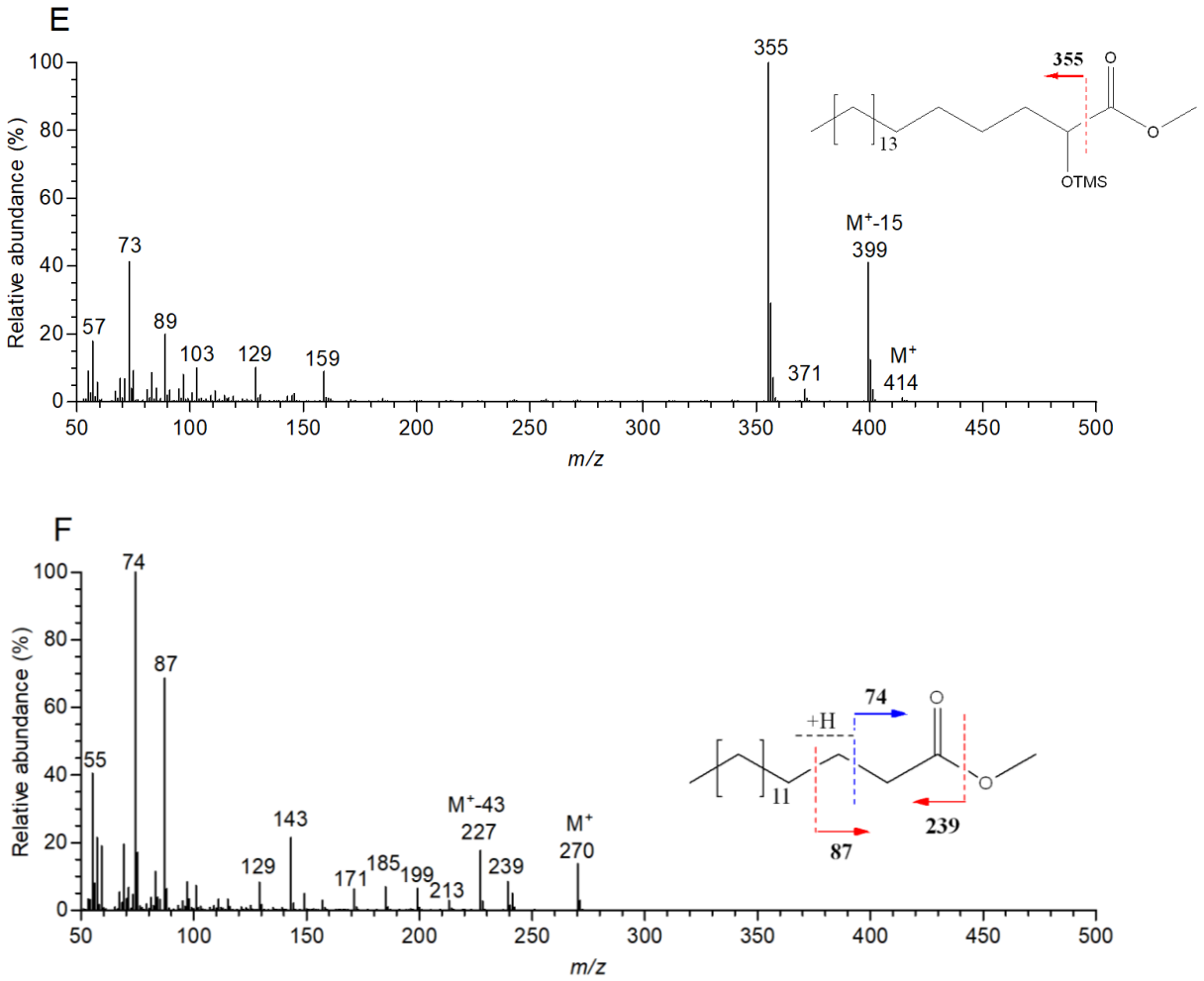

Figure 3.1: **GC-MS analysis of the TMS-derivatized lipids obtained after transmethylation of the extracts from *Hv*DMH-expressing *E. coli* cells. A.** Total ion chromatogram of the total lipids. Mass spectra of **B.** heneicosan-2-one standard, **C.** heneicosan-2-ol standard, **D.** β-hydroxy palmitic acid methyl ester, **E.** α-hydroxy eicosanoic acid methyl ester standard**,** and **F.** palmitic acid methyl ester. Inserts show molecular structures and the predominant fragments. M^+-15 fragments corresponds to the loss of a methyl group.

MKs and alkan-2-ols were found to present similar homolog distributions, with $C_{15:1}$ dominating both compound classes with 84.8% and 88.2%, respectively (Figure 3.2). The saturated C_{15} homologs constituted 8.1% and 5.0% of the total MKs and alkan-2-ols, respectively, along with small amounts of additional MK homologs including C_{13} (3%), $C_{13:1}$ (0.9%) and $C_{17:1}$ (2.7%) and alkan-2-ols C_{13} (5.1%) and $C_{17:1}$ (1.4%).

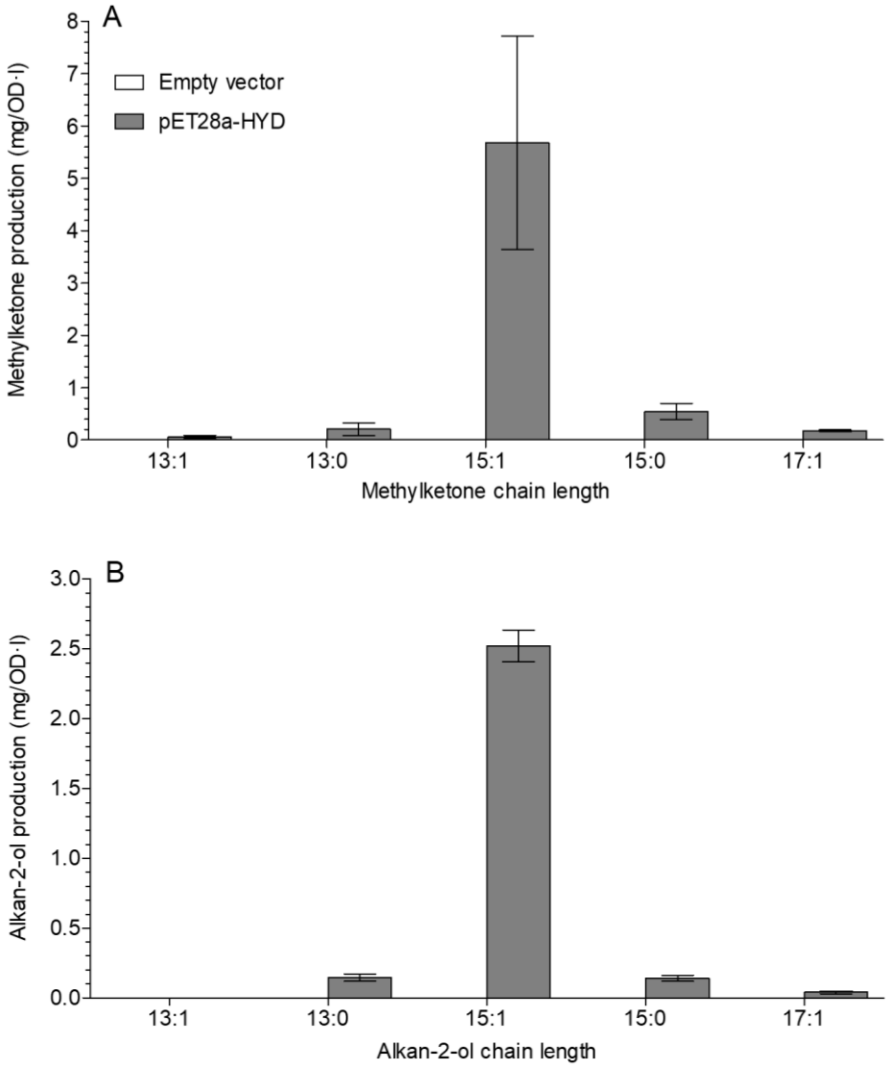

Figure 3.2: **CG-MS analysis of extracted lipids from *E. coli* expressing *Hv*DMH.** Absolute amounts of **A.** methylketones and **B.** alkan-2-ols detected based on quantification using 2-heneicosanone and 2-heneicosanol as internal standards, respectively. Experiments were performed in biological triplicates. Error bars show standard deviation. Methylketones and alkan-2-ols were not detected in the empty-vector control samples.

On the other hand, the BHFAs detected comprised a range of even-chain length homologs between C_{12} and C_{16}, with C_{14} and C_{16} both saturated and unsaturated. Lipid extracts from the empty-vector control samples contained two BHFA homologs, the saturated C_{14} and C_{16}, at significantly lower amounts than in the DMH-expressing *E. coli*. Despite the high variability of the determined

amounts of the different BHFA homologs between the biological replicates, C_{14} was the predominant homolog (57.9% of the compound class), accompanied by $C_{16:1}$ (27.3%) and $C_{16:0}$ (12.1%) and small amounts of $C_{12:0}$ and $C_{14:1}$ (Figure 3.3).

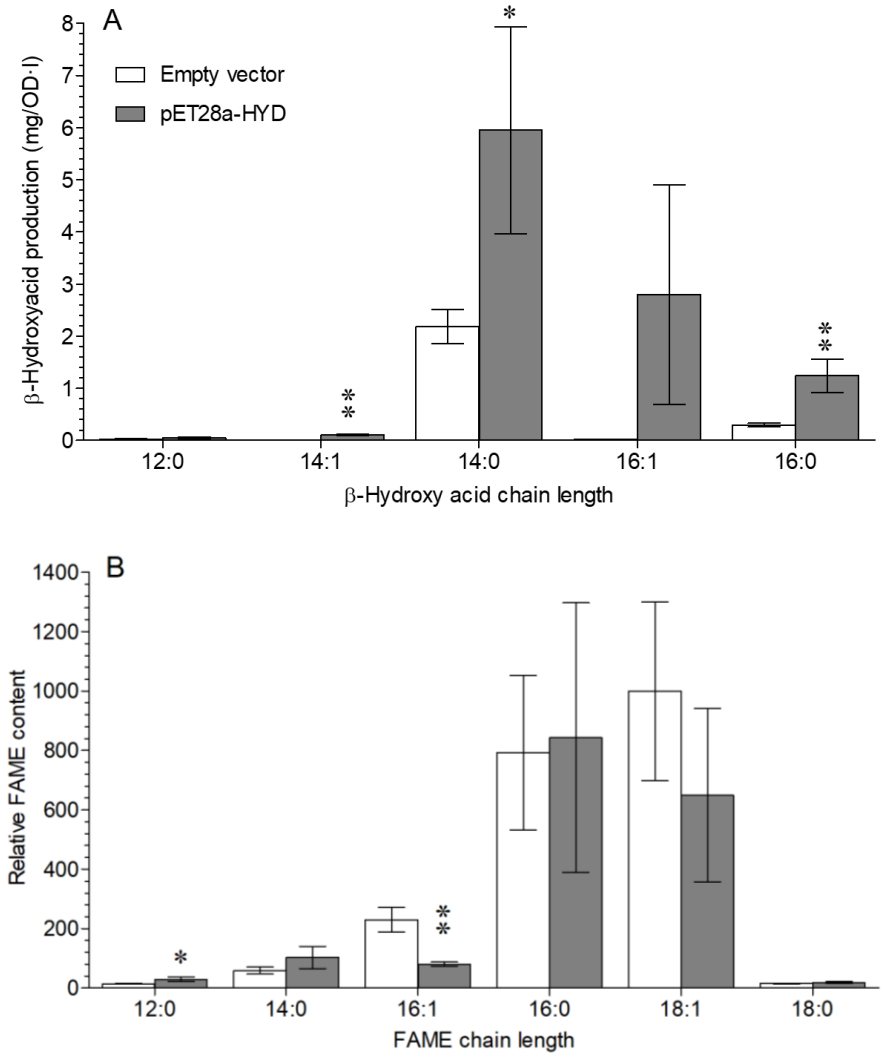

Figure 3.3: **CG-MS analysis of extracted lipids from *Hv*DMH-expressing *E. coli* cells.** Exact amounts of **A.** BHFAs quantified using 2-hydroxy eicosanoic acid methyl ester as internal standard and **B.** relative amounts of FAMEs, quantified using heneicosan-2-one as internal standard, detected on the total extracted lipids from *E. coli* cell expressing *Hv*DMH and their respective empty-vector control samples. Experiments were performed in biological triplicates. Error bars show standard deviation. *p<0.05, **p<0.01.

Analysis of the total fatty acids in the *E. coli* cells determined after transmethylation resulted in detection of a range of FAME homologs ranging from C_{12} to C_{19}, with $C_{16:0}$ and $C_{18:1}$ accumulating to similar amounts in the empty-vector and the *Hv*DMH-expressing samples. Instead, the $C_{16:1}$ FAME accompanying them had lower abundance in *Hv*DMH-expressing *E. coli* cells as compared to the empty-vector control, while C_{12} FAME accumulated to significantly higher levels in the *Hv*DMH-expressing *E. coli*.

3.4 Discussion

Characterization of *Hv*DMH by heterologous expression in *E. coli* revealed the involvement of this enzyme in the production of MKs, alkan-2-ols and BHFAs. Whilst BHFA production was directly detected, MKs and alkan-2-ol were considered to be derivate products from the BKFAs as suggested by earlier studies on TEs displaying analogous functions to *Hv*DMH, such as ALTs or MKSs. However, it could not be determined whether BKFA decarboxylation occurs primarily due to spontaneous decarboxylation during cell culture, lysis and extraction, or whether this reaction catalyzed by either *Hv*DMH, as reported for MKS-1[54], or by an endogenous *E. coli* decarboxylase. The biosynthetic relation between MKs and alkan-2-ols and, therefore, the presence of an active endogenous *E. coli* reductase, is indicated by the very similar chain length distribution and unsaturation degrees between the two compound classes.

Hence, *Hv*DMH was found to be involved in the formation of C_{14}, $C_{14:1}$, C_{16}, $C_{16:1}$ ad $C_{18:1}$ BKFAs, reflecting the complex acyl-ACP pool in *E. coli* including saturated and unsaturated acyls. Interestingly, the *E. coli* acyl-ACP pool composition, as determined by FA profiling, showed significant differences to the acyl distribution found in the BKFA products, suggesting that

*Hv*DMH has a higher preference for unsaturated than for saturated substrates. Interestingly, the proportions of saturated and unsaturated products match previous reports on the characterization of TEs such as MKS-2 in *E. coli*[57]. However, as unsaturated acyl-ACPs are present in plant plastids at much lower concentrations that saturated acyl-ACPs, the formation of unsaturated BKFAs might not be significant *in planta*. More interesting is the observation that *Hv*DMH was active towards interception and release of C_{14}, C_{16} and C_{18} BKFA homologs. Adding up saturated and unsaturated MK and alkan-2-ol products, the homologs C_{14}, C_{16} and C_{18} were found to be present in relative abundance of 4.3%, 93.4% and 2.3%, respectively, confirming that C_{16} BKFA was the predominant product of *Hv*DMH in agreement with previous research[29], and that small amounts of C_{14} and C_{18} BKFAs were also produced.

The observed effect of *Hv*DMH on enhancing the levels of free BHFA in *E. coli* suggests that *Hv*DMH also possesses activity towards the formation of this compound class. However, the large variation in the BHFA levels between replicates, especially for the predominant homologs as reported before[21], may indicate that these compounds result from an indirect alteration of fatty acid *de novo* biosynthesis prompted by the presence of *Hv*DMH rather than due to a direct activity of the enzyme. Previous studies demonstrating that BHFA were poor substrates for alkan-2-ol ester formation[17], and the mismatch found here between the chain length profiles of the BHFA products and the β-diketone-related compounds make it unlikely that the BHFAs serve as intermediates on respective pathways. Nonetheless, it cannot be completely ruled out at this point that *Hv*DMH may have side-activity towards the formation BHFA that can be transformed into various β-diketone-related compounds.

Analysis of the total FAs in *Hv*DMH-expressing and empty-vector control *E. coli* cells also served to evaluate a possible additional activity of DMH towards the production of free FAs, similar to

other TEs such as FATs or ALTs. The most notable difference between the total acyl profiles of the control and the *Hv*DMH-expressing *E. coli* was in the amounts of $C_{16:1}$ FA and C_{12} FA, whereas the other FAs were not altered by *Hv*DMH expression. The effect observed on $C_{16:1}$ FA could well be due to the strong activity of *Hv*DMH intercepting $C_{16:1}$ BKFA, the precursor for $C_{16:1}$ FA. The small but significant increase on C_{12} FA is hence the only activity that can be assigned to *Hv*DMH towards the formation of free FAs. Nevertheless the FA profiling results overall argue against a prominent function of *Hv*DMH in producing free FAs.

Overall, it can be concluded that the main activity of *Hv*DMH involves the formation of BKFAs rather than of BHFAs or FAs. Even though the relative abundances of each homolog can be influenced by the endogenous acyl-ACP pool in *E. coli*, a similar distribution of BKFAs may occur *in planta*. Interestingly, the BKFA profile produced by *Hv*DMH matches the profile of esterified alkan-2-ols found in barley *cv.* Morex spikes and flag leaf sheaths, but not that of the precursors for β-diketones according to previous hypotheses for the biosynthesis, where C_{18} BKFA was expected as the predominant precursor. Therefore, the current results further underline the possibility that β-diketones are biosynthesized through a pathway involving mechanisms differing from those hitherto assumed. Instead, the present results suggest that C_{14}, C_{16} and C_{18} BKFA are the precursors for all the β-diketone homologs and isomers found in barley, with C_{16} BKFA as the predominant product of *Hv*DMH and hence the most likely precursor for the predominant C_{31} 14,16-diketone (C_{31} 16,18-diketone). This finding implies that the diketone is formed either by elongation of C_{16} BKFA or via head-to-head condensation between C_{16} BKFA and C_{16} acyl-CoA. However, the complete incorporation of labeled C_{16} FA into C_{31} 14,16-diketone (C_{31} 16,18-diketone) observed in earlier studies[15] strongly favors head-to-head condensation over elongation of C_{16} BKFA. Hence, further experiments attempting the characterization of *Hv*DMP will have

consider both, the current pathway involving elongation and the alternative mechanism involving head-to-head condensation. In addition, the three BKFA homologs identified here as products of *Hv*DMH will need to be tested as candidate precursors giving rise to the repertoire of β-diketone homologs and isomers identified in barley *cv.* Morex wax.

Chapter 4: *In vivo* and *in vitro* functional characterization of barley DMP

4.1 Introduction

4.1.1 Polyketide synthases

Found in plants, fungi and bacteria, polyketide synthase (PKS) enzymes catalyze the biosynthesis of a broad range of polyoxygenated natural products. The important pharmacological activities displayed by some of their products has prompted intense research into this type of enzymes, resulting in extensive characterizations of many PKSs as well as determination of their crystal structure, together allowing their manipulation for the production of repertoires of unnatural compounds with valuable properties[59].

Generally, PKSs act by catalyzing the formation of polyketides via decarboxylative head-to-tail condensation of a starter molecule, and successive incorporation of two- or three-carbon units by extenders such as malonyl- or methylmalonyl-CoA, respectively, via Claisen condensation. The wide range of starters reported to be accepted by the different types of PKSs, the differences in the number of extender incorporations they can perform, as well as the possible additional activities such as functional group modifications or final cyclization of the polyketide leads to a large diversity of PKS products[60].

PKSs have been divided into three classes, designated as type-I, type-II and type-III PKSs, all of them sharing the same mechanisms for C–C bond-formation but differentiated through the architecture of their catalytic domains[61,62,63]. Type I PKSs are single proteins containing multiple modules acting as acyl carrier protein, a ketosynthase and an acyltransferase, catalyzing extender loading, condensation between the growing polyketide and the extender, and the translocation of

the growing polyketide between domains and/or modules, respectively. In contrast, type II PKSs consist of a multienzyme complex of separable proteins performing respective functions. Both types of PKSs can catalyze multiple rounds of extender addition, depending on the number of modules or the specific substrate-binding pocket geometry. In addition, further domains can also be present, carrying out diverse reductive modifications of the β-keto group before the next round of chain extension. Elongation terminates by the action of a TE which, at the same time, may catalyze the cyclization of the resulting polyketide.

Type III PKSs, instead, are a divergent PKS family that resulted from extended evolution. Type III PKSs are homodimer proteins all sharing a conserved catalytic triad of cysteine, histidine and asparagine, which catalyze the decarboxylative head-to-tail condensation between acyl-CoA starters and multiple units of malonyl-CoA[64]. The condensation starts with the acyl-CoA starter loading and covalent binding to the catalytic cysteine side chain. Starter extension then occurs by activation of the extender (malonyl- or methylmalonyl-CoA) in the enzyme active site via decarboxylation and nucleophilic C-C bond formation between the enolate anion and the growing chain via Claisen condensation. Type III PKSs are characterized by their promiscuity for different CoA-starters, and in some cases they also accept extenders other than malonyl-CoA or methylmalonyl-CoA, such as a β-keto acid (BKA), in these cases undergoing extension via head-to-head condensation. These diverse mechanisms will be the topic of the following sections.

4.1.2 The diversified mechanisms of plant type III PKS

Identified in 1970s[65], chalcone synthase (CHS) was the first plant type III PKS characterized. Since then, plant type III PKSs have been referred to as CHS-like PKSs. CHSs are the most common and widely distributed type III PKSs in higher plants, mediating the biosynthesis of chalcone by

catalyzing the condensation between a *p*-coumaroyl-CoA starter and three units of malonyl-CoA. CHSs also possess TE and cyclase activity, mediating the release of a tetraketide intermediate and its final cyclization and aromatization (Figure 4.1). The chalcone produced by CHSs serves as substrate for downstream enzymes which, by performing diverse modifications on the precursor, give rise to the multiple chalcone-derived compounds such as flavonoids, with important functions in protecting plants from UV radiation or attracting pollinators[66] and many medicinal properties[67,68].

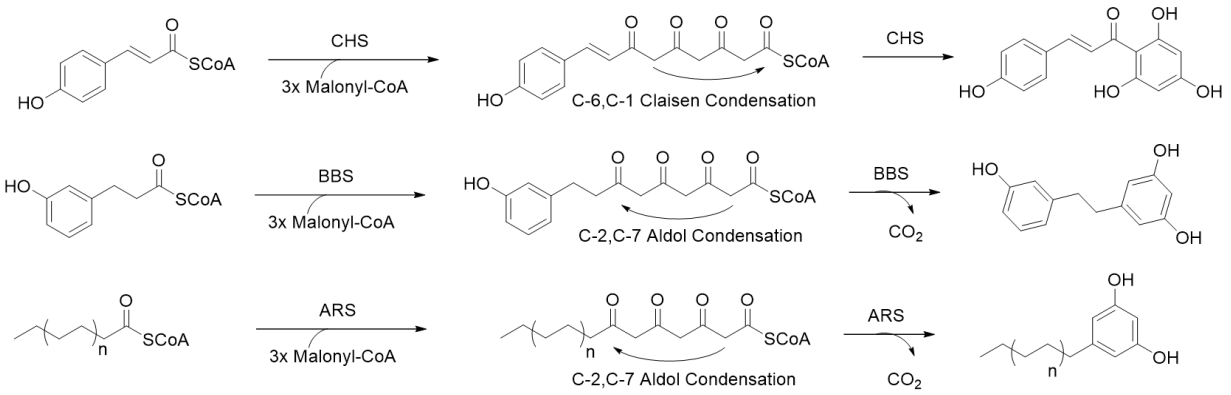

Figure 4.1: **Comparison of the different starter substrates and number of malonyl units incorporated among divergent plant type III PKSs to yield the broad repertoire of polyketide products.**

The vast majority of type III PKSs characterized so far act through mechanisms analogous to that of CHS. For example, CHS, stilbene synthase and coumaroyl triacetic acid synthase all accept *p*-coumaryl-CoA starter and perform the same number of malonyl-CoA incorporations, but cyclize the resulting tetraketide by C-6,C-1 Claisen condensation, by C-2,C-7 aldol condensation with a loss of CO_2, or by lactonization, respectively. Other CHS-like enzymes differ in their preference for acyl-CoA starters where, for example, bibenzyl synthase (BBS), homoeriodictyol/eriodictyol synthase, and benzophenone synthase use the aromatic coumaroyl-CoA-derivatives as starters,

while olivetol synthase or alkylresorcinol synthase (ARS) use aliphatic acyl-CoA precursors of different chain length[69,70].

Among the extensive repertoire of plant type III PKSs, just two have been shown to not display malonyl-CoA head-to-tail condensation activity and to catalyze a head-to-head condensation between various aromatic acyl-CoA starters and aromatic or aliphatic BKAs instead. This mechanism is used by curcumin synthase (CURS) and curcuminoid synthase (CUS) for the synthesis of diverse curcuminoids and gingerols, compounds with known beneficial activities for human health.

4.1.3 CUS and CURS a non-CHS-like plant type III PKSs

Diketide-CoA synthase (DCS) and CURS, two type III PKSs isolated from *Curcuma longa,* turmeric, were characterized *in vitro* to show that their combined activity was responsible for the biosynthesis of the different curcuminoids found in turmeric rhizome. Specifically, DCS acts as a CHS-like PKS catalyzing the condensation between feruloyl-CoA and, with reduced preference, *p*-coumaroyl-CoA and cinnamoyl-CoA, and one unit of malonyl-CoA to form the respective diketide-CoAs with high efficiency. CURS was found to act downstream on the curcuminoid biosynthesis pathway, presenting both TE activity, catalyzing the hydrolysis of the resulting diketide-CoA to yield free aromatic BKAs, and head-to-head condensation activity, catalyzing the reaction between BKA and, preferentially, a second feruloyl-CoA starter[71]. Two additional CURS enzymes have been identified in turmeric, CURS-2 and CURS-3, just differentiated by their preference for the different aromatic acyl-CoAs used as second starter. CURS-2 was found to prefer feruloyl-CoA as starter, whereas CURS-3 accepted both feruloyl-CoA and *p*-coumaroyl-CoA (Figure 4.2 A). Together, the three CURSs were able to form the different curcuminoids

found in turmeric plant, curcumin, demethoxycurcumin and bisdemethoxycurcumin[72]. These were the first plant type III PKS reported to not follow the traditionally assumed role of plant type III PKSs in catalyzing exclusively head-to-tail condensations of acyl-CoA starter with malonyl-CoA extenders.

Further studies identified another type III PKS, CUS, in *Oryza sativa*, rice, a plant species belonging to the Poaceae family. This enzyme was found also capable of producing curcuminoids *in vitro*[73]. However, since curcuminoids have not been identified in rice plant, the function of CUS *in planta* still remains to be elucidated. In contrast to CURS, CUS alone catalyzes the condensation of the first acyl-CoA starter with a single unit of malonyl-CoA, the hydrolysis of the CoA group to form BKAs, and the head-to-head condensation between the resulting BKA and a second starter, leading to the formation of curcuminoids. CUS was observed to have primarily preference for *p*-coumaroyl-CoA as starter and β-keto-*p*-coumaric acid as extender substrate among the various common aromatic acyl-CoA derivatives. It is worth noting that free BKAs were not detected in the *in vitro* experiments with CURS and CUS, suggesting that these products were not released by the enzyme.

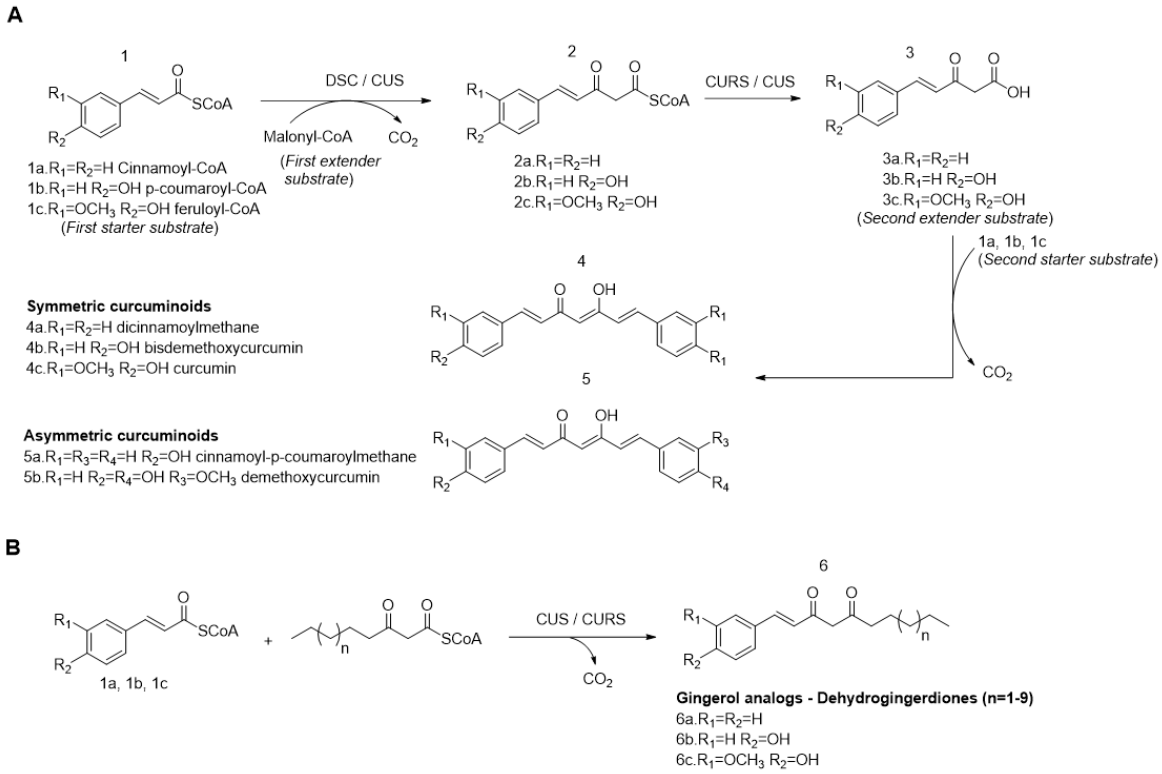

Figure 4.2: ***In vitro* activity of CURS and CUS A.** Mechanism for curcuminoid derivative biosynthesis catalyzed by the combined action of DCS and CURS (including CURS, CURS-2 and CURS-3) or by CUS (adapted from Rodriges *et* al.[74]) and **B.** biosynthesis of dehydrogingerdione derivatives by CUS and CURS.

More interesting was the observation that rice CUS and turmeric CURS also accept aliphatic β-keto-acyl-CoA and BKFA extenders *in vitro*, leading to the formation of different dehydrogingerols (Figure 4.2 B), analogs to the gingerols found in the rhizome of *Zingiber officinale*, the ginger plant. This provided first evidence that a plant type III PKS can accept these types of substrates as extenders, even though not as part of the enzyme *in planta* function.

Further studies were carried out involving heterologous expression of CUS in *E. coli* together with β-oxidation pathway enzymes from *S. cerevisiae*, to allow the endogenous production of different β-keto fatty acyl-CoAs from a set of externally fed fatty acids[75]. The results revealed that CUS accepts various β-ketoacids with odd- and even-numbered chain lengths ranging from C_6 to C_{14} as

extenders, in combination with cinnamoyl-CoA, *p*-coumaroyl-CoA or feruloyl-CoA as starters[76]. Even though the biosynthesis of gingerols in ginger remains to be elucidated, these results suggests that a CUS-like enzyme may be involved in the formation of a possible dehydrogingerdione precursor.

Barley DMP has been assumed to act as a CHS-like PKS enzyme in the formation of β-diketones, through successive condensation of three malonyl-CoAs with a β-keto-acyl-CoA starter. The resulting tetraketides were thought to be elongated by FAE complexes, similar to the majority of wax compounds. However, after *Hv*DMH was characterized as a TE forming BKFAs, the role of *Hv*DMP had to be revisited, and this PKS enzyme has since been assumed to perform the condensation of just two malonyl-CoA units onto a BKFA starter.

Following the identification of the cer-cqu gene cluster, the sequence and structure of *Hv*DMP could be determined. Computational modeling predicted a folding structure of this enzyme characteristic of a type III PKS[20], and phylogenetic analysis revealed high sequence similarity between barley DMP and *Z. officinale* CUS[21]. Even though these recent contributions to the knowledge on *Hv*DMP should now facilitate the study of its biochemical function, the enzyme activity still remains to be determined. Specifically, the question remains whether *Hv*DMP acts as a CHS-like PKS using malonyl-CoA extenders as previously assumed, or if catalyzes the head-to-head condensation of fatty acyl-CoA starters with BKFA extenders. In this chapter, the two alternative activities of *Hv*DMP will be evaluated first *in vivo* and then *in vitro,* using heterologous expression of *Hv*DMP in yeast combined with exogenous feeding of the pathway intermediates known to be formed by *Hv*DMH (see Chapter 3). In addition, the specificity of *Hv*DMP for the different substrates required to generate the different β-diketone homologs and isomers identified in barley *cv.* Morex (see Chapter 2) will be studied in order to decipher their biosynthesis.

4.2 Materials and methods

4.2.1 Synthesis of authentic standards

4.2.1.1 C_{14}, C_{16}, C_{17} and C_{18} β-ketoacid methyl esters

C_{14}, C_{16}, C_{17} and C_{18} β-ketoacyl methyl esters were synthesized via Meldrum's acid as described by Brinkerhoff et al.[77]. For synthesis of C_{16} β-ketoacyl methyl ester, 2 g of myristic acid (Sigma-Aldrich) were dissolved in 10 ml of CH_2Cl_2 and 2 g of DCC (Sigma-Aldrich) (1 eq.) were added. Separately, 1.6 g of Meldrum's acid (TCI) (1 eq.) were dissolved in 20 ml of pyridine followed by 1.9 g of 4-dimethylaminopyridine (Sigma-Aldrich) (1 eq.). Both solutions were allowed to stir at room temperature for 15 min before being combined and stirred at room temperature for another 16 h. Then, solvent was evaporated under vacuum and, without previous purification, the solid was redissolved in 20 ml of methanol, 2 drops of concentrated H_2SO_4 were added, and the mixture was refluxed for 16 h. Reaction products were extracted with ethyl ether (3x 10 ml). Organic fractions were then combined and washed with NaH_2CO_3, distilled water and saturated NaCl (1x 10 ml each). The organic fraction was dried with Na_2SO_4 and solvent evaporated under vacuum. The resulting solid was then purified by column chromatography ($CHCl_3$). 0.84 g of pure C_{16} β-ketoacid methyl ester was obtained, resulting in a 34% overall yield as determined by GC-MS (Figure B.1).

The C_{14}, C_{17} and C_{18} β-ketoacid methyl esters were synthesized following the same methodology but using lauric acid, pentadecanoic acid and palmitic acid (Sigma-Aldrich) as starting reagents, respectively. Similar yields were obtained for all homologs.

4.2.1.2 C_{14}, C_{16}, C_{17} and C_{18} β-keto fatty acids

The BKFAs were obtained via acidic hydrolysis of corresponding methyl esters at low temperature. For that, 0.5 g of purified β-keto methyl ester (Section 4.2.1.1) were dissolved in 20 ml of glacial acetic acid, and five drops of concentrated HCl were added. To minimize product decarboxylation, the solution was allowed to react at 10ºC for a week. Then, 20 ml of deionized water and 20 ml of ethyl ether were added, the organic phase washed with deionized water (3x 10 ml), and the solvent evaporated under vacuum. GC-MS showed that the crude contained non-hydrolyzed methyl ester and BKFA as main products, accompanied by small amounts of the decarboxylation product, methylketone. BKFA was obtained by flash column chromatography ($CHCl_3$) (Figure B.2) with <65% yield and stored at 4ºC prior to its use. The recovered methyl ester was subjected to hydrolysis in successive batches of substrate preparation.

4.2.1.3 Pentatriacontane-14,16-dione

Pentatriacontane-14,16-dione was synthesized in an analogous manner to hentriacontane-14,16-dione as described in Section 2.2.7.3 and with similar yields, using eicosanol (Sigma Aldrich) as starting material (Figure B.2).

4.2.2 DNA construct for yeast expression and transformation (performed in collaboration with Y. Sun)

To construct the vector for expressing *Hv*DMP along with *At*LACS1 (*Arabidopsis thaliana* long chain acyl-CoA synthetase 1) in yeast, the coding sequence of *At*LACS1 (AT2G47240.1) was first amplified from Arabidopsis stem cDNA with Phusion polymerase (NEB) by primers 5'-AGAGGATCCATGAAGTCTTTTGCGGCTAAG-3' (forward) and 5'-

AGAGTCGACTGAGATTTTCTTTGAGGCCAAT-3’ (reverse). The product was inserted into the pESC-TRP yeast expression vector with C-terminal MYC epitope tag, behind the galactose-inducible promoter GAL1 to give the initial construct pESC-TPR-GAL1::AtLACS1-MYC. Then, *Hv*DMP was subcloned from pET28-HvDMP using primers 5’-TCTGAATTCATGGCAGGCAGCTCACC-3’ (forward) and 5’-GGACTAGTAGCCATTTTTTCTTGAGAGCGC-3’ (reverse) and spliced into the pESC-TPR-GAL1::AtLACS1-MYC vector, C-terminally in frame with FLAG epitope tag, resulting in the pESC-TPR-GAL1::AtLACS1-MYC-GAL10::HvDMP-FLAG vector. The resulting construct was transformed into *E. coli* DH10B competent cells. The transformants were screened on LB plates containing 100 µg/ml ampicillin and verified by colony PCR, restriction digestions and Sanger sequencing.

The pESCTPR-GAL1::AtLACS1-MYC-GAL10::HvDMP-FLAG vector was amplified in *E. coli*, isolated and purified, and then transformed into yeast strain INVSc1 (*MATa* his3D1 leu2 trp1-289 ura3-52). Three verified positive individual yeast lines were grown in 2 ml liquid minimal medium lacking the appropriate amino acids supplied with 2% glucose and grown at 28℃ overnight, the resulting yeast cultures were mixed with glycerol and stored at -80 ℃ for further use. INVSc1 yeast cells transformed with pESCTPR-GAL1::AtLACS1 served as negative control.

4.2.3 Yeast *in vivo* assay

The three selected yeast colonies co-expressing *Hv*DMP and *At*LACS1 were cultured in appropriate liquid minimal medium supplemented with 2% glucose at 28℃ overnight. The yeast cells were then cultured in liquid minimal medium supplemented with 2% galactose at 28℃ for 16 h to induce the expression of target genes. The yeast cells were transferred to 30 ml liquid

minimal medium based on phosphate buffer (20 mM sodium phosphate, 300 mM sodium chloride, pH 7.4) supplemented with 2% galactose.

In vivo assays were initiated by supplying yeast cells with the corresponding substrate, C_{14} BKFA C_{16} BKFA, C_{17} BKFA or C_{18} BKFA (Section 4.2.1.2) to a final concentration of the medium of 0.22 mM from 20 mM ethanolic stock solutions. For assays involving BKFA and FA co-feeding, same concentration of BKFA was used, whereas FAs were added to a final concentration of 1.2 mM of capric acid (C_{10} FA) or undecanoic acid (C_{11} FA) from 0.8 M ethanolic stock solutions, and heptadecanoic acid (C_{17} FA), deuterium-labeled $^{2}H_{31}$-palmitic acid or $^{2}H_{2}$-palmitic acid to a final concentration of 0.22 mM from 0.1 M ethanolic stock solutions. For assays involving BKFA supply combined with a range of FAs, lauric acid (C_{12} FA), tridecanoic acid (C_{13} FA), myristic acid (C_{14} FA) and pentadecanoic acid (C_{15} FA) were added to a final concentration of 1.2 mM, 0.66 mM, 0.33mM and 0.33 mM, respectively, from ethanolic stock solutions of 0.8 M, 0.8 M, 0.5 M and 0.5 M, respectively (all FAs were obtained from Sigma-Aldrich). After 24 h incubation at 22ºC, a 5 ml aliquot was taken, cells were collected by centrifugation and washed with distilled water (3x 30 ml), and the pellet was subject to transesterification and products analyzed by GC-MS as described in Sections 3.2.3.1 and 3.2.3.2, respectively. Yeast cells from the remaining suspension were collected by centrifugation, washed with distilled water (3x 30 ml) and resuspended in 3 ml of distilled water to which 0.5 mm glass beads and 40 µl of pentatriacontane-14,16-dione internal standard 0.02 mg/ml in $CHCl_3$ were added and cells were then lysed by vortexing the suspension (5x 2 min).

Lipidic compounds were then extracted using $CHCl_3$ (5x 4ml), the organic fractions were combined and dried with Na_2SO_4. Finally, the solution was concentrated at 70ºC under a gentle N_2 steam, transferred into autosampler vials provided with inserts and dried at 70ºC under a gentle N_2

steam. Extracts were BSTFA-derivatized and analyzed by GC-MS as described in Sections 2.2.4 and 2.2.5, respectively. All assays were accompanied by their respective non-feeding and negative controls.

4.2.4 Recombinant *Hv*DMP production (performed in collaboration with Y. Sun)

A selected colony of *E. coli* BL21 (DE3) carrying pET28-HvDMP (section 3.2.2) was grown in 1 ml LB medium with kanamycin in 37 ℃ overnight. *E. coli* BL21 (DE3) carrying the empty vector pET28-TEVH was used as control. A 1 ml aliquot of sample was taken, diluted in 100 ml LB medium supplemented with kanamycin and grown at 37℃. Recombinant His-HvDMP protein expression was then induced by adding IPTG to a concentration of 500 µM followed by incubation at 16℃ overnight. *E. coli* cells were collected by centrifugation at 10,000 *g*, resuspended in lysis buffer (20 mM sodium phosphate, 300 mM sodium chloride, 10 nM imidazole and 0.1% Triton X-100; pH 7.4) and lysed by sonication at 4℃. Recombinant His-HvDMP was purified by Ni-NTA affinity column chromatography with HisPur Ni-NTA resin (Invitrogen) following the manufacturer's protocol. The presence and purity of His-HvDMP in the collected fractions was verified by sodium dodecylsulphate polyacrylamide gel electrophoresis. Selected fractions were then combined and dialyzed in dialysis buffer (0.1 M Na_2HPO_4/ NaH_2PO_4, 2.5 mM DTT, 10 mM $MgCl_2$, 0.025% Triton X-100; pH 7.4) at 4℃ and protein concentration was determined by Bardford's assay using Protein Assay Dye Reagent Concentrate and bovine serum albumin standards (Bio-Rad). The obtained protein was immediately used for the assays.

4.2.5 *Hv*DMP *in vitro* assays

In vitro assays were carried out by incubating purified recombinant protein with the respective substrates in 3 ml of 50 mM phosphate buffer (pH 7.4) containing 2.5 mM DTT, 10 mM $MgCl_2$ and 0.025% Triton X-100. C_{14} BKFA, C_{16} BKFA, C_{18} BKFA (Section 4.2.1.2), malonyl-CoA lithium salt (Sigma-Aldrich), myristoyl-CoA lithium salt (Sigma-Aldrich) and palmitoyl-CoA lithium salt (Sigma-Aldrich) were used as substrates for the different assays. A final concentration of 0.22 mM of BKFA added from a 20 mM ethanolic stock solution and 0.22 mM of myristoyl-CoA and palmitoyl-CoA added from 4.1 mM and 4.5 mM aqueous stock solutions, respectively, were employed for all the *in vitro* assays. Malonyl-CoA, instead, was added to a concentration of 0.44 mM from a 5.3 mM aqueous stock solution. 50 µg of purified recombinant *Hv*DMP was employed in all assays. After incubation at room temperature for 14 h, reactions were quenched by adding 200 µl of 10% H_2SO_4, and lipids were extracted using $CHCl_3$ (3x 1 ml). Organic fractions were then combined, dried with Na_2SO_4, concentrated at 70ºC under a gentle N_2 steam and transferred into autosampler vials provided with inserts. All assays were accompanied by their respective controls with boiled protein (100 ºC for 30 min)

4.3 Results

4.3.1 *In vivo* characterization of *Hv*DMP by yeast heterologous expression combined with BKFA feeding

To test whether *Hv*DMP has biochemical activity for β-diketone formation either via elongation or via condensation between a BKFA and fatty acyl-CoA, the enzyme was heterologously expressed in yeast supplied with exogenous C_{16} BKFA substrate.

As BKFAs undergo spontaneous decarboxylation in solution[55], fresh BKFA solutions were prepared for each assay and substrate purity and concentration determined by CG-MS. Substrate stability after yeast feeding and incubation at 22ºC for 24 h was evaluated, observing that after incubation less than 60% of the fed BKFA had undergone decarboxylation and that yeast displayed efficient growth. In addition, a final concentration of 0.22 mM of BKFA in the incubation media, buffered at pH 7.4, was found suitable for yeast feeding and was used for all the yeast experiments. Higher concentrations of BKFA led to substrate precipitation observed by naked eye.

Interestingly, GC-MS analysis of lipids extracted from yeast cells expressing *Hv*DMP revealed the presence of β-diketones (Figure 4.3). Specifically, C_{29} 12,14-diketone (C_{29} 16,18-diketone), C_{31} 14,16-diketone (C_{31} 16,18-diketone) and the unsaturated $C_{31:1}$ 14,16-diketone ($C_{31:1}$ 16,18-diketone) were detected in the lipid mixture. The structures of these β-diketones were assigned based on their mass spectral characteristics and GC retention times in comparison to standards and literature information. One of the yeast lipids was found to have GC-MS characteristics identical to C_{31} 14,16-diketone (C_{31} 16,18-diketone) authentic standard and the corresponding compound identified in barley *cv.* Morex wax (for references visit Chapter 2). The other diketones found in the yeast extract were identified based on corresponding GC-MS characteristics matching those of barley wax components, except for the unsaturated $C_{31:1}$ 14,16-diketone ($C_{31:1}$ 16,18-diketone). Its structure was elucidated based on its mass spectrum similar to C_{31} 14,16-diketone (C_{31} 16,18-diketone) with two of the α-fragments and M^+ and M^+-18 presenting *m/z* values reduced by two units. In contrast, none of the β-diketones were detected in any of the negative and non-feeding controls.

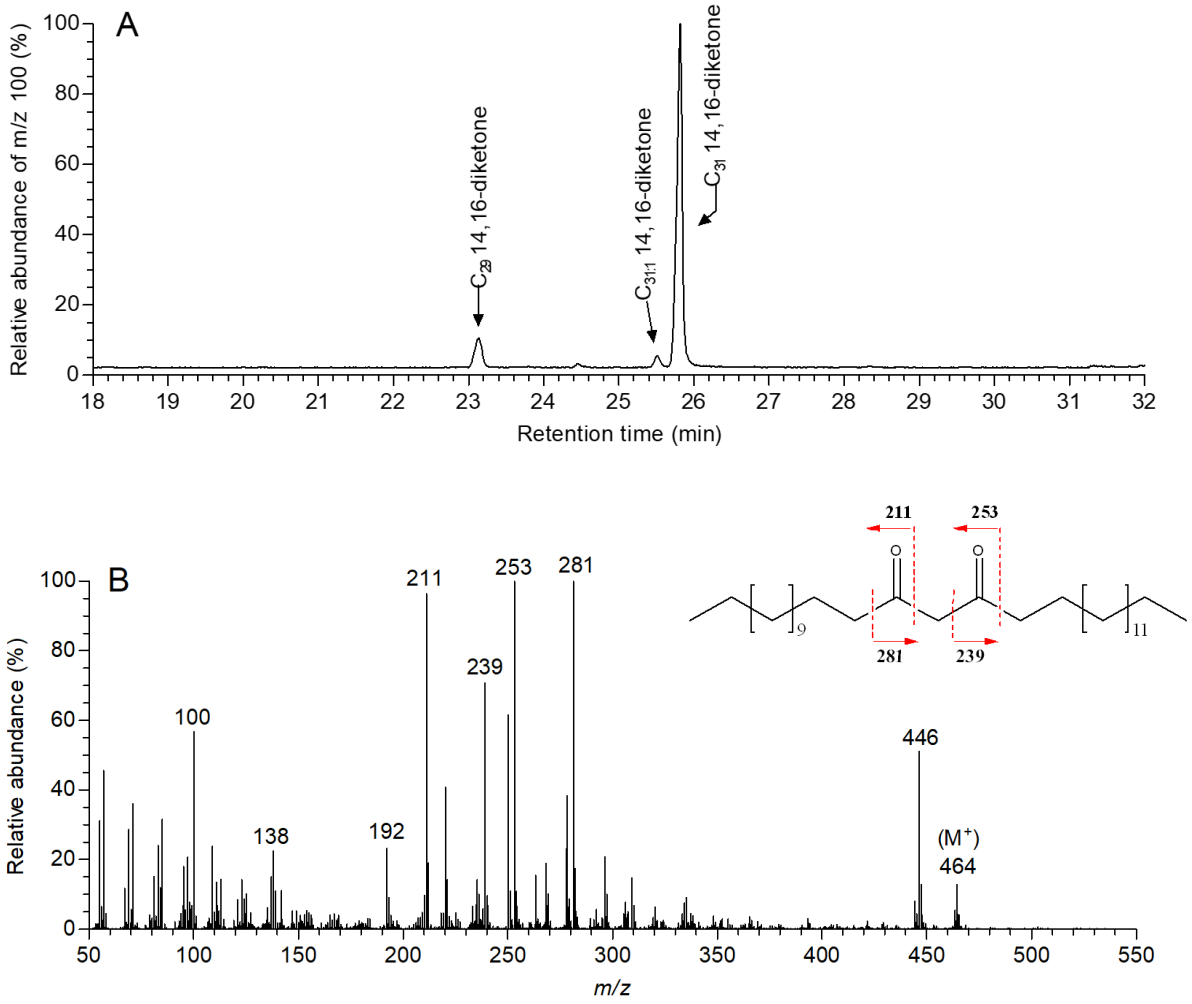

Figure 4.3: **GC-MS analysis of the lipid mixture extracted from yeast expressing *Hv*DMP supplemented with C_{16} BKFA A.** *m/z* 100 extracted ion chromatogram and **B.** mass spectrum of the detected C_{31} 14,16-diketone (C_{31} 16,18-diketone).

4.3.2 Evaluating the direct incorporation of BKFAs and FAs into β-diketone mediated by *Hv*DMP

Direct incorporation of BKFAs and FAs into the β-diketones was studied by feeding *Hv*DMP-expressing yeast with either odd-chain length BKFA or odd-chain length FA combined with even-chain length BKFA. Thus, the formation of unnatural even-chain length β-diketones, indicative of the incorporation of the entire odd-chain length moiety was explored.

Firstly, DMP-expressing yeast cells were incubated with equimolar amounts of C_{15} FA and C_{16} BKFA. GC-MS analysis of the extracted yeast lipids revealed the production of C_{30} 14,16-diketone (C_{30} 15,17-diketone) as the principal β-diketone, accompanied by small amounts of two odd-chain length β-diketones, C_{29} 14,16-diketone and C_{31} 14,16-diketone (C_{31} 16,18-diketone), structures that were assigned based on their mass spectral characteristics and GC retention times in comparison to standards and literature information (Figure 4.4 A and 4.4 C). Interestingly, the structure of the unnatural even-chain length β-diketone, C_{30} 14,16-diketone (C_{30} 15,17-diketone), combined an odd- and an even-chain length acyl moiety, with the carbonyls allocated at C-15 and C-17 (or C-14 and C-16) whereas C_{29} 14,16-diketone and C_{31} 14,16-diketone (C_{31} 16,18-diketone), both presented two even-chain length acyl moieties.

Secondly, direct incorporation of BKFAs into β-diketones was studied by co-feeding of the odd-chain length C_{17} BKFA and C_{14} FA to yeast expressing *Hv*DMP. In the resulting lipid extracts, C_{30} 14,16-diketone (C_{30} 15,17-diketone) was the dominating homolog (Figure 4.4 B and 4.4 D), accompanied by smaller amounts of C_{31} 15,17-diketone, C_{32} 16,18-diketone (C_{32} 15,17-diketone) and C_{33} 15,17-diketone (C_{33} 17,19-diketone). In this case, all identified β-diketones combined an odd- and an even-chain length acyl moiety with the carbonyl groups allocated at C-15 and C-17.

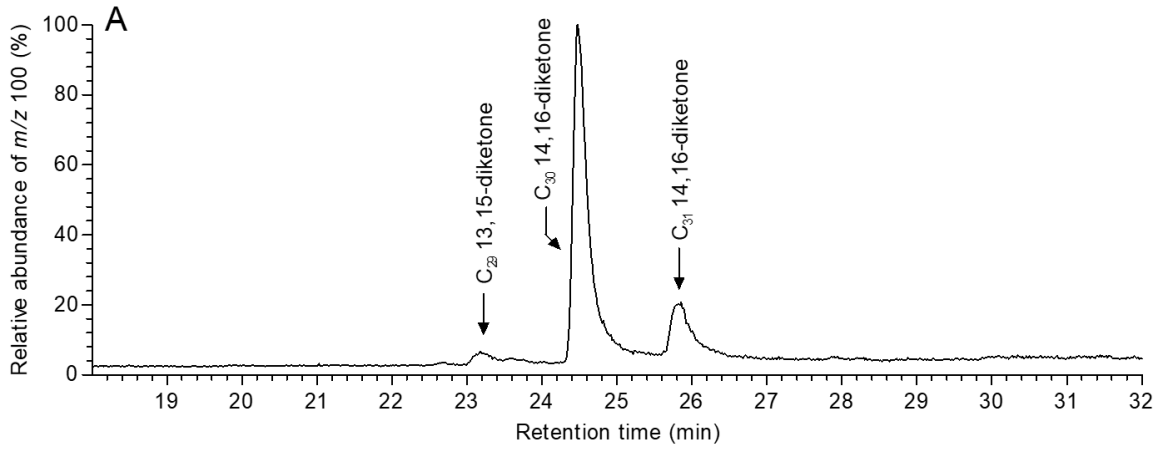
A
Relative abundance of m/z 100 (%)
Retention time (min)
C29 13,15-diketone
C30 14,16-diketone
C31 14,16-diketone

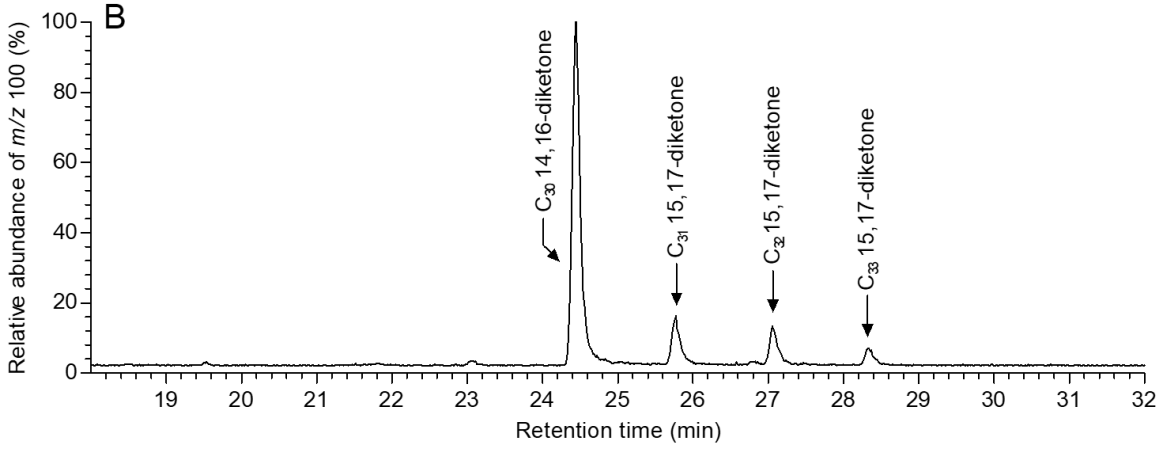
B
Relative abundance of m/z 100 (%)
Retention time (min)
C30 14,16-diketone
C31 15,17-diketone
C32 15,17-diketone
C33 15,17-diketone

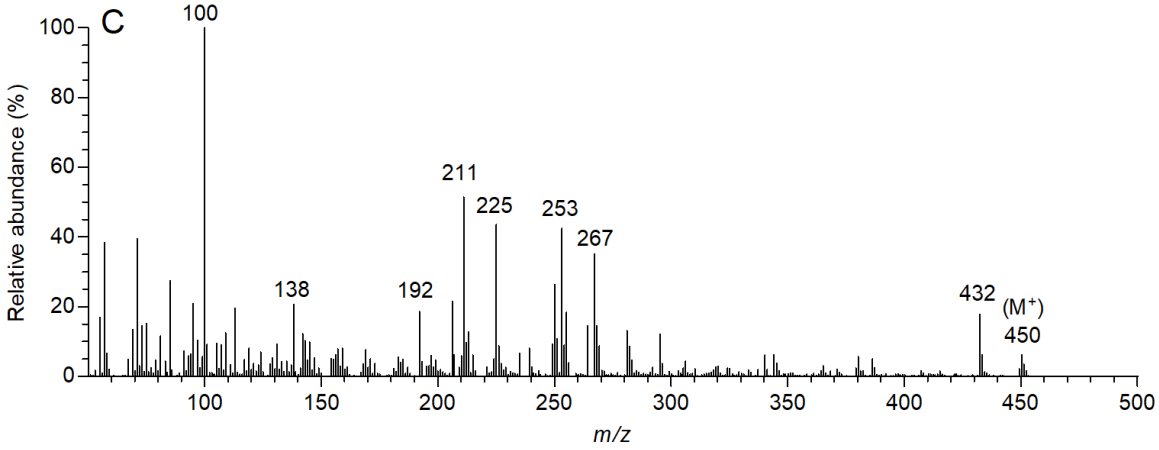
C
Relative abundance (%)
m/z
100
138
192
211
225
253
267
432
(M+)
450

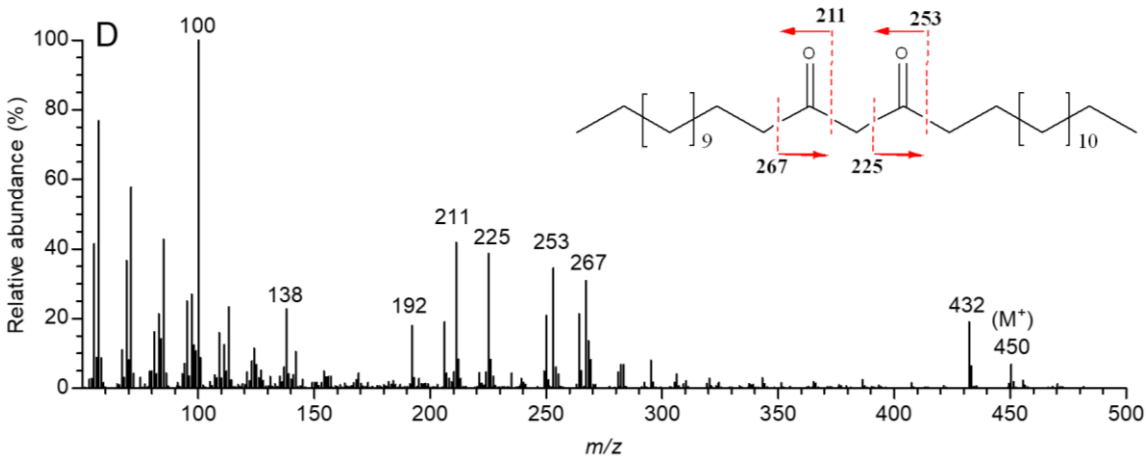

Figure 4.4: **GC-MS analysis of the extracted yeast lipids from *Hv*DMP-expressing yeast fed with odd-chain length FA or BKFA. A**. *m/z* 100 extracted ion chromatogram of the extracted lipids from *Hv*DMP-expressing yeast co-fed with C_{15} FA and C_{16} BKFA and B. C_{17} BKFA and C_{14} FA. C. and D. show the MS spectrum of the predominant β-diketone detected in each assay, respectively. In both cases, this β-diketone was identified as C_{30} 14,16-diketone (C_{30} 15,17-diketone)

Finally, complete incorporation of the FAs into the β-diketones was tested by yeast co-feeding of C_{16} BKFA with different deuterium-labeled FAs.

Feeding of palmitic acid with all acyl hydrogens exchanged for deuterium ($^2H_{31}$ C_{16} FA) along with C_{16} BKFA to yeast expressing *Hv*DMP resulted in the formation of mainly unlabeled C_{31} 14,16-diketone (C_{31} 16,18-diketone) as before. Interestingly, it was accompanied by small amounts of a compound with shorter retention time and with similar mass spectral characteristics. Specifically, it presented two of the α-fragment ions diagnostic for C_{31} 14,16-diketone (C_{31} 16,18-diketone), *m/z* 211 and 253, accompanied by two fragments, *m/z* 270 and 312, with masses 31 units higher than those of the unlabeled C_{31} diketone. Similarly, a molecular ion 31 atomic mass unit (amu) higher than that of the unlabeled compound was found. In addition, the spectrum presented a peak *m/z* 103 consistent with a double McLafferty rearrangement on both sides of the β-diketo group, one of them involving a double-deuterated α-methylene and γ-deuterium transfer, and the other one involving an unlabeled α-methylene and single γ-hydrogen transfer. Two other

abundant fragments were found to accompany *m/z* 103, *m/z* 102 and 104, indicating that other types of fragmentation might also occur, however the identity of those fragments could not be assigned.

The mass spectral characteristics of this compound and its GC retention relative to the unlabeled homolog[78] led to the identification of this compound as $^{2}H_{31}$ C_{31} 14,16-diketone ($^{2}H_{31}$ C_{31} 16,18-diketone) (Figure 4.5 A).

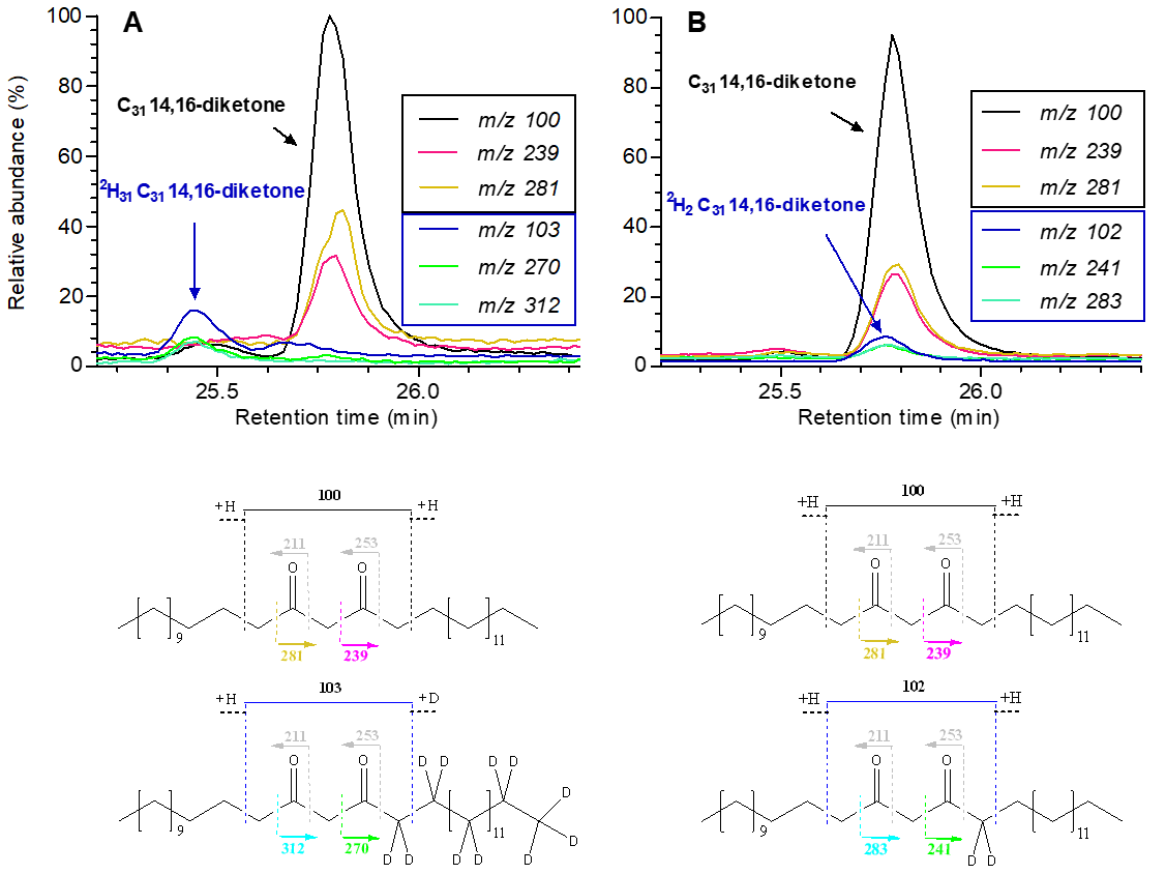

Figure 4.5: **Extracted single ion chromatograms of the most characteristic fragment ions of the deuterium-labeled β-diketones.** Super-imposed chromatograms showing **A.** $^{2}H_{31}$-labeled and unlabeled C_{31} 14,16-diketone (C_{31} 16,18-diketone) as a result of $^{2}H_{31}$-C_{16} FA feeding and **B.** $^{2}H_{2}$-labeled and the unlabeled C_{31} 14,16-diketone (C_{31} 16,18-diketone) resulting from $^{2}H_{2}$-C_{16} FA feeding. Structures underneath indicate the proposed fragmentation of the different compounds.

An analogous experiment was performed by co-feeding C_{16} BKFA with C_{16} FA labeled with two deuteriums on C-2 (2,2-^2H palmitic acid). In this case fragment ions consistent with the presence of $^2H_2$-labeled C_{31} 14,16-diketone (C_{31} 16,18-diketone) were detected eluting only slightly before the peak of unlabeled-diketone, hence making it difficult to obtain a clean mass spectrum for this compound. However, the presence of two characteristic α-fragments, *m/z* 183 and 241, as well as the base peak *m/z* 102 corresponding to the double McLafferty fragment diagnostic for β-diketones, permitted the identification of $^2H_2$ C_{31} 14,16-diketone ($^2H_2$ C_{31} 16,18-diketone) (Figure 4.5 B). Both feeding assays thus led to the formation of similar amounts of deuterium-labeled β-diketone relative to the unlabeled C_{31} β-diketone.

4.3.3 Testing the preference of *Hv*DMP for different BKFA substrates

Preferences of *Hv*DMP for different BKFAs were tested by feeding C_{14}, C_{16} and C_{18} BKFAs to yeast expressing the enzyme and analysis of the resulting β-diketones by GC-MS. C_{35} 14,16-diketone (C_{35} 18,20-diketone) authentic standard was used as internal standard for quantification of the exact amounts of each β-diketone and to allow comparison between the different experiments. Detection of β-diketone in all the experiments indicated that *Hv*DMP was capable of accepting all three BKFAs to form diverse β-diketones, including primarily odd- but also small amounts of even-chain-length and unsaturated β-diketones (Figure 4.6 A).

Feeding of C_{16} BKFA to *Hv*DMP-expressing yeast resulted in 27.2 µg/OD·l of β-diketones, whereas C_{14} BKFA and C_{18} BKFA feeding gave 5.3 µg/OD·l and 18.3 µg/OD·l of β-diketones, respectively (Figure 4.6 B). C_{16} BKFA feeding, resulted in the formation of four different β-diketones, with C_{31} 14,16-diketone (C_{31} 16,18-diketone) dominating (82.2% of the total β-

diketones) along with C_{29} 14,16-diketone (11.3%) and small amounts of the $C_{31:1}$ 14,16-diketone ($C_{31:1}$ 16,18-diketone) and 14,16 C_{30}-diketone (15,17 C_{30}-diketone) (5.5% and 1.0%, respectively).

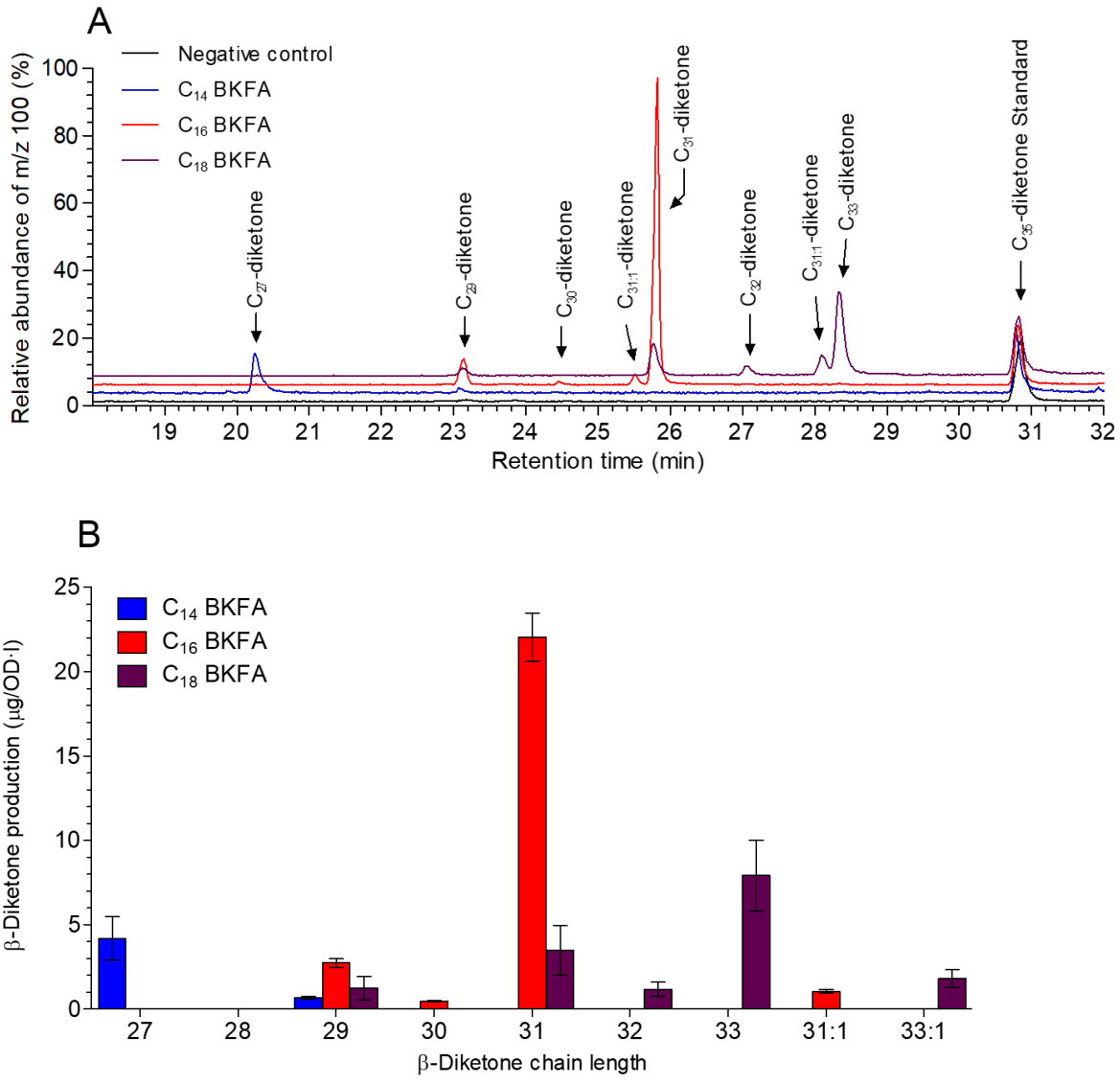

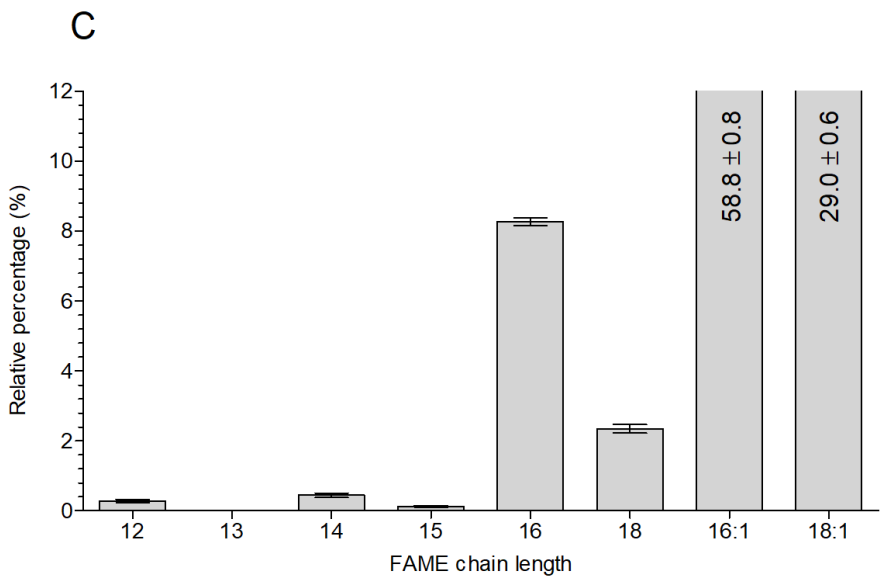

Figure 4.6: **GC-MS analysis of the total lipids extracted from *Hv*DMP-expressing yeast after incubation with C_{14}, C_{16} and C_{18} BKFAs. A** *m/z* 100 extracted ion chromatograms obtained from each independent feeding. **B.** Quantification of the β-diketones formed in each assay using C_{35} 14,16-diketone (C_{35} 18,20-diketone) as internal standard. **C.** Shows the relative percentages of FAMEs obtained from yeast cells transmethylation reaction for the three yeast colonies used. n=3, error bars represents standard deviations.

Feeding of C_{18} BKFA to *Hv*DMP-expressing yeast resulted primarily in the symmetric C_{33} 16,18-diketone (49% of the total β-diketones), together with C_{31} 14,16-diketone (C_{31} 16,18-diketone) (21%) and C_{29} 12,14-diketone (C_{29} 16,18-diketone) (9%), an unsaturated 16,18 $C_{33:1}$-diketone, and an even-chain length homolog C_{32} 15,17-diketone (C_{32} 16,18-diketone). Finally, feeding of C_{14} BKFA led to production of two β-diketone homologs, C_{27} 12,14-diketone (C_{27} 14,16-diketone) and C_{29} 12,14-diketone (C_{29} 16,18 C_{29}-diketone), accounting for 83% and 17% of the total β-diketones, respectively.

Fatty acyl profile of the three yeast colonies used for this experiment by transmethylation of diverse acyl lipids into respective fatty acyl methyl ester (FAME) species, was used as a proxy to assess the endogenous acyl-CoA pools available as substrates for *Hv*DMP in the cells. Unsaturated $C_{16:1}$ and $C_{18:1}$ FAMEs accounted for almost the 88% of the total acyls, with no other unsaturated

homologs detectable (Figure 4.6 C). Saturated C_{16} and C_{18} FAMEs accounted for 12% and 8% of the total acyl pool, respectively. In addition, small amounts of the shorter C_{14} (0.4%) and C_{12} (0.3%) FAMEs were found, together with C_{15} FAME (0.1%) as the only odd FAME detectable.

To test the preference of *Hv*DMP for various fatty acyl-CoA substrates, yeast expressing the enzyme were fed BKFA together with a range of FAs. The mixture of fed FAs was optimized based on the previously determined endogenous yeast fatty acyl profile, with the goal to obtain a more homogenous overall fatty acyl-CoA pool. However, feeding of large amounts of FAs from ethanolic stock solutions impeded yeast growth, resulting in β-diketone amounts too low to be detected. Hence, the lower and higher ranges of FAs accepted by *Hv*DMP together with C_{16} BKFA were first determined, so that FA amounts in both ranges could then be optimized independently. *Hv*DMP-expressing yeast fed with C_{10} and C_{11} FAs produced C_{29} 14,16-diketone and C_{31} 14,16-diketone (C_{31} 16,18-diketone), but C_{25} and C_{26} β-diketones could not be detected, showing that endogenous C_{14} and C_{16} acyls were readily accepted by the enzyme as in previous assays but the exogenous mid-chain length FAs were not. Similarly, co-feeding of C_{16} BKFA with C_{17} FA also yielded C_{31} 14,16-diketone (C_{31} 16,18-diketone) and C_{29} 14,16-diketone, but not the C_{32} homolog expected from direct incorporation of C_{17} FA. In addition, as yeast endogenous C_{18} acyl-CoA was found to not be incorporated in any of the previous *in vivo* experiments, this was also assumed to not be accepted by *Hv*DMP.

Based on the FA feeding experiments thus far, only C_{12} to C_{15} FAs needed to be supplied for further competition assays along with endogenous C_{16} acyl substrate. With the aim to roughly balance the amounts of all these fatty acyl-CoAs, yeast cells were supplemented with C_{15} and C_{14} FAs to final medium concentrations of 0.33 mM each, C_{13} FA was fed to a concentration of 0.66 mM and C_{12}

FA to 1.2 mM. Co-feeding of these FAs with C_{16} BKFA led to the production of five different β-diketones with odd- and even-numbered chain lengths (Figure 4.7 A). In particular, C_{27} 12,14-diketone (C_{27} 14,16-diketone), C_{28} 13,15-diketone (C_{28} 14,16-diketone), C_{29} 14,16-diketone, C_{30} 15,17-diketone (C_{30} 14,16-diketone) and C_{31} 14,16-diketone (C_{31} 16,18-diketone) accumulated to 0.8 µg/OD·l, 2.5 µg/OD·l, 3.7 µg/OD·l, 2.9 µg/OD·l and 1.1 µg/OD·l, respectively, as determined by integration of extracted ion GC-MS traces (*m/z* 100) against internal standard pentatriacontane-14,16-dione (Figure 4.7 B). The total amount of β-diketones produced in this assay was reduced compared to previous experiments without FA feeding, from average total productions of 27.2 µg/OD·l to 11.0 µg/OD·l.

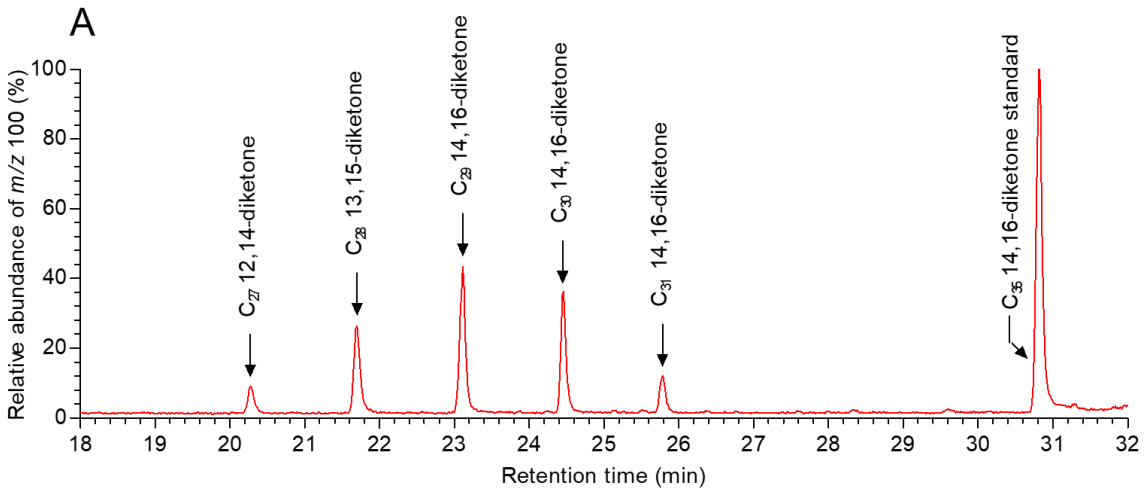

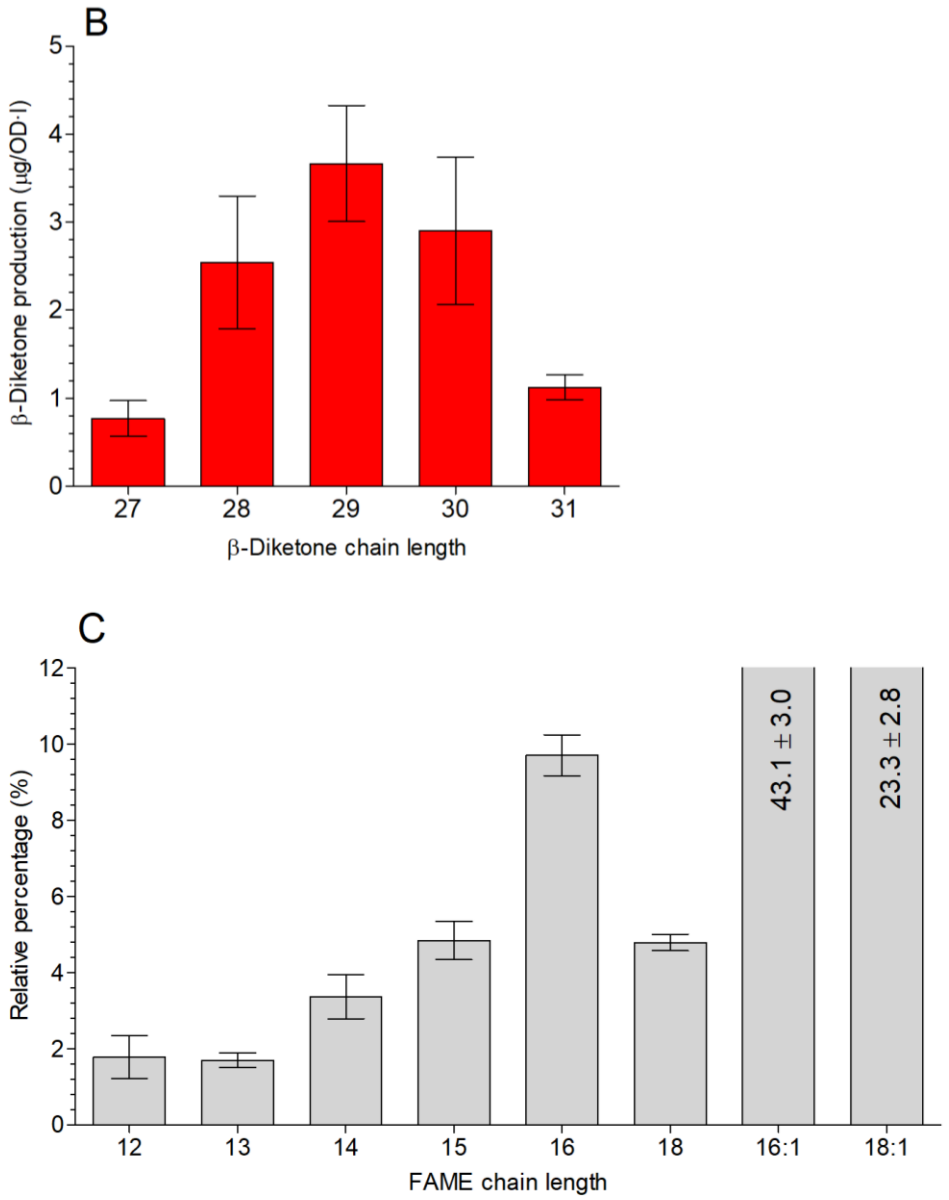

Figure 4.7: **GC-MS analysis of the total lipids extracted from *Hv*DMP-expressing yeast after incubation with C_{16} BKFA and a mixture of C_{12} - C_{15} FAs. A** *m/z* 100 extracted ion chromatogram showing the different β-diketones produced. **B.** Shows the altered FAME profile obtained from the three yeast colonies after FAs feeding and incubation. n=3, error bars represents standard deviation.

4.3.4 In vitro characterization of *Hv*DMP

4.3.4.1 Evaluating whether *Hv*DMP can form triketides or tetraketides from a C_{16} BKFA precursor

A set of *in vitro* assays was carried out to test whether *Hv*DMP has CHS-like PKS activity (catalyzing the formation of polyketides via successive condensations of a BKFA or a fatty acyl-CoA precursor with malonyl-CoA units) and/or an activity of *Hv*DMP analogous to CUS (catalyzing the formation of β-diketones via head-to-head condensation between a BKFA and a fatty acyl-CoA). For this, purified recombinant *Hv*DMP was incubated with C_{16} BKFA and two equivalents of malonyl-CoA, or C_{14} acyl-CoA and two equivalents of malonyl-CoA, and with equimolecular amounts of C_{16} BKFA and C_{14} acyl-CoA. In all the assays, the same amounts of BKFA were fed as in the *in vivo* assays, and all assays were accompanied by a negative control where substrate was incubated with previously boiled protein.

Lipids extracted from assays of feeding C_{16} BKFA or C_{14} acyl-CoA together with malonyl-CoA were analyzed by GC-MS without prior derivatization. Total ion chromatograms were compared with those of respective boiled-protein controls to search for compounds formed by *Hv*DMP, but no additional peaks were detected that would indicate possible *Hv*DMP products. To search specifically for triketide and tetraketide products, extracted ion chromatograms of diagnostic ions were further analyzed. In particular, detailed searches focused on the characteristic fragment ions *m/z* 85 and 100 of 2,4-diketones expected to result from triketides[79], and the ions *m/z* 85, 100, 127 and 142 of 2,4,6-triketones expected from tetraketides (Figure 4.8). However, no compounds with respective fragment combinations could be detected in any of the samples.

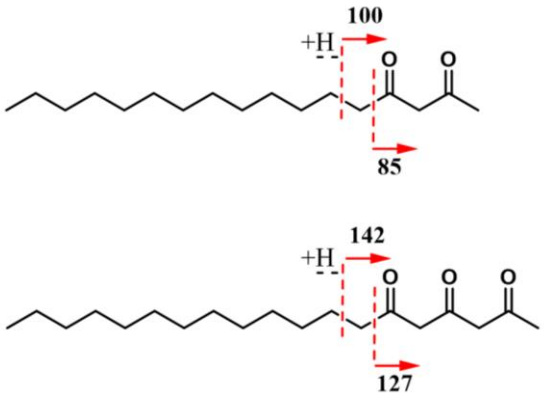

Figure 4.8: **Structure and diagnostic GC-MS fragments of the expected products from degradation of C_{18} 3,5 diketoacid (triketide) and C_{20} 3,5,7 triketoacid (tetraketide).**

Finally, the presence of *Hv*DMP-derived products in lipids from assays involving *Hv*DMP incubation with C_{16} BKFA and C_{14} acyl-CoA was investigated. Respective total ion chromatograms showed a peak eluting at 23.1 min that was missing in respective boiled-protein controls, and that was identified as C_{29} 14,16-diketone based on its mass spectral characteristics. Other β-diketone homologs could not be detected, either in total ion chromatograms or in extracted ion chromatograms of the characteristic fragment *m/z* 100.

4.3.4.2 *Hv*DMP preferences between different BKFAs and fatty acyl-CoAs for formation of β-diketones

In a first experiment, the preference of *Hv*DMP between C_{14}, C_{16} or C_{18} BKFA substrates was tested by incubating recombinant protein with C_{14} acyl-CoA. To ensure competition between the BKFAs, each of them was fed in the same amount as C_{14} acyl-CoA, making the latter the limiting substrate. The lipids extracted after incubation comprised three β-diketones, C_{27} 12,14-diketone (C_{27} 14,16-diketone), 14,16 C_{29}-diketone and 14,16 C_{31}-diketone (16,18 C_{31}-diketone) (Figure 4.9 A), resulting from incorporation of C_{14}, C_{16} or C_{18} BKFA, respectively. Integration of selected ion

chromatograms (*m/z* 100) revealed that approximately 82% of the total β-diketones were formed by C_{14} BKFA, 16% by C_{16} BKFA, and 2% by C_{18} BKFA.

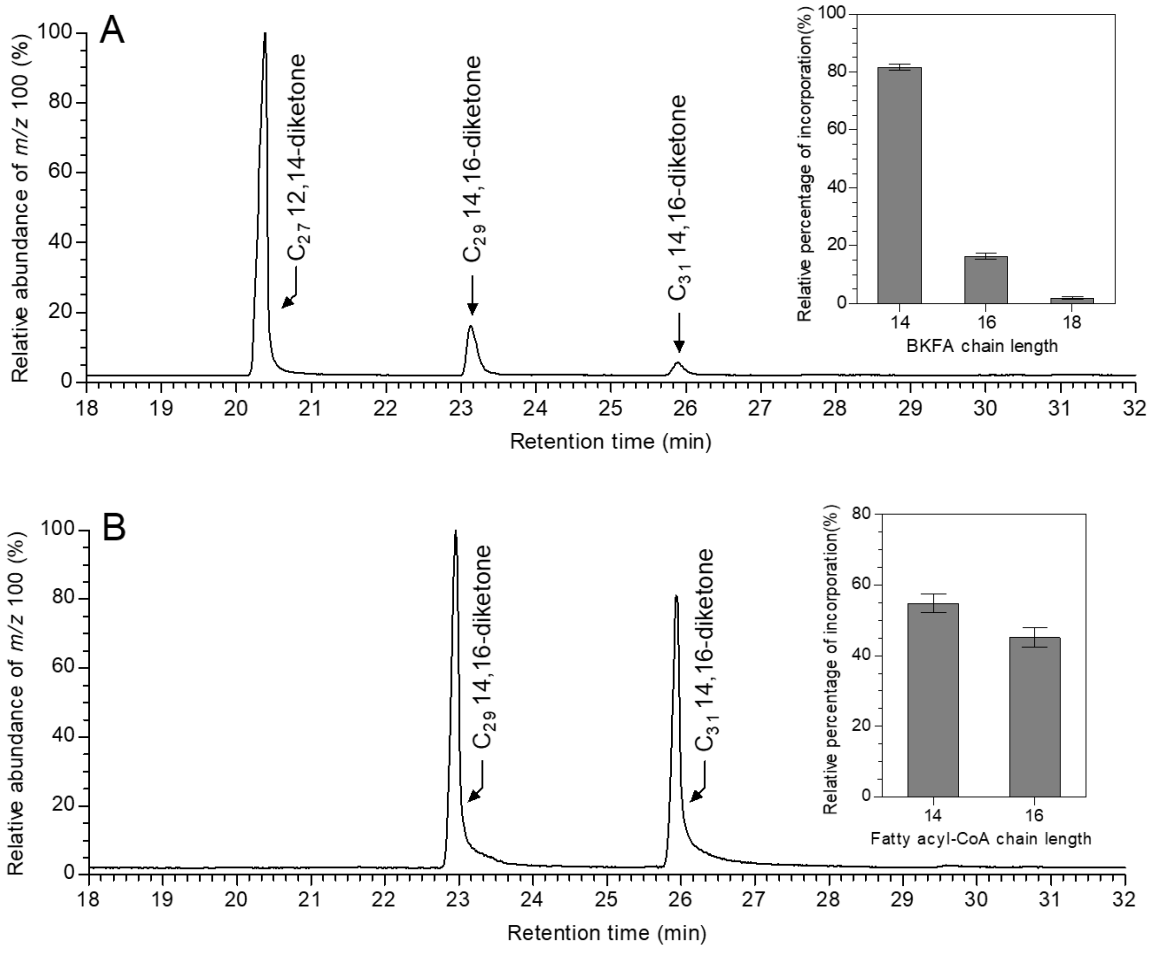

Figure 4.9: **GC-MS analysis of the lipids extracted from the media after *Hv*DMP incubation with different BKFAs and fatty acyl-CoAs. A.** *m/z* 100 extract ion chromatogram showing the different β-diketones produced after protein incubation with C_{14} BKFA, C_{16} BKFA, C_{18} BKFA and C_{14} acyl-CoA and **B.** C_{14} acyl-CoA, C_{16} acyl-CoA and C_{16} BKFA. Insert panels show the relative percentage of incorporation of each BKFA or fatty acyl-CoA determined by the relative abundance of their respective β-diketones among the total β-diketones formed. n=3, error bars represents standard deviation.

In a second experiment, the preference of *Hv*DMP between different fatty acyl-CoAs was also tested *in vitro*. For this, purified protein was incubated with C_{16} BKFA and a mixture of C_{14} and C_{16} acyl-CoAs, with all three compounds at equal concentrations to ensure competition between

the acyl-CoAs and C_{16} BKFA as limiting substrate. The lipid mixtures resulting from these assays contained two β-diketones, identified as C_{29} 14,16-diketone and C_{31} 14,16-diketone (C_{31} 16,18-diketone) in relative amounts of 55% of and 45%, respectively (Figure 4.9 B), showing that *Hv*DMP had a slight preference for C_{14} acyl-CoA.

4.4 Discussion

4.4.1 Formation of β-diketones in yeast expressing *Hv*DMP

Heterologous expression of proteins in yeast combined with exogenous feeding has been widely used to study the activity of plant enzymes involved in the biosynthesis of wax compounds[80] or products of specialized metabolism with high pharmacological value[81,82]. Yeast has been established as a suitable organism for heterologous expression especially for studying membrane-associated proteins. In contrast to prokaryotic systems like *E. coli*, yeast has endomembrane systems, hence offering a suitable environment for membrane-associated proteins and resulting in protein folding similar to the native plant cells. Since the barley DMP enzyme was expected to be localized in the ER, yeast was selected for experiments characterizing the *in vivo* activity of this enzyme.

Feeding of *Hv*DMP-expressing yeast with C_{16} BKFA alone resulted in the formation of a series of β-diketones. Negative controls either harboring empty vector or lacking the exogenous substrate showed that the β-diketones were derived from the activity of *Hv*DMP and that the enzyme required C_{16} BKFA as substrate. However, based on these assays alone, it is impossible to distinguish whether the β-diketone products are formed via a tetraketide intermediate and further elongation or via head-to-head condensation between BKFA and endogenous fatty acyl-CoA. On

the one hand, tetraketide formation and elongation would require several endogenous factors in the yeast host, including further substrates and downstream processing enzymes: (1) *Hv*DMP would require malonyl-CoA co-substrate for formation of the tetraketide intermediate, and this common precursor of many metabolic pathways is present in the yeast environment; (2) elongation of the tetraketide intermediate would have to rely on FAE enzyme complexes, and the wild-type yeast strain used here is known to have analogous activities, since it accumulates VLCFAs up to C_{26}[10], however FAE enzyme complexes catalyzing acyl-CoA elongation up to C_{32} are presumably not present; (3) decarboxylation of the elongation products into β-diketones requires enzymes analogous to Arabidopsis CER1 and CER3, however yeast are unlikely to have respective enzyme activities since they do not produce corresponding alkanes. Hence, it seems very unlikely that the β-diketones found here in wild-type yeast expressing *Hv*DMP are formed via elongation and decarboxylation. In contrast, it seems feasible that the observed β-diketones are formed by head-to-head condensation of BKFA with endogenous fatty acyl-CoAs, since the latter co-substrates are common yeast metabolites and the overall process does not require further endogenous enzyme activities.

4.4.2 Direct incorporation of entire FA moieties into β-diketones via head-to-head condensation

The suggested ability of *Hv*DMP to catalyze the head-to-head condensation between a BKFA and a fatty acyl-CoA was tested first by performing experiments with exogenous feeding of either odd-chain length BKFAs or FAs, and analysis of the unnatural even-chain length β-diketones. When C_{15} FA and C_{16} BKFA were fed to yeast expressing *Hv*DMP, mainly the even-chain length C_{30} 14,16-diketone (C_{30} 15,17-diketone) was formed, indicating incorporation of an odd-chain length

precursor. Specifically, the position of the carbonyls strongly suggested that exogenous FA was taken up by the yeast cells, activated into the corresponding CoA ester (most likely facilitated by the co-expressed LACS1), and that the acyl moiety was condensed directly with C_{16} BKFA, without prior modification of the acyl carbon skeleton. The additional formation of C_{29} 14,16-diketone and C_{31} 14,16-diketone (C_{31} 16,18-diketone) can be explained by the presence of yeast endogenous C_{14} and C_{16} acyl-CoAs that may have served for *Hv*DMP-catalyzed condensation with the C_{16} BKFA substrate.

Direct incorporation of the entire acyl moiety was corroborated in a second set of experiments using deuterium-labeled FAs as exogenous substrate. Feeding of $^{2}H_{31}$-C_{16} FA together with C_{16} BKFA led to the production of $^{2}H_{31}$-C_{31} 14,16–diketone ($^{2}H_{31}$-C_{31} 16,18–diketone), confirming that the hydrocarbon structure of the FA was incorporated directly, without prior modification through other metabolic processes. However, much less labeled than unlabeled C_{31} 14,16–diketone (C_{31} 16,18–diketone) was found, in contrast to the previous experiment where more exogenous C_{15} acyl than endogenous C_{16} acyl was incorporated. The lower incorporation of $^{2}H_{31}$-labeled C_{16} FA may reflect a preference of *Hv*DMP for the slightly shorter substrate and/or, conversely, a preference of yeast enzymes competing for the lipid substrates to utilize C_{16} rather than C_{15} acyls. However, the relatively poor incorporation of labeled C_{16} FA substrate may also be due to discrimination against this substrate either during uptake and activation by *At*LACS1 or during condensation by *Hv*DMP. While it is currently impossible to assess which of these factors may have led to the reduced overall incorporation rates, the discrimination may be further tested using exogenous FA substrate labeled with fewer deuterium atoms. To investigate this, yeast expressing *Hv*DMP were incubated with $^{2}H_{2}$ C_{16} FA and C_{16} BKFA under the same conditions as in the previous experiment involving $^{2}H_{31}$ C_{16} FA. The results showed that $^{2}H_{2}$-C_{31} 14,16–diketone ($^{2}H_{2}$-

C_{31} 16,18–diketone) was formed, however the relative amount of labeled β-diketone was similar to the previous experiment with $^{2}H_{31}$-labeled species. Taken together, these results indicate that either discrimination against labeled substrates was mainly due to deuterium labels on C-2 of the FA molecules, or that indeed *Hv*DMP showed a preference for C_{15} acyl substrate.

4.4.3 Direct incorporation of entire BKFA moieties into β-diketones via head-to-head condensation

Similar to previous tests on FA substrates of *Hv*DMP, further experiments tested whether the BKFA moiety was also incorporated into β-diketones without prior modification. To this end, C_{17} BKFA and C_{14} FA substrates were fed to yeast expressing *Hv*DMP, and C_{30} 14,16-diketone (C_{30} 15,17-diketone) was found to be the main β-diketone formed. All other homologs detected also had an odd-chain length acyl moiety of the same length (C_{15}), suggesting that they were all formed from the same BKFA precursor with odd-numbered chain length through condensation with different acyl-CoAs (all with even-numbered chain lengths). Together, these results suggest that the BKFA precursor is incorporated into the β-diketone product without prior modification of the carbon skeleton, in its entirety except for the carboxyl carbon. The present results further show that the same β-diketone, C_{30} 14,16-diketone (C_{30} 15,17-diketone), can be formed either from C_{16} BKFA and C_{15} FA or from C_{17} BKFA and C_{14} FA, overall confirming that β-diketone biosynthesis proceeds via a head-to-head condensation mechanism between both substrates.

Interestingly, earlier experiments had already shown that incubation of barley spike tissue with C_{15} FA leads to the formation of C_{30} 14,16-diketone (C_{30} 15,17-diketone)[16], most likely due to activity of *Hv*DMP. In these experiments, radioactive label on C-1 of the C_{15} FA substrate was found on C-16 of the β-diketone product, leading to the conclusion that C_{15} FA was first converted into C_{17}

BKFA and then elongated/decarboxylated into β-diketone product. However, the product labelling pattern may equally well be explained by the alternative mechanism for β-diketone formation, via head-to-head condensation of C_{16} BKFA and C_{15} acyl-CoA units. Both alternative mechanisms may now be distinguished based on the present results, showing that C_{30} 14,16-diketone (C_{30} 15,17-diketone) can indeed be formed from C_{15} FA, however it does not have to be converted into C_{17} BKFA for this but can be condensed directly with C_{16} BKFA instead.

Final confirmation of the activity of *Hv*DMP was achieved by its *in vitro* characterization, avoiding interference from endogenous enzymes or substrates. Both hypotheses for the biochemical activity of *Hv*DMP were tested, invoking either the formation of tri- and tetraketides via malonyl-CoA incorporation or head-to-head condensation of BKFA and acyl-CoA. Incubation of *Hv*DMP with either BKFA or fatty acyl-CoA as starter substrate and malonyl-CoA as extender did not result in the formation of polyketides, neither in the form of tri- and tetraketide intermediates nor of β-diketone end products. However, incubation of *Hv*DMP with C_{16} BKFA and C_{14} acyl-CoA yielded C_{29} 14,16-diketone, thus corroborating the decarboxylative head-to-head condensation as the primary mechanism through which *Hv*DMP catalyzes the formation of β-diketones.

4.4.4 Characterizing *Hv*DMP preference for different BKFA and FA chain lengths

In order to understand the formation of the different β-diketones found in barley *cv.* Morex waxes, the chain length preferences of all enzymes on the pathway leading to these products must be tested. Therefore, the *in vitro* and *in vivo* assays testing the *Hv*DMP activity were further developed to enable an evaluation of the enzyme preferences for different fatty acyl-CoAs and BKFAs.

First, *in vitro* assays involving competition between all the *Hv*DMH products (as tested in *E. coli*), C_{14} BKFA, C_{16} BKFA and C_{18} BKFA, for C_{14} acyl-CoA demonstrated that the three BKFAs were

accepted as substrates for β-diketone biosynthesis, with distinct preference for shorter BKFA chain lengths. On the other hand, *in vitro* assays involving competition between C_{14} and C_{16} acyl-CoA for C_{16} BKFA revealed a preference for the shorter of the two acyl substrates.

Then, *in vivo* assays were performed to further study the *Hv*DMP preferences for different fatty acyl-CoAs as a function of the BKFA. The yeast system used offers a broad range of endogenous fatty acyl-CoA chain lengths (C_{12} to C_{18}, including odd-chain length and unsaturated species), hence avoiding the need to supplement expensive or not commercially available fatty acyl-CoAs. Furthermore, it was shown that the pool of fatty acyl-CoAs available for β-diketone formation could be altered by feeding FAs to the yeast, therefore permitting to augment fatty acyl homologs that occur a relatively low concentration in yeast. The *in vivo* assays confirmed that C_{14} BKFA, C_{16} BKFA and C_{18} BKFA were all accepted by *Hv*DMP, and that the enzyme *Hv*DMP had preferences for certain fatty acyl-CoA chain lengths depending on the BKFA chain length. To quantify the FA preferences, the amounts of each β-diketone formed can be assessed relative to the abundance of the acyl incorporated into it (determined by FA profiling of the yeast used), leading to ratios of β-diketone amounts per FA substrate present.

The *in vivo* assays performed without feeding exogenous FA showed that C_{14} BKFA was preferentially condensed with C_{14} acyl-CoA, resulting in C_{27} 12,14-diketone (C_{27} 14,16-diketone) (Figure 4.10 A). Interestingly, this β-diketone is not found in barley wax, but its formation had been reported for tissue slices incubated with labeled C_{14} FA[16]. To a much lesser extent, *Hv*DMP also condensed C_{14} BKFA with C_{16} acyl units to yield C_{29} 12,14-diketone (C_{29} 16,18-diketone), while other fatty acyl-CoA homologs were not accepted as co-substrates along with C_{14} BKFA.

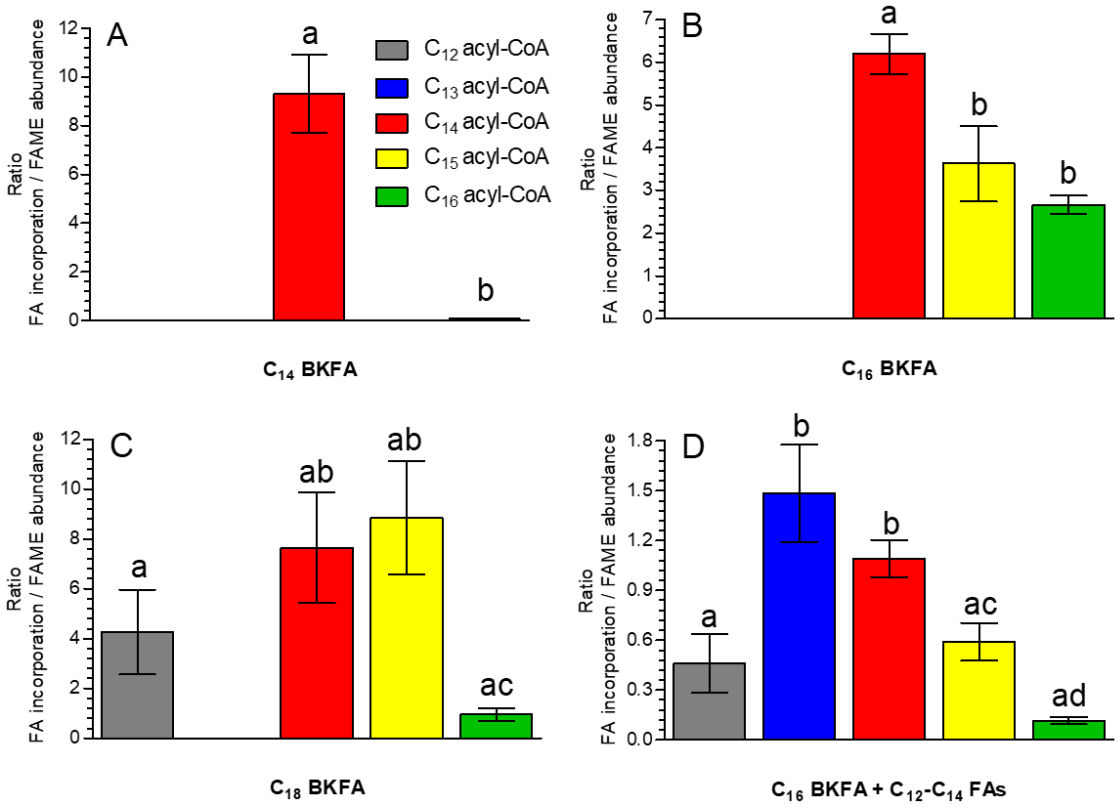

Figure 4.10: ***Hv*DMP preference for different fatty acyl-CoA chain lengths as a function of the BKFA.** Yeast *in vivo* assays showed that *Hv*DMP had preference for certain fatty acyl-CoAs when supplied with **A,** C_{14} BKFA, **B,** C_{16} BKFA and **C,** C_{18} BKFA. **D.** Further assays involving co-feeding of C_{16} BKFA with C_{12} to C_{15} FA showed that *Hv*DMP had a preference peaking at C_{13} acyl-CoA. Preferences were determined based on the ratio between β-diketone amounts produced in each sample and the relative abundance, in the same sample, of the fatty acyl-CoA incorporated into each homolog. n=3, error bars represent standard deviation. Anova post hoc Tukey tests were performed on the different data sets ($p<0.05$).

Further *in vivo* assays (also without feeding exogenous FA) showed that C_{16} BKFA is condensed with yeast endogenous C_{14}, C_{15} and C_{16} acyl-CoAs to form C_{29}, C_{30} and C_{31} β-diketones, respectively (Figure 4.10 B). C_{14} acyl-CoA was the preferred substrate for *Hv*DMP in combination with C_{16} BKFA, with lesser activities on C_{15} and C_{16} acyl-CoAs (that were not significantly different). Finally, C_{18} BKFA was condensed with endogenous C_{12}, C_{14}, C_{15} and C_{16} acyl-CoAs into C_{29}, C_{31}, C_{32} and C_{33} β-diketones, respectively. This BKFA substrate was preferentially

combined with C_{15} and C_{14} acyl-CoA, less with C_{12} acyl-CoA (not significantly different), and in a low extent with C_{16} acyl-CoA (significantly different) (Figure 4.10 C).

It is worth noting that the total acyl profiles determined here can be taken only as a rough proxy for the acyl-CoA pool compositions, since the method used for generating the methyl esters likely released acyls from membrane phospholipids and glycolipids, thus including lipid metabolism end products rather than transient precursors. As saturated and unsaturated C_{16} and C_{18} FAs are the predominant FAs incorporated into membranes[83], the relative abundance of respective CoAs may be over-estimated by total acyl profiling. Nevertheless, the FA profiles reported here closely match the fatty acyl-CoA profiles of other wild-type yeast strains with no fatty acid elongation alterations[84].

It should also be noted that the relatively low amounts of endogenous C_{12} to C_{15} acyls (as compared to C_{16}) may have led to somewhat inaccurate quantifications, and thus over-estimated product: substrate ratios for respective chain lengths. To overcome these issues, *Hv*DMP-expressing yeast were co-fed with C_{16} BKFA and C_{12} to C_{15} FAs to compensate for the low endogenous levels of these short substrate homologs. Feeding was restricted to these chain lengths, since acyl chain lengths below C_{12} and above C_{16} had not been incorporated into β-diketones in previous experiments. The exogenous supplement of FAs led to a more homogenous acyl profile, as shown by total acyl analysis of the resulting yeast cells. Co-feeding with C_{16} BKFA then corroborated the preference of *Hv*DMP for C_{14} acyl-CoA in the presence of this BKFA, with lower activity for C_{12}, C_{15} and C_{16} acyls (not significantly different) (Figure 4.10 D). Interestingly, *Hv*DMP had similar preference for C_{13} acyl and C_{14} acyl (not significantly different), which had not been observed in previous assays due to the low amounts of endogenous C_{13} acyl-CoA in yeast. Overall, *Hv*DMP showed inverse selectivities between its two substrates, where the longer BKFAs were

preferentially condensed with shorter acyls and vice versa. Moreover, *Hv*DMP had a much lower activity on unsaturated FA-CoA substrates compared to corresponding saturated acyls, independently of the BKFA.

The enzyme immediately upstream of *Hv*DMP on the pathway, *Hv*DMH, delivers mainly C_{16} BKFA as substrate for β-diketone formation, and the present assays showed that *Hv*DMP can condense this substrate with a relatively broad range of fatty acyl-CoA co-substrates. However, among the preferred co-substrates of *Hv*DMP, C_{13} - C_{15} acyl-CoAs are likely present in the barley ER only at very low concentrations, while C_{16} acyl-CoA is known to occur in relatively high amounts. Accordingly, the corresponding C_{28} – C_{30} β-diketones are found at very low concentrations in barley wax, or not at all, while C_{31} β-diketone is found as a major wax constituent. The sharp chain length distribution of wax β-diketones is, thus, mostly due to the strongly dominating acyl-CoA chain length along with the equally narrow profile of BKFAs delivered by *Hv*DMH. Overall, the chain length preferences found here in various assays are in agreement with the β-diketone chain length profiles observed in the wax product mixtures. It can be concluded that the β-diketone homolog profile is dictated largely by the chain length distribution within the available pools of its two substrates, and relatively little by the preferences of *Hv*DMP between various substrate homologs.

Chapter 5: **Conclusions and future directions**

5.1 *Hv*DMH catalyzes the formation of the β-diketone precursors C_{14}, C_{16} and C_{18} BKFAs in *E.coli.*

*Hv*DMH, previously designated as CER-Q, has been recognized as the first enzyme acting on the β-diketone biosynthesis pathway for more than 40 years. Its biochemical activity has long been speculated, mostly assuming that this enzyme is involved in Claisen-type C-C bond formation. However, the recent identification of the encoding gene enabled a tentative biochemical characterization, revealing that *Hv*DMH is a TE with primary function towards the formation of C_{16} BKFA. These initial results prompted a re-evaluation of the long-standing assumption that β-diketones are formed by elongation of a C_{18} precursor, and they opened the possibility that β-diketones are instead formed by head-to-head condensation of BKFA and acyl-CoA.

Here, it was firstly confirmed that *Hv*DMH has activity towards the formation of BKFAs, rather than free fatty acids or β-hydroxy fatty acids as shown for other TEs. Specifically, it was observed that, in agreement with the previous partial characterization, C_{16} BKFA is its principal product and that *Hv*DMH also possesses, to a lower extent, preference towards the formation of C_{14} and C_{18} BKFAs. Based on previous characterization of other TEs similar to *Hv*DMH, it may be assumed that the *Hv*DMH chain length preference observed in *E. coli* is similar to that *in planta*. Approaches such as transient expression of *Hv*DMH in tobacco are needed to confirm this. Meanwhile, it should be noted that the homolog distribution of alkan-2-ol esters in barley *cv.* Morex wax matches the BKFA product profile of *Hv*DMH observed in *E. coli.* Therefore, it seems very likely that this first enzyme on the β-diketone biosynthesis pathway generates C_{14}, C_{16} and C_{18} BKFAs *in planta*.

In addition, the strong activity of *Hv*DMH observed in *E. coli* and its primary sequence including a predicted transit peptide sequence both suggest that *Hv*DMH is localized in the plastids *in planta*, where it may intercept β-keto acyl-ACP intermediates during *de novo* biosynthesis of fatty acids. However, its subcellular localization still remains to be proven in future research.

5.2 β-Diketones are biosynthesized via head-to-head condensation between BKFAs and fatty acyl-CoAs catalyzed by *Hv*DMP

Here, it was shown that the primary activity of *Hv*DMP does not involve the formation of tetraketides from BKFA precursors, but that this enzyme instead displays a strong activity, *in vivo* and *in vitro*, towards condensing BKFAs and fatty acyl-CoAs into β-diketones. As observed from *in vivo* assays with labeled substrates, entire FA molecules were incorporated into the β-diketones, indicating that a mechanism involving BKFA decarboxylative condensation with fatty acyl-CoAs, as proposed for CUS and CURS, must occur. The results obtained here, thus, indicate that *Hv*DMP is the third plant type-III PKS identified to catalyze a head-to-head condensation between β-ketoacids and acyl-CoA substrates *in planta*. This mechanism could be further corroborated by *in vitro* assays, analogous to the ones presented in this research, involving the use of C-1 labeled BKFA substrates and determining if the label is lost during β-diketone formation, indicating that BKFA decarboxylation occurs in the process.

Moreover, it has been determined that *Hv*DMP specificity towards the different fatty acyl-CoAs is linked to BKFA chain length. Specifically, *Hv*DMP is capable of accepting fatty acyl-CoAs ranging from C_{12} to C_{16} and BKFAs from C_{14} to C_{18}. In particular, *Hv*DMP accepts a narrow range of fatty acyl-CoAs, preferably C_{14} acyl-CoA together with C_{14} BKFA. However, *Hv*DMP also catalyzes the condensation of C_{16} and C_{18} BKFAs with a range of fatty acyl-CoAs (C_{12} to C_{16}),

with inverse chain length preferences between the two substrates. The observed preferences must be regulated by the size and geometry of the enzyme substrate-binding pocket/s, similar to other type-III PKSs. A more detailed understanding of the condensation mechanism of *Hv*DMP may be expected from determination of its crystal structure as well as a more detailed characterization including enzyme kinetics studies in the future.

In addition, the subcellular localization of *Hv*DMP should be determined, to test whether it has access to both its substrates. Interestingly, the BKFA precursor is thought to be generated in plastids, while the acyl-CoA substrates are likely formed in the ER. *Hv*DMP must, therefore, reside in either of these compartments, and one of its substrates must be transported between them.

5.3 A revised pathway for biosynthesis of the β-diketone-related compounds in barley (*Hordeum vulgare*)

Four decades of intense research into the biosynthesis of β-diketones resulted in extended barley wax mutant collections and large sets of experiments involving feeding of different radiolabeled substrates, spurring progress in our understanding of the biosynthesis of these particular wax compounds. The great advances since then due to modern sequencing technologies have revealed the identity of the enzymes involved in the biosynthesis of β-diketone-related compounds, and this in turn has enabled the current research leading to the revision of the β-diketone-forming pathway (Figure 5.1).

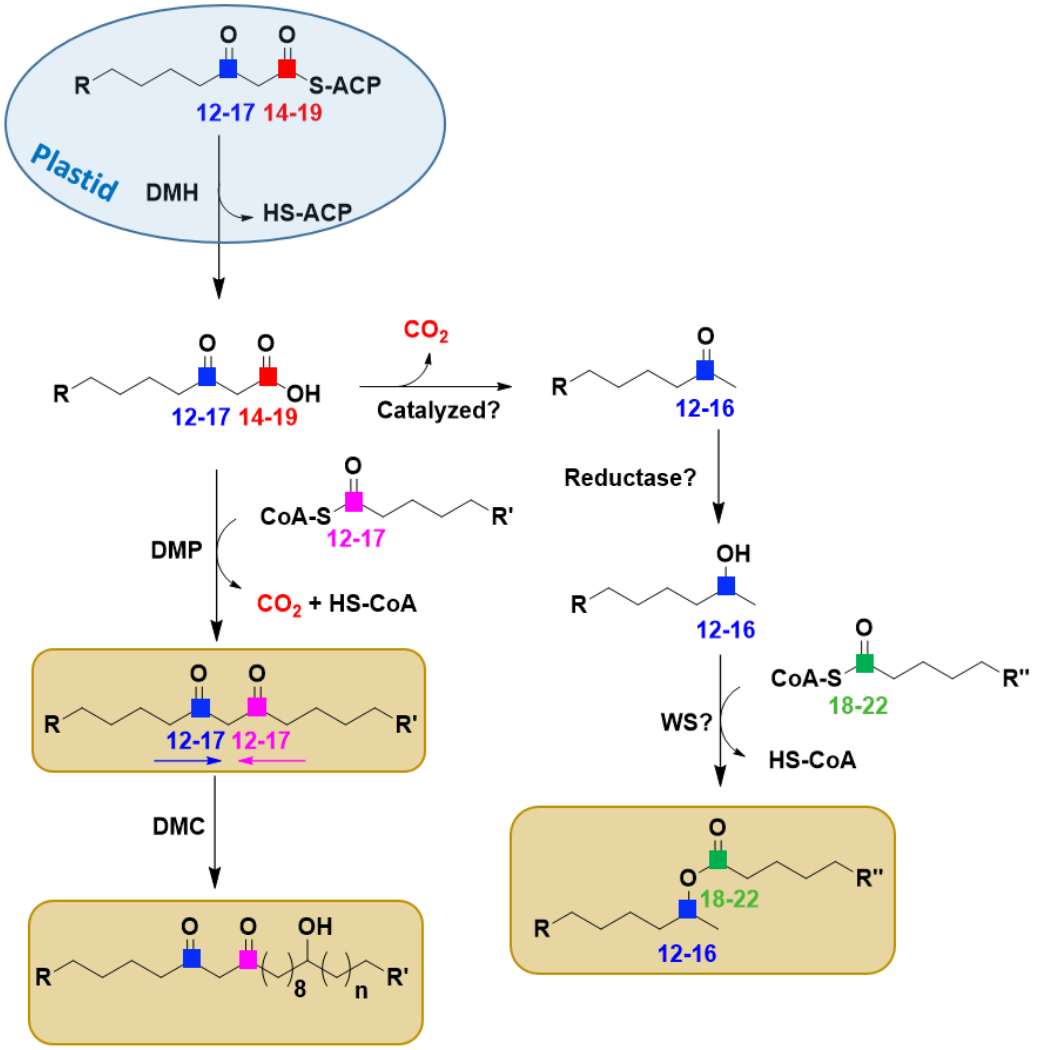

Figure 5.1: **Revised pathway leading to the formation of the different β-diketone-related compounds found in barley *cv.* Morex waxes.** A novel mechanism for β-diketone biosynthesis involving head-to-head condensation between BKFAs and fatty acyl-CoAs is proposed. The carbonyl carbon lost during BKFA decarboxylation either for methylketone formation or condensation with a fatty acyl-CoA is indicated in red. The carbonyl carbons incorporated into the β-diketones from the BKFA and the fatty acyl-CoA are indicated in blue and pink, respectively. Based on the β-diketone homolog and isomer distribution in barley *cv.* Morex wax, all the possible chain length for both precursors are indicated. Arrows indicate the two possible nomenclatures for β-diketones given by the BKFA or the acyl-CoA moiety based on their respective chain lengths. Among the four different hydroxy-β-diketones identified in barley *cv.* Morex wax, the two symmetric homologs (5-hydroxy-nonacosane-14,16-dione and 7-hydroxy-tritriacontane-16,18-dione) can be indistinguishably hydroxylated at both moieties, whereas for the two asymmetric isomers (23-hydroxy-nonacosane-12,14-dione and 25-hydroxy-hentriacontane-14,16-dione) hydroxylation occurs at the acyl-CoA moiety, assuming C_{16} acyl-CoA as the primary acyl-CoA homolog incorporated into the β-diketones.

In the new model for β-diketone biosynthesis, *Hv*DMH is the first enzyme along the pathway producing BKFAs, the central precursors for all β-diketone-derived compounds. Specifically, *Hv*DMH provides BKFAs with chain lengths ranging from C_{14} to C_{18}, mainly C_{16} BKFA. Then, BKFA decarboxylation, spontaneous or enzymatically catalyzed, leads to the formation of methylketones, which, in barley, have been shown to be reduced by a currently unidentified reductase and incorporated into alkan-2-ol esters through esterification with C_{18} to C_{22} FAs, catalyzed by a WS. Even though some WS candidates have been proposed, this enzyme still remains to be identified[21].

In parallel, BKFAs also serve as substrate for *Hv*DMP, which catalyzes the head-to-head condensation of the BKFAs with fatty acyl-CoAs to form β-diketones. Even though at this point the exact chain length of both substrates used by *Hv*DMP *in planta* cannot be assessed, the different β-diketone homologs and isomers identified in this study suggest two major alternatives of BKFA and fatty acyl-CoA chain length combinations (Figure 5.2). Ultimately, these alternatives can be distinguished only based on the exact BKFA chain lengths produced by *Hv*DMH *in planta* and the availability of endogenous fatty acyl-CoAs in plant epidermal cells.

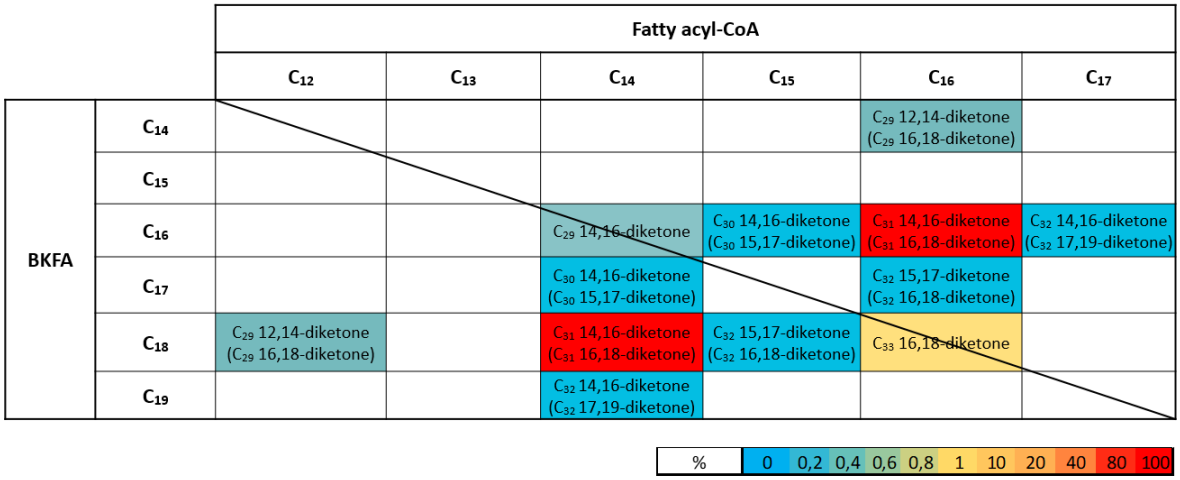

Figure 5.2: **Heat map representing the approximate β-diketone amounts found in barley *cv.* Morex spike wax and the different combinations of BKFAs and FAs leading to their formation.** Colors represent the relative abundance (%) of each isomer. The black line divides the two alternatives through which asymmetric β-diketones can be biosynthesized.

The first alternative is in agreement with the alkan-2-ol chain length profile, the observed activity of *Hv*DMH in *E. coli* and, interestingly, also with early tissue incubation experiments. It involves C_{16} BKFA as a predominant precursor which is preferentially condensed with C_{16} acyl-CoA, producing the major β-diketone homolog, C_{31}. C_{16} BKFA may also, to a smaller extent, be condensed with other fatty acyl-CoAs in the chain length range C_{14} - C_{17}. In addition, minor amounts of C_{14} to C_{18} BKFAs will also be condensed with C_{16} acyl-CoA into the other β-diketone homologs and isomers found in barley wax. However, some of the observed homolog and isomer distributions do not match respective substrate preferences found in the feeding experiments presented here, suggesting that product profiles *in planta* are determined by substrate pool composition as well as enzyme substrate preference. In particular, the current results imply that C_{16} is the main acyl-CoA chain length incorporated into β-diketones. It seems very plausible that C_{16} acyl-CoA is indeed the major homolog in barley epidermal ER, based on fatty acyl-CoA profiles of Arabidopsis total leaf tissue showing strong predominance of this acyl-CoA chain

length[85]. However, further research is needed to assess the acyl-CoA distribution in relevant barley tissues.

The second alternative involves C_{18} BKFA as the predominant BKFA that is condensed primarily with C_{14} acyl-CoA and, less, with C_{12} to C_{16} acyl-CoAs. Other, minor BKFA homologs would also be condensed with C_{14} acyl-CoA, giving rise to the rest of the β-diketone homologs and isomers. Interestingly, this alternative fits with the determined preference of *Hv*DMP for C_{14} acyl-CoA independently of the BKFA chain length. However, the stronger preference of *Hv*DMP for C_{14} acyl-CoA cannot account for the big differences in abundances between the C_{33} and the C_{31} β-diketones found in barley wax, necessitating that larger amounts of C_{14} acyl-CoA are available in epidermal cells as compared to C_{16} acyl-CoA. Given the acyl-CoA profiles in Arabidopsis and other species, this seems rather unlikely. In addition, the presence of large amounts of C_{14} acyl-CoA in epidermal cells, together with the presence of C_{14} BKFA (as indicated by corresponding ester profiles), should lead to the formation of C_{27} β-diketone. The finding that this diketone cannot be detected in barley wax then argues further against high C_{14} acyl-CoA amounts and, thus, this overall pathway alternative. It would also imply substantial enzyme specificities that seem unlikely, including alkan-2-ol ester formation regulated by WS preference rather than by the relative abundance of alkan-2-ols and *Hv*DMH chain length specificity varying between *E. coli* and barley.

Finally, a combination of both alternative chain length combinations also seems unlikely, since the formation of C_{16} and C_{18} BKFA by *Hv*DMH in similar amounts would not match either the alkan-2-ol ester profile or the β-diketone profile found in barley. As shown in this study, C_{16} and C_{18} BKFAs are both preferentially condensed with C_{14} acyl-CoA, hence comparable amounts of

C_{29} 14,16-diketone and C_{31} 14.16-diketone (C_{31} 16,18-diketone) would be expected if both BKFAs were present.

All the current evidence taken together, it seems very likely that β-diketone formation proceeds mainly via C_{16} BKFA rather than C_{18} BKFA. Ultimately, both scenarios may be distinguished by determining the activity of *Hv*DMH *in planta*, to determine the composition of BKFAs available as substrate pool for *Hv*DMP. Respective investigations should be flanked by experiments determining the fatty acyl-CoA profile in barley epidermal cells, specifically in the β-diketone-producing organs, to determine the precise chain length of the precursors leading to the formation of the different β-diketones.

5.4 Hydroxy-β-diketone biosynthesis in *Hordeum vulgare*

Earlier studies suggested that *Hv*DMC performs the hydroxylation of β-diketones into hydroxy-β-diketones. Based on this, the discovery of novel hydroxy-β-diketone homologs and isomers in this study now enables further inferences on the activity of this enzyme. The relative abundances of the three hydroxy-β-diketone homologs detected here, C_{29}, C_{31} and C_{33}, matched the relative abundances of respective β-diketones with corresponding chain lengths, strongly suggesting that these serve as precursors for hydroxylation. Moreover, the finding that the predominant hydroxy-β-diketone has the hydroxyl group almost exclusively on C-25 (or C-7 counting form the opposite end) indicates that the *Hv*DMC enzyme is capable of recognizing the C_{16} moiety of the molecule and to perform the hydroxylation almost exclusively at C-7. In contrast, the C_{29} homolog, composed of two isomers of the β-diketo group, showed substantial variation of the hydroxyl group positions. The two isomers with hydroxyls at C-23 (C-7 counting from the end of the molecule) and C-25 (C-5 counting from the end of the molecule) were found in similar abundance. Even

though the position of the hydroxyl group on either side of the β-diketone group could not be unambiguously confirmed, these results indicate that each isomer is hydroxylated at different positions. Interestingly, β-diketone homologs lacking C_{16} moieties, such as the symmetric C_{29} 14,16-diketone, may be hydroxylated preferentially at C-5, suggesting that *Hv*DMC is capable of specifically performing the hydroxylation ten carbons away from the β-diketo group.

Further characterization of *Hv*DMC is required to corroborate the suggested activity of this enzyme as presented here based on the different hydroxy-β-diketones found in barley wax. However, *Hv*DMC characterization *in vivo* or *in vitro* may be challenging due to the highly hydrophobic nature of its substrates. Hence, reconstruction of the β-diketone biosynthesis pathway in yeast, by co-expressing *Hv*DMC and *Hv*DMP, might be a good approach in order to generate β-diketones available for *Hv*DMC and permit a more extended characterization of this enzyme.

5.5 Biosynthesis of β-diketone-derived compounds in other plant species

In wheat (*Triticum aestivum*), the gene loci *W1*, *W2* and *W3* are responsible for the formation of β-diketone-derived compounds and have been shown to each comprise genes homologous to the barley *CER-C, CER-Q* and *CER-U* genes[21]. In addition, closely related *CER-CQU* gene orthologues have also been identified in more distant grass species such as switchgrass (*Panicum virgatum*). Hence, the pathway presented here might also be extrapolated to these species. For more distant species such as *Eucalyptus* or carnation (*Dianthus caryophyllus*), among others, also known to have β-diketone-related compounds in their waxes, it still needs to be demonstrated if the *CER-C, CER-Q* and *CER-U* genes have been conserved, and if β-diketone biosynthesis there also occurs analogously to Poaceae species[20]. This will be an interesting question to answer in the future.

Overall, the research presented here represents an important step forward for our understanding of the biosynthesis of the predominant wax compounds in barley leaf sheath, peduncle and spikes, the β-diketones. It is also very likely that this might be extrapolated to the closely related species, wheat. Hence, this research may enable the breeding of new cultivars of these two cereal species, extensively cultivated worldwide, with enhanced drought resistance and higher production yield associated to larger presence of β-diketones on their surfaces[86].

Bibliography

1. Jetter, R., Kunst, L., & Samuels, A. L. (2007). Composition of plant cuticular waxes. *Annual Plant Reviews Volume 23: Biology of the Plant Cuticle*, 145-181.
2. Antoniou Kourounioti, R. L., Band, L. R., Fozard, J. A., Hampstead, A., Lovrics, A., Moyroud, E. & Glover, B. J. (2013). Buckling as an origin of ordered cuticular patterns in flower petals. *Journal of the Royal Society Interface*, *10*(80), 20120847.
3. Buschhaus, C., & Jetter, R. (2011). Composition differences between epicuticular and intracuticular wax substructures: how do plants seal their epidermal surfaces?. *Journal of experimental botany*, *62*(3), 841-853.
4. Koch, K., & Ensikat, H.-J. (2008). The hydrophobic coatings of plant surfaces: epicuticular wax crystals and their morphologies, crystallinity and molecular self-assembly. *Micron*, *39*(7), 759-772.
5. Bargel, H., Koch, K., Cerman, Z., & Neinhuis, C. (2006). Evans Review No. 3: Structure–function relationships of the plant cuticle and cuticular waxes—a smart material?. *Functional Plant Biology*, *33*(10), 893-910.
6. Lee, S. B., & Suh, M. C. (2015). Advances in the understanding of cuticular waxes in *Arabidopsis thaliana* and crop species. *Plant cell reports*, *34*(4), 557-572.
7. Kunst, L., & Samuels, A. (2003). Biosynthesis and secretion of plant cuticular wax. *Progress in lipid research*, *42*(1), 51-80.
8. Jenks, M. A., Tuttle, H. A., Eigenbrode, S. D., & Feldmann, K. A. (1995). Leaf epicuticular waxes of the *eceriferum* mutants in Arabidopsis. *Plant physiology*, *108*(1), 369-377.
9. Lardizabal, K. D., Metz, J. G., Sakamoto, T., Hutton, W. C., Pollard, M. R., & Lassner, M. W. (2000). Purification of a jojoba embryo wax synthase, cloning of its cDNA, and production of high levels of wax in seeds of transgenic Arabidopsis. *Plant physiology*, *122*(3), 645-656.
10. Bernard, A., Domergue, F., Pascal, S., Jetter, R., Renne, C., Faure, J.-D., Haslam, R., Napier, J., René Lessire, & R. Joubès, J. (2012). Reconstitution of plant alkane biosynthesis in yeast demonstrates that Arabidopsis ECERIFERUM1 and ECERIFERUM3 are core components of a very-long-chain alkane synthesis complex. *The Plant Cell*, *24*(7), 3106-3118.
11. Greer, S., Wen, M., Bird, D., Wu, X., Samuels, L., Kunst, L., & Jetter, R. (2007). The cytochrome P450 enzyme CYP96A15 is the midchain alkane hydroxylase responsible for formation of secondary alcohols and ketones in stem cuticular wax of Arabidopsis. *Plant physiology*, *145*(3), 653-667.
12. Wang, Y., Wang, M., Sun, Y., Wang, Y., Li, T., Chai, G., Jiang, W., Shan, L., Li, C., Xiao, E., & Wang, Z. (2014). FAR5, a fatty acyl-coenzyme A reductase, is involved in primary alcohol biosynthesis of the leaf blade cuticular wax in wheat (*Triticum aestivum L.*). *Journal of Experimental Botany*, *66*(5), 1165-1178.
13. von Wettstein-Knowles, P. (1972). Genetic control of β-diketone and hydroxy-β-diketone synthesis in epicuticular waxes of barley. *Planta*, *106*(2), 113-130.
14. Netting, A. G., and Penny von Wettstein-Knowles (1976). Biosynthesis of the β-diketones of barley spike epicuticular wax. *Archives of biochemistry and biophysics* 174(2), 613-621.
15. Mikkelsen, J. D., & von Wettstein-Knowles, P. (1978). Biosynthesis of β-diketones and hydrocarbons in barley spike epicuticular wax. *Archives of biochemistry and biophysics*, *188*(1), 172-181.

16. Mikkelsen, J. D. (1979). Structure and biosynthesis of β-diketones in barley spike epicuticular wax. *Carlsberg Research Communications*, *44*(3), 133.
17. Mikkelsen, J. D. (1984). Biosynthesis of esterified alkan-2-ols and β-diketones in barley spike epicuticular wax: Synthesis of radioactive intermediates. *Carlsberg Research Communications*, *49*(3), 391.
18. von Wettstein-Knowles, P., & Søgaard, B. (1980). The *cer-cqu* region in barley: gene cluster or multifunctional gene. *Carlsberg Research Communications*, *45*(2), 125.
19. von Wettstein-Knowles, P. (2012). Plant Waxes. (Chichester, UK: John Wiley & Sons).
20. Schneider, L. M., Adamski, N. M., Christensen, C. E., Stuart, D. B., Vautrin, S., Hansson, M., Uauy, C., & von Wettstein-Knowles, P. (2016). The Cer-cqu gene cluster determines three key players in a β-diketone synthase polyketide pathway synthesizing aliphatics in epicuticular waxes. *Journal of experimental botany*, *67*(9), 2715-2730.
21. Hen-Avivi, S., Savin, O., Racovita, R. C., Lee, W. S., Adamski, N. M., Malitsky, S., ... & Friedlander, G. (2016). A metabolic gene cluster in the wheat W1 and the barley *Cer-cqu* loci determines β-diketone biosynthesis and glaucousness. *The Plant Cell*, *28*(6), 1440-1460.
22. von Wettstein-Knowles, P. (2017). The polyketide components of waxes and the *Cer-cqu* gene cluster encoding a novel polyketide synthase, the β-diketone synthase, DKS. *Plants*, *6*(3), 28.
23. von Wettstein-Knowles, P. (1969). 5. Gene Action. *Barley Genetics: Proceedings*, *2*, 146.
24. von Wettstein-Knowles, P., & Netting, A. G. (1976). Composition of epicuticular waxes on barley spikes. *Carlsberg Research Communications*, *41*(5), 225.
25. von Wettstein-Knowles, P., & Netting, A. G. (1976). Esterified alkan-1-ols and alkan-2-ols in barley epicuticular wax. *Lipids*, *11*(6), 478-484.
26. von Wettstein-Knowles, P. (1976). Biosynthetic relationships between β-diketones and esterified alkan-2-ols deduced from epicuticular wax of barley mutants. *Molecular and General Genetics MGG*, *144*(1), 43-48.
27. Trka, A., & Streibl, M. (1974). Mass spectra of long-chain aliphatic β-diketones and some of their derivatives. *Collection of Czechoslovak Chemical Communications*, *39*(2), 468-474.
28. Tulloch, A. P., & Hogge, L. R. (1978). Gas chromatographic—mass spectrometric analysis of β-diketone-containing plant waxes: Use of trimethylsilyl ethers. *Journal of Chromatography A*, *157*, 291-296.
29. Adamski, N. M., Bush, M. S., Simmonds, J., Turner, A. S., Mugford, S. G., Jones, A., Findlay, K., Pedentchouk, N., von Wettstein-Knowles, P. & Uauy, C. (2013). The *Inhibitor of wax 1* locus (*Iw1*) prevents formation of β-and OH-β-diketones in wheat cuticular waxes and maps to a sub-c M interval on chromosome arm 2 BS. *The Plant Journal*, *74*(6), 989-1002.
30. Mascher, M., H. Gundlach, A. Himmelbach, S. Beier, S. O. Twardziok, T. Wicker, V. Radchuk, C. Dockter, P. E. Hedley, J. Russell, M. Bayer, L. Ramsay, H. Liu, G. Haberer, X.-Q. Zhang, Q. Zhang, R. A. Barrero, L. Li, S. Taudien, M. Groth, M. Felder, A. Hastie, H. Šimková, H. Staňková, J. Vrána, S. Chan, M. Muñoz-Amatriaín, R. Ounit, S. Wanamaker, D. Bolser, C. Colmsee, T. Schmutzer, L. Aliyeva-Schnorr, S. Grasso, J. Tanskanen, A. Chailyan, D. Sampath, D. Heavens, L. Clissold, S. Cao, B. Chapman, F. Dai, Y. Han, H. Li, X. Li, C. Lin, J. K. McCooke, C. Tan, P. Wang, S. Wang, S. Yin, G. Zhou, J. A. Poland, M. I. Bellgard, L. Borisjuk, A. Houben, J. Doležel, S. Ayling, S. Lonardi, P. Kersey, P. Langridge, G. J. Muehlbauer, M. D. Clark, M. Caccamo, A. H. Schulman, K. F. X. Mayer, M. Platzer, T. J. Close, U. Scholz, M. Hansson, G. Zhang, I. Braumann, M. Spannagl, C. Li, R. Waugh and N.

Stein (2017). A chromosome conformation capture ordered sequence of the barley genome. *Nature*, 544, 427.
31. Muccio, Z., & Jackson, G. P. (2009). Isotope ratio mass spectrometry. *Analyst*, *134*(2), 213-222.
32. Sessions, A. L. (2006). Isotope-ratio detection for gas chromatography. *Journal of separation science*, *29*(12), 1946-1961.
33. Chikaraishi, Y., Naraoka, H., & Poulson, S. R. (2004). Carbon and hydrogen isotopic fractionation during lipid biosynthesis in a higher plant (*Cryptomeria japonica*). *Phytochemistry*, *65*(3), 323-330.
34. Collister, J. W., Rieley, G., Stern, B., Eglinton, G., & Fry, B. (1994). Compound-specific δ 13C analyses of leaf lipids from plants with differing carbon dioxide metabolisms. *Organic Geochemistry*, *21*(6-7), 619-627
35. Chikaraishi, Y., & Naraoka, H. (2007). δ13C and δD relationships among three n-alkyl compound classes (n-alkanoic acid, n-alkane and n-alkanol) of terrestrial higher plants. *Organic Geochemistry*, *38*(2), 198-215.
36. Chikaraishi, Y. 13 C/12 C Signatures in Plants and Algae." (2014): 95-123
37. Bi, X., Sheng, G., Liu, X., Li, C., & Fu, J. (2005). Molecular and carbon and hydrogen isotopic composition of n-alkanes in plant leaf waxes. *Organic Geochemistry*, *36*(10), 1405-1417.
38. Guo, Y., Li, J. J., Busta, L., & Jetter, R. (2018). Coverage and composition of cuticular waxes on the fronds of the temperate ferns *Pteridium aquilinum, Cryptogramma crispa, Polypodium glycyrrhiza, Polystichum munitum* and *Gymnocarpium dryopteris*. *Annals of botany*, *122*(4), 555-568.
39. Lindquist, P. J., Svensson, L. T., & Alexson, S. E. (1998). Molecular cloning of the peroxisome proliferator-induced 46-kDa cytosolic acyl-CoA thioesterase from mouse and rat liver: Recombinant expression in *Escherichia coli*, tissue expression, and nutritional regulation. *European journal of biochemistry*, *251*(3), 631-640.
40. Robbi, M., Van Schaftingen, E., & Beaufay, H. (1996). Cloning and sequencing of rat liver carboxylesterase ES-4 (microsomal palmitoyl-CoA hydrolase). *Biochemical Journal*, *313*(3), 821-826.
41. Svensson, L. T., Engberg, T. S., Aoyama, T., Usuda, N., Alexson, E. S., & Hashimoto, T. (1998). Molecular cloning and characterization of a mitochondrial peroxisome proliferator-induced acyl-CoA thioesterase from rat liver. *Biochemical Journal*, *329*(3), 601-608.
42. Cantu, D. C., Chen, Y., & Reilly, P. J. (2010). Thioesterases: a new perspective based on their primary and tertiary structures. *Protein Science*, *19*(7), 1281-1295.
43. Guerra, D. J., Ohlrogge, J. B., & Frentzen, M. (1986). Activity of acyl carrier protein isoforms in reactions of plant fatty acid metabolism. *Plant physiology*, *82*(2), 448-453.
44. Suh, M. C., Schultz, D. J., & Ohlrogge, J. B. (1999). Isoforms of acyl carrier protein involved in seed-specific fatty acid synthesis. *The Plant Journal*, *17*(6), 679-688
45. Pollard, M. R., Anderson, L., Fan, C., Hawkins, D. J., & Davies, H. M. (1991). A specific acyl-ACP thioesterase implicated in medium-chain fatty acid production in immature cotyledons of *Umbellularia californica*. *Archives of biochemistry and biophysics*, *284*(2), 306-312.
46. Voelker, T. (1996). Plant acyl-ACP thioesterases: chain-length determining enzymes in plant fatty acid biosynthesis. In *Genetic engineering* (pp. 111-133). Springer, Boston, MA.

47. Jones, A., Davies, H. M., & Voelker, T. A. (1995). Palmitoyl-acyl carrier protein (ACP) thioesterase and the evolutionary origin of plant acyl-ACP thioesterases. *The Plant Cell*, *7*(3), 359-371.
48. Davies, H. M., Anderson, L., Fan, C., & Hawkins, D. J. (1991). Developmental induction, purification, and further characterization of 12: 0-ACP thioesterase from immature cotyledons of *Umbellularia californica*. *Archives of Biochemistry and Biophysics*, *290*(1), 37-45.
49. Dörmann, P., Voelker, T. A., & Ohlrogge, J. B. (1995). Cloning and expression in Escherichia coli of a novel thioesterase from Arabidopsis thaliana specific for long-chain acyl-acyl carrier proteins. *Archives of Biochemistry and Biophysics*, *316*(1), 612-618.
50. Salas, J. J., & Ohlrogge, J. B. (2002). Characterization of substrate specificity of plant FatA and FatB acyl-ACP thioesterases. *Archives of Biochemistry and Biophysics*, *403*(1), 25-34.
51. Dörmann, P., Voelker, T. A., & Ohlrogge, J. B. (2000). Accumulation of palmitate in Arabidopsis mediated by the acyl-acyl carrier protein thioesterase FATB1. *Plant Physiology*, *123*(2), 637-644.
52. Kalinger, R. S., Pulsifer, I. P., & Rowland, O. (2018). Elucidating the substrate specificities of acyl-lipid thioesterases from diverse plant taxa. *Plant Physiology and Biochemistry*, *127*, 104-118.
53. Kalinger, R. S., Pulsifer, I. P., & Rowland, O. (2018). Elucidating the substrate specificities of acyl-lipid thioesterases from diverse plant taxa. *Plant Physiology and Biochemistry*, *127*, 104-118.
54. Fridman, E., Wang, J., Iijima, Y., Froehlich, J. E., Gang, D. R., Ohlrogge, J., & Pichersky, E. (2005). Metabolic, genomic, and biochemical analyses of glandular trichomes from the wild tomato species *Lycopersicon hirsutum* identify a key enzyme in the biosynthesis of methylketones. *The Plant Cell*, *17*(4), 1252-1267.
55. Kornberg, A., Ochoa, S., & Mehler, A. H. (1948). Spectrophotometric studies on the decarboxylation of β-keto acids. *Journal of Biological Chemistry*, *174*(1), 159-172.
56. Ben-Israel, I., Yu, G., Austin, M. B., Bhuiyan, N., Auldridge, M., Nguyen, T., Schauvinhold, I., Noel, J., Pichersky, E., & Fridman, E. (2009). Multiple biochemical and morphological factors underlie the production of methylketones in tomato trichomes. *Plant physiology*, *151*(4), 1952-1964.
57. Yu, G., Nguyen, T. T., Guo, Y., Schauvinhold, I., Auldridge, M. E., Bhuiyan, N., Ben-Israel, I., Iijima, Y., Fridman, E., Noel, J. & Pichersky, E. (2010). Enzymatic functions of wild tomato methylketone synthases 1 and 2. *Plant physiology*, *154*(1), 67-77.
58. Antonious, G. F. (2001). Production and quantification of methyl ketones in wild tomato accessions. *Journal of Environmental Science and Health, Part B*, *36*(6), 835-848.
59. Katz, L. (2009). The DEBS paradigm for type I modular polyketide synthases and beyond. *Methods in enzymology*, *459*, 113-142.
60. Shen, B. (2003). Polyketide biosynthesis beyond the type I, II and III polyketide synthase paradigms. *Current opinion in chemical biology*, *7*(2), 285-295.
61. Keatinge-Clay, A. T. (2012). The structures of type I polyketide synthases. *Natural product reports*, *29*(10), 1050-1073.
62. Weissman, K. J. (2006). The structural basis for docking in modular polyketide biosynthesis. *ChemBioChem*, *7*(3), 485-494.
63. Staunton, J., & Weissman, K. J. (2001). Polyketide biosynthesis: a millennium review. *Natural product reports*, *18*(4), 380-416.

64. Abe, I., & Morita, H. (2010). Structure and function of the chalcone synthase superfamily of plant type III polyketide synthases. *Natural product reports*, *27*(6), 809-838.
65. Kreuzaler, F., & Hahlbrock, K. (1972). Enzymatic synthesis of aromatic compounds in higher plants: Formation of naringenin (5, 7, 4′-trihydroxyflavanone) from *p*-coumaroyl coenzyme A and malonyl coenzyme A. *FEBS letters*, *28*(1), 69-72.
66. Dixon, R. A., & Paiva, N. L. (1995). Stress-induced phenylpropanoid metabolism. *The plant cell*, *7*(7), 1085.
67. Jang, M., Cai, L., Udeani, G. O., Slowing, K. V., Thomas, C. F., Beecher, Moon, R. C. (1997). Cancer chemopreventive activity of resveratrol, a natural product derived from grapes. *Science*, *275*(5297), 218-220.
68. Li, R., Kenyon, G. L., Cohen, F. E., Chen, X., Gong, B., Dominguez, J. N., & Rosenthal, P. J. (1995). In vitro antimalarial activity of chalcones and their derivatives. *Journal of medicinal chemistry*, *38*(26), 5031-5037.
69. Suzuki, Y., Kurano, M., Esumi, Y., Yamaguchi, I., & Doi, Y. (2003). Biosynthesis of 5-alkylresorcinol in rice: incorporation of a putative fatty acid unit in the 5-alkylresorcinol carbon chain. *Bioorganic chemistry*, *31*(6), 437-452.
70. Paniego, N. B., Zuurbier, K. W., Fung, S. Y., van der Heijden, R., Scheffer, J. J., & Verpoorte, R. (1999). Phlorisovalerophenone synthase, a novel polyketide synthase from hop (*Humulus lupulus L*.) cones. *European journal of biochemistry*, *262*(2), 612-616.
71. Katsuyama, Y., Kita, T., Funa, N., & Horinouchi, S. (2009). Curcuminoid biosynthesis by two type III polyketide synthases in the herb Curcuma longa. *Journal of Biological Chemistry*, *284*(17), 11160-11170.
72. Katsuyama, Y., Kita, T., & Horinouchi, S. (2009). Identification and characterization of multiple curcumin synthases from the herb *Curcuma longa*. *FEBS letters*, *583*(17), 2799-2803.
73. Katsuyama, Y., Matsuzawa, M., Funa, N., & Horinouchi, S. (2007). In vitro synthesis of curcuminoids by type III polyketide synthase from *Oryza sativa*. *Journal of Biological Chemistry*, *282*(52), 37702-37709.
74. Rodrigues, J. L., Prather, K. L., Kluskens, L. D., & Rodrigues, L. R. (2015). Heterologous production of curcuminoids. *Microbiol. Mol. Biol. Rev.*, *79*(1), 39-60.
75. Katsuyama, Y., Ohnishi, Y., & Horinouchi, S. (2010). Production of Dehydrogingerdione Derivatives in *Escherichia coli* by Exploiting a Curcuminoid Synthase from *Oryza sativa* and a β-Oxidation Pathway from *Saccharomyces cerevisiae*. *Chembiochem*, *11*(14), 2034-2041.
76. Katsuyama, Y., Miyazono, K. I., Tanokura, M., Ohnishi, Y., & Horinouchi, S. (2011). Structural and biochemical elucidation of mechanism for decarboxylative condensation of β-keto acid by curcumin synthase. *Journal of Biological Chemistry*, *286*(8), 6659-6668.
77. Brinkerhoff, R. C., Tarazona, H. F., de Oliveira, P. M., Flores, D. C., D'Oca, C. D. R. M., Russowsky, D., & D'Oca, M. G. M. (2014). Synthesis of β-ketoesters from renewable resources and Meldrum's acid. *RSC Advances*, *4*(91), 49556-49559.
78. Matucha, M., Jockisch, W., Verner, P., & Anders, G. (1991). Isotope effect in gas—liquid chromatography of labelled compounds. *Journal of Chromatography A*, *588*(1-2), 251-258.
79. Racovita, R. C., & Jetter, R. (2016). Identification of Polyketides in the Cuticular Waxes of *Triticum aestivum cv*. Bethlehem. *Lipids*, *51*(12), 1407-1420.
80. Rowland, O., Zheng, H., Hepworth, S. R., Lam, P., Jetter, R., & Kunst, L. (2006). CER4 encodes an alcohol-forming fatty acyl-coenzyme A reductase involved in cuticular wax production in Arabidopsis. *Plant Physiology*, *142*(3), 866-877.

81. Galanie, S., Thodey, K., Trenchard, I. J., Interrante, M. F., & Smolke, C. D. (2015). Complete biosynthesis of opioids in yeast. *Science*, *349*(6252), 1095-1100.
82. Brown, S., Clastre, M., Courdavault, V., & O'Connor, S. E. (2015). De novo production of the plant-derived alkaloid strictosidine in yeast. *Proceedings of the National Academy of Sciences*, *112*(11), 3205-3210.
83. Swan, T. M., & Watson, K. (1997). Membrane fatty acid composition and membrane fluidity as parameters of stress tolerance in yeast. *Canadian journal of microbiology*, *43*(1), 70-77.
84. Færgeman, N. J., Black, P. N., Zhao, X. D., Knudsen, J., & DiRusso, C. C. (2001). The Acyl-CoA Synthetases Encoded within FAA1 andFAA4 in *Saccharomyces cerevisiae* Function as Components of the Fatty Acid Transport System Linking Import, Activation, and Intracellular Utilization. *Journal of Biological Chemistry*, *276*(40), 37051-37059.
85. Larson, T. R., & Graham, I. A. (2001). Technical advance: a novel technique for the sensitive quantification of acyl CoA esters from plant tissues. *The Plant Journal*, *25*(1), 115-125.
86. Richards, R. A., H. M. Rawson, and D. A. Johnson (1986). Glaucousness in wheat: its development and effect on water-use efficiency, gas exchange and photosynthetic tissue temperatures. *Functional Plant Biology* 13(4), 465-473.

Appendices

Appendix A Supplementary data from Chapter 2

Table A.1 **Composition of the alkane-2-ol esters isolated from barley *cv.* Morex spikes**

Chain length	Relative abundance (%)	Esterified alkan-2-ol chain length (%)		
		13	15	17
33	8.3	11.8	88.2	-
35	58.5	-	100.0	-
36	3.0	-	100.0	-
37	30.3	-	40.9	59.1

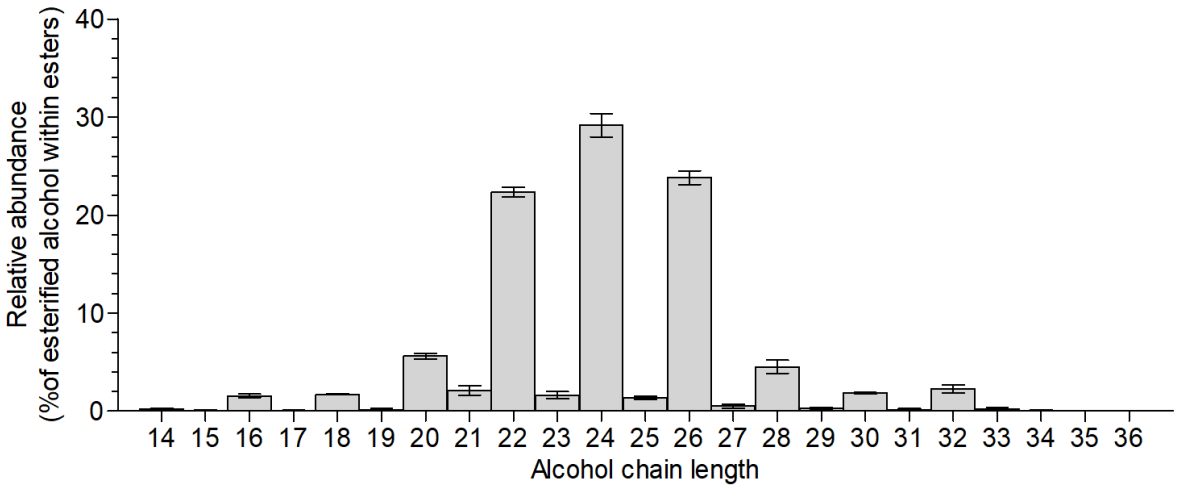

Figure A.1: **Chain length distribution of the esterified alcohol moiety on alkane-1-ol esters.** Bars represent the averages of three independent replicates, error bars corresponds to standard deviation.

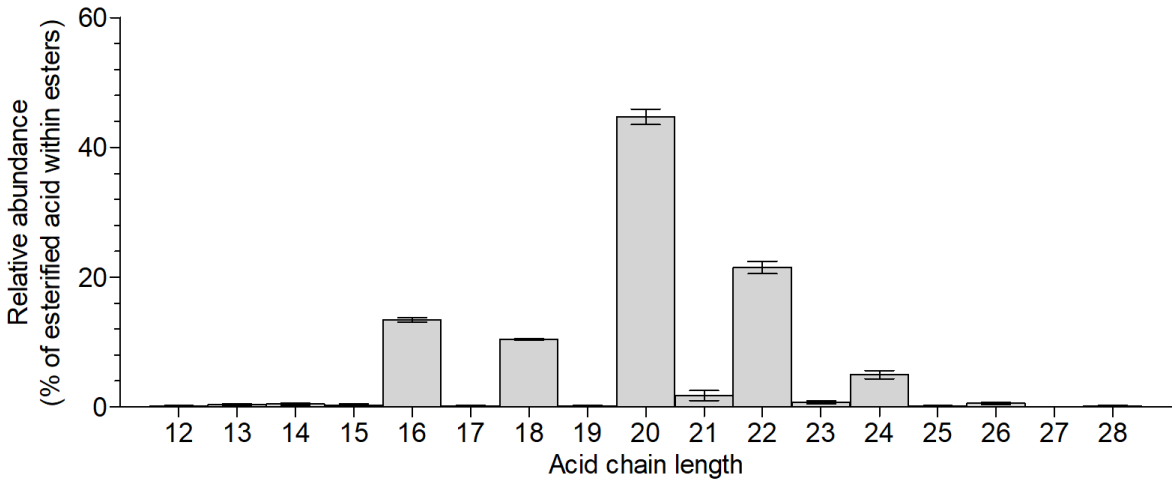

Figure A.2: **Chain length distribution of the esterified acyl moiety on alkane-1-ol esters.** Bars represent the averages of three independent replicates, error bars corresponds to standard deviation.

Appendix B Supplementary data from Chapter 4

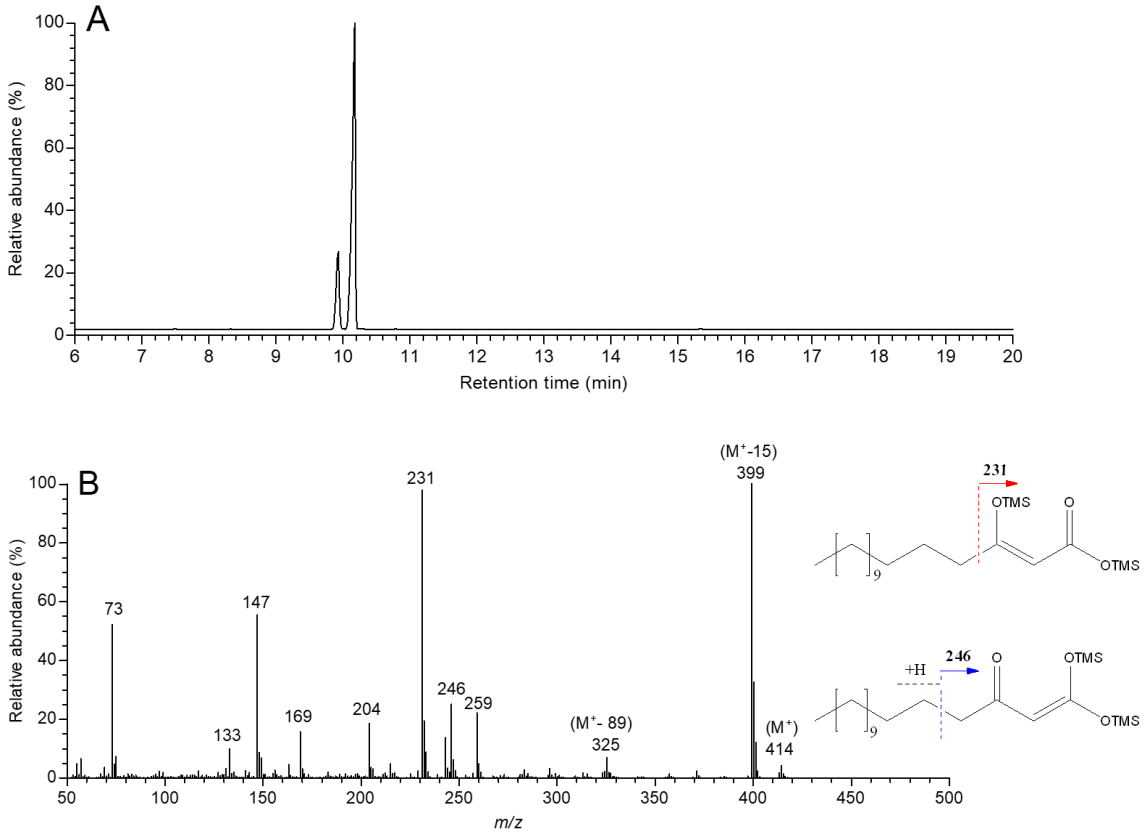

Figure B.1: **GC-MS analysis of the synthetized β-keto-palmitic acid methyl ester. A.** GC-MS chromatogram and **B.** mass spectrum of the purified β-keto-palmitic acid methyl ester.

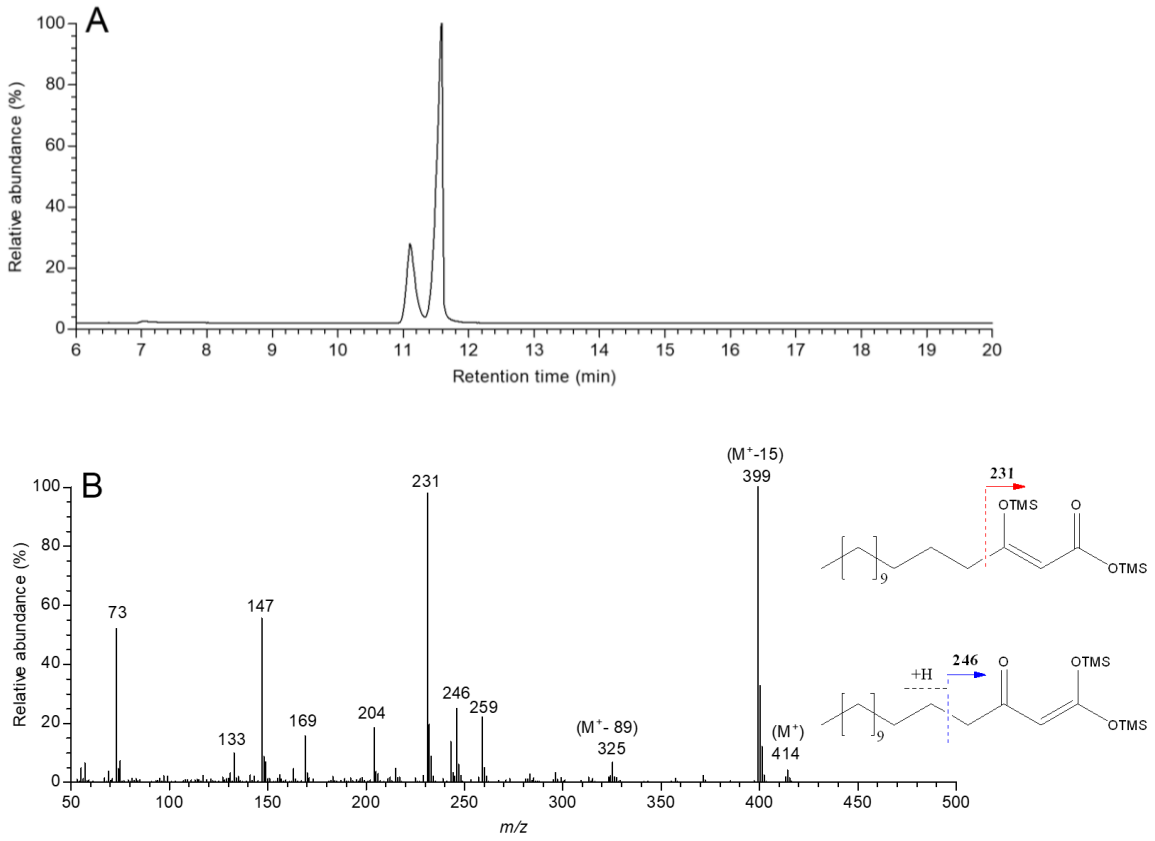

Figure B.2: **GC-MS analysis of the synthetized β-keto palmitic acid (C_{16} BKFA) used for yeast feeding. A.** GC-MS chromatogram of the purified C_{16} BKFA and **B.** mass spectrum

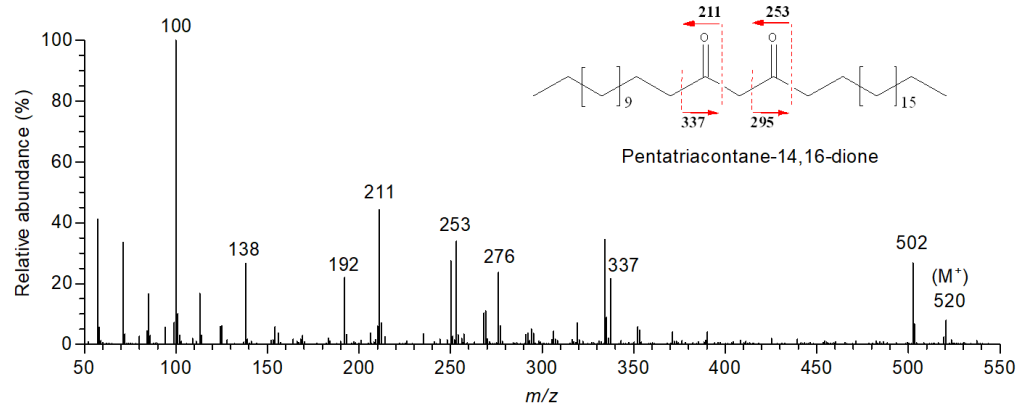

Figure B.3: **Mass spectrum of the pentatriacontane-14,16-dione authentic standard.**